THE INTERPRETATION OF MEDIO-LATERAL REACTION FORCES IN HUMAN LOCOMOTION USING BODY COORDINATE SYSTEMS

by

Subramaniam Balakrishnan

A THESIS

SUBMITTED TO THE FACULTY OF GRADUATE STUDIES

IN PARTIAL FULFILLMENT OF THE REQUIREMENTS FOR THE DEGREE

OF DOCTOR OF PHILOSOPHY

THE UNIVERSITY OF MANITOBA

DEPARTMENT OF MECHANICAL ENGINEERING

WINNIPEG, MANITOBA

March 1982

THE INTERPRETATION OF MEDIO-LATERAL REACTION FORCES IN HUMAN LOCOMOTION USING BODY COORDINATE SYSTEMS

BY

SUBRAMANIAM BALAKRISHNAN

A thesis submitted to the Faculty of Graduate Studies of the University of Manitoba in partial fulfillment of the requirements of the degree of

DOCTOR OF PHILOSOPHY

ABSTRACT

The research work reported in this dissertation focuses on the mathematical interpretation of force plate measurements for normal and abnormal locomotion. A force plate large enough (approximately 16 sq. ft. in area) to accomodate many types of abnormal gait normally encountered by the clinician was developed. The force plate was sufficiently sensitive to ground-reaction force measurements in all the three principal spacial directions to allow the measurement of the subtle changes in ground-reaction as a result of injury to any of the supporting limbs.

A simple three dimensional model is proposed in order to interpret the significance of reaction parameters. The model input, in the form of displacement patterns of limb segments and ground-reaction forces were obtained using bi-plane photography and force plate measurements respectively. The mathematical model proposed relates the dynamics of upper body motion to those of the lower extremity in support phase. A set of symmetry parameters highly indicative of gait disruption have been defined. The parameters of symmetry which relate reaction forces as measured by the force plate to asymmetrical characteristics of pathological gait have not been previously defined in the literature.

The present work relates the measured reaction force patterns to the upper body motions using the principle of impulse and momentum and force and moment equilibrium. In the majority of investigations on gait analysis the moments and forces at various limb joints have been expressed in the general reference frame. In the present study,

movements of the segments are related to the angular rotations of the body fixed coordinate system. Special coordinate transformation techniques have been proposed and are general enough to accept the large angular rotations characteristic of pathological gait. The moments in the moving upper body coordinate system are then related to ground-reaction forces through the parameters developed. In this way, the compensatory maneuver brought about by the upper body in the event of injury to one of the supporting members is better understood and quantified.

The use of the force plate and the mathematical model to develop gait parameters for clinical studies is illustrated by analysing certain subjects with joint dysfunction. The set of force and moment parameters developed have been used to indicate the degree of symmetry in the various planes of motion. The parameters have helped identify gait abnormalities, as well as to quantify them. Through cooperation with subjects undertaking physiotherapy, data have been taken and demonstrate the use of the gait parameters developed for clinical monitoring of injury recovery rate.

ACKNOWLEDGEMENT

I pursued my Ph.D. program primarily to fulfill the wishes of my grandpa, Prof. S.A. Mani. Sadly he is not around to read this thesis. I wish to dedicate this thesis to the fond memories of my grandpa.

During my period of research at the University of Manitoba, I have been very fortunate in having Dr. A.B. Thornton-Trump as my thesis advisor. I wish to acknowledge Dr. Thornton-Trump for the excellent support throughout the period of my research. He gave me the freedom to complete the work in my own way and I wish to express my sincere gratitude to him by saying, 'Thank you Sandy, I could not have made it without your support'.

This dissertation has benefited greatly from the discussions I had with numerous persons. That broadened my comprehension of the problems undertaken. I acknowledge with gratitude the valuable suggestions given by Mr. Wayne Brodland while working out the various transformation techniques reported in this thesis. The asistance offered to me by Mr. Art Quanbury of the Rehibilitation center for children and Mr. Chris Snow of St. Boniface Hospital, is also greatly appreciated. I wish to thank Mr. J. Sewell for his assistance in hardware construction.

Mrs. Violet Lee, who typed this thesis, has done an excellent job. She was very co-operative and understanding in doing the typing in a short time. My sincere thanks are due to her. During my stay at the University of Manitoba, the friendly staff at the Dept. of Engineering were always willing to help me. The assistance from everyone of them is greatly appreciated.

I will fail in my duty if I did not thank my family and a few others. They have been waiting patiently, miles away. I can only tell them "Thank you, I appreciate your best wishes, I will have better times ahead".

Finally, the funding provided by the National Research Council through a Grant to Dr. A.B. Thornton-Trump is gratefully acknowledged.

TABLE OF CONTENTS

LIST OF FIGURES

LIST OF TABLES

NOMENCLATURE

a, b, c	Constants representing the angular orientation of reference coordinate axes at center of gravity and the hip displacement vector
a_1, b_1, c_1	Components of **'r'** in the reference frame $X_2\ Y_2\ Z_2$
a_2, b_2, c_2	components of **'h'** in the reference frame $X_1\ Y_1\ Z_1$
$\mathbf{h}$	position vector between hip and center of gravity defined in reference frame $X_1\ Y_1\ Z_1$
h_s	position vector between hip and center of gravity in body neutral position defined in reference frame $X_1\ Y_1\ Z_1$
ℓ	length of lower limb in the body neutral position
$\mathbf{M}$	moment vector at any joint in the body
M_j	total moment at the jth joint due to muscular forces
M_{j_r}	moment produced by the ground-reaction at the jth joint
$\mathbf{M}_{j_g}$	moment due to gravity forces of leg segments below the jth joint
M_{j_i}	moment at the jth joint due to inertial forces of the leg segments below the jth joint
M_B	moment vector in the reference frame at the center of gravity of body
M_B^b	moment vector in the body coordinate system at the center of gravity of the body
$M_{B_X}, M_{B_Y}, M_{B_Z}$	components of moments in the upper body reference system
$M_{B_X}^b, M_{B_Y}^b, M_{B_Z}^b$	components of moments in the upper body coordinate axes
M_H	vector moment in the reference frame at the hip joint
$\mathbf{P}$	position vector normal to the plane containing the position vectors **'T'** and **'h'**

$\mathbf{r}$	position vector of the lower limb (between ground and hip joint)
$\mathbf{R}$	ground-reaction vector at the foot
R_X, R_Y, R_Z	components of ground-reaction forces in the reference frame
$\mathbf{T}$	vector normal to the plane containing the reference Z_1 axis and the neutral position hip vector $\mathbf{h}_s$
$T_{S \rightarrow H}$	Transformation matrix for the lower limb
$T_{S \rightarrow B}$	Transformation matrix for the upper body
$V^I, V^{II}, V^{III}, V^{IV}$	components of the position vector 'r' on the reference X, Y, Z, axis and XY plane respectively
X_1, Y_1 Z_1	reference frame fixed at the center of gravity parallel to the earth frame X_E Y_E Z_E
X_2, Y_2, Z_2	reference frame fixed at the hip joint, parallel to the earth frame
X_E, Y_E, Z_E	General coordinate axes fixed to the reference point located outside the body
X^b, Y^b, Z^b	body centered coordinate system at center of gravity
X^h, Y^h, Z^h	body centered coordinate system at hip joint
ψ, θ, ϕ	general Eulerian angles
ψ_ℓ, θ_ℓ, ϕ_ℓ	Eulerian rotation angles of the body coordinate system at the hip joint
ψ_b, θ_b, ϕ_b	Eulerian rotation angle of the body coordinate system at the CG
'ν'	angle between the reference axis Z_1 and the position vector '$\mathbf{h}_s$'

CHAPTER I

INTRODUCTION

1.1 Definition of Locomotion

Locomotion in the most general sense is defined as change of place. The rhythmical, alternating movement of the limbs of the human body to accomplish this change of place is referred to as human bipedal locomotion. Walking from one place to another on two legs seems to be a simple act but it is a complex interaction between the forces generated within the body and several external forces acting on it. In order to produce or prevent motion at any major limb joint in the body, millions of energy transformations are triggered within the body. The resulting movement of the center of gravity of the body from one place to another (in the safest, most efficient and pain-free manner) will be termed normal human locomotion and is one of the primary functions of the neuro-musculo-skeletal system. In the case of normal gait, the movement of the limbs are more or less symmetrical with respect to the median plane. The various planes normally considered by anatomists and clinicians for defining motions of the body are shown in Fig. 1. In the case of pathological or abnormal gait the movement of the limbs even though alternating, need not necessarily be symmetrical.

The human control system automatically interrelates changing conditions in the force-motion-position system at scores of joints and the end product is the resultant ground-reaction force at the foot. The major locations for the control of the ground-reaction force in each leg are the ankle, knee and hip. By proper regulation of moments about each of these joints, the nervous system controls the magnitude and direction of the

ground-reaction force and consequently controls the movement of the center of gravity of the body. In the case of certain joint dysfunctions and neuro-musculo-skeletal disease, the precise and efficient regulation mechanism of the movement of the body does not function well. A person's ability to apply and control forces and moments is often impaired. In the event of amputation of one of the major joints or extremities, a prosthesis restores the possibility of locomotion for an amputee. Usually, a prosthesis is purely a passive device having no active elements corresponding to muscle. Amputee gait therefore requires an adaptation in body kinetics and a change in the utilization of remaining musculature in order to ambulate from one place to another. This kind of compensation from other musculature would in general be found for any pathological gait condition and the readjustment is a highly individual characteristic. Exaggerated motions in some limb segments and reduced motions in others, resulting in a totally different ground reaction force[9], may be viewed as an attempt by the individual to preserve as low a level of gait energy expenditure as possible. Therapeutic intervention of many sorts, such as assist devices, orthotic devices, prosthetics, rehabilitative surgery and a range of exercise techniques represent attempts to improve abnormal gait or represent attempts to develop more normal or stable gait positions.

From time to time anatomists, mathematicians and physicists have occupied themselves with problems concerning human gait and to trace the roots of such study would lead one almost to antiquity. Parameters that are observable on a subject's gait such as time duration of support of each leg on the floor, the duration of swing of each leg, angular rotation of ankle, knee and hip joints are all interrelated. The characteristics

of normal gait determined with respect to these physical parameters have been attempted by several researchers. Forces and moments at various limb joints during normal locomotion have also been investigated and approximated using models of varying degrees of complexity. A brief review of various studies is presented in the next chapter. A complete description of human gait would involve consideration and measurement of both the kinematics and kinetics of the extremities of the limb segments. Such knowledge, by itself, is not of much value to the clinician until it is integrated and reduced to a simpler concept of locomotion. Deductions can then be drawn, clinical progress quantified, and treatment inferred from the analysis of the clinical problems that confront him. Such locomotion analysis would then help determine the type and extent of gait disorder resulting from pathological processes.

1.2 Gait Study in the Past and Scope of Present Study

The distinction of being a path finder in human locomotion study should go to Borelli[1] since he was the first to determine the center of gravity of the human body and to propose a fundamental concept of muscle action. He described the forward displacement of the center of gravity beyond the supporting area of the foot and the manner in which the forward swinging of the limbs saves the body from losing balance. Following this study, very little was accomplished in the study of locomotion for nearly one hundred years. The period which could be termed the observational period of studies in gait started with Wilhem and Edward Weber[2]. Several studies of alternation of swing and support, the inclinations of the lower limbs in either phase, the relationship between the duration and

length of the step, the rhythm of alternation in walking and running, were attempted during this period. Once photography was established as a medium of recording the phases of gait, the way was open for more quantitative investigations of velocities, accelerations and moving forces, - an outstanding paper being the classic work of Braune and Fischer[3]. From this time, newer approaches to human gait opened up wider possibilities. With the availability of hybrid computing systems, a comprehensive picture of human locomotion was made possible. Synchronized data relevant to muscular activities, trajectories of several cardinal points on the body and the various forces underfoot, with and without the imposition of special constraints such as pace period have been undertaken by researchers such as Murray[4,5]. With the application of high speed computing systems to gait study, the scope of investigation has increased manyfold in recent times.

To study those aspects of locomotion which are most germane for patient gait evaluation and thus aid in the design of better prosthetic and orthotic devices has been the aim of several researchers in recent years. Floor torques and floor reaction forces have been measured and applied to the calculation of forces and moments at various joints of the body. These measurements and calculations are analyzed in conjunction with limb displacement data and EMG signals from various groups of muscles. Normal human gait has been the theme of investigation in the majority of studies. In a normal human gait the movement of the limbs on either side of the median plane[Fig. 1] is more or less symmetrical and, hence, measurements have been mostly made on one limb in the plane of progression. Such measurements have been assumed to be adequate. In the

case of pathological gait the movement of the limb in the three dimensional space need not be symmetrical[9], and hence measurements have to be made in three dimensional space. Such measurement and the analysis that follow have required relatively elegant instrumentation and mathematical models. The concept of using a force plate (a device that measures the reaction force between the foot and the ground) was not available to most of the investigators and gait study was restricted to calculation of velocity and acceleration of the moving limbs of the body. Frame-by-frame analysis of the motion picture film of the subject moving in a laboratory environment resulted in composite tracings and stick diagrams showing the position of body segments. The energy levels and power flow across human limb joints were assumed to represent the characteristics of human movement. The advent of a force plate by Cunningham and Brown[6] in 1951 increased the scope of gait studies. Thus in addition to the kinematic information on the movement of the limbs, the kinetic information through the ground forces is available to the researchers. Force plates reported in literature are rather small in size (approximately 2 to 3 square feet in area) and the subjects have to constantly aim in order to step on the force plate. This aiming could result in a constraint on the walk. Some of the subjects investigated as part of a preliminary study on Legg Perthes Braces[10] showed a very broad compass gait and it would be difficult to accomodate such pathological gait on a small force plate. As pointed out earlier, in the case of pathological or abnormal gait the compensation for loss of function in one limb or joint usually comes from other limbs or joints of the body. A reduced force or motion in one plane of motion, may give rise to a larger

and above normal level of forces or motion in another plane. This brings into focus the necessity of three dimensional measurement for adequately representing pathological gait. Mathematical models for human body movement reported in literature vary from a simple one link segment model to the nine link segment model used by Ramey and Yang[71]. Some of the three-dimensional models reduce their clinical applicability due to their complexity.

In the case of three dimensional displacement measurements, additional difficulties arise from the use of several cameras. Because of the solid, irregular and opaque nature of human body segments, the same target fixed to the body may not be seen by all the cameras at all times. Solutions for such problems will have to be developed.

The critical period for stability of human body during its ambulation occurs when it is being supported on only one of the lower limbs. One of the valuable biomechanical variables for the assessment of any human movement is the time history of the moments at each joint. The effect of all agonist and antagonist muscle activity is shown by these kinetic patterns. The net effect of the movement of the body about the point of support at the ground results in a time varying net ground-reaction force. As part of the present work the design and development of a force plate capable of accurately measuring the ground reaction force components in three mutually perpendicular directions was undertaken. The force plate is required to be large enough to accommodate disrupted gait without altering a subject's stride. The increased mass of a large force plate will tend to lower the natural frequency of the system as well as lower the sensitivity in measurements. The design investigated attempts

to keep the natural frequency of the system well above the measurement range and provide a good resolution for force measurement in all three directions.

Since normal locomotion has been investigated by several researchers, the present study will focus on the use and mathematical interpretation of force plate measurements for abnormal or pathological gait conditions. The use of models to analyse locomotion in abnormal gait conditions has not been reported. A set of parameters will be defined which are highly indicative of gait disruption but show smaller variation in normal gait.

In order to describe the net locomotion posture, a simple mathematical model that would present an integrated picture of locomotion of the upper body with respect to the lower limb will be proposed. The spatial kinematics of limb segments in three dimensional space will have to be determined and the use of biplane photography for obtaining three dimensional movement of the body segments will be illustrated. The traditional locomotion analysis considers the motion in a moving coordinate system, parallel to the general reference axes, and the computations are reported primarily in the sagittal plane. In the present study the movement will be described in the moving body coordinate system and special coordinate transformation techniques for obtaining these from measured limb marker positions will be proposed. Finally, the use of force and displacement measurements and the mathematical model along with the set of parameters for analysing the characteristics of gait disruption on certain abnormal gait conditions will be reported.

1.3 General Statement of Goals.

Several weaknesses in gait analysis up to the present prevent their full clinical use. These weaknesses will be more fully defined during the literature review in Chapter 2 and are summarized at the end of that chapter. However, there are two over-riding difficulties in the usual clinical gait laboratory. The first is the lack of accurate three dimensional reaction force data taken simultaneously with displacement data. The second difficulty is the length of time required for the data abstraction and analysis. The first difficulty can be overcome by the development of a suitable force plate system, which is one of the objectives of this work. The difficulty of data abstraction and analysis is caused, in part, by a lack of simple parameters which give clear indications of abnormal gait. Often, extremely complex mathematics is applied yielding conclusions quite beyond clinical interpretation. In this work the objective is to use mathematical models to develop simple parameters which allow a clinical assessment of gait normality, based on reaction force measurement and related changes in body segment displacements and motions.

CHAPTER 2

LITERATURE REVIEW

2.1 General Layout

A review of literature on human locomotion studies presented in this chapter would indicate the constant interest and advancements made in this field. For the sake of convenience in presentation, the literature review in this chapter is divided into five sections which are reviews of: the normal gait cycle, the force plates used in locomotion analysis, the displacement measurement techniques, the joint models and some mathematical gait models. Areas where further work is most desirable are identified in detail.

2.2 Review of Normal Gait

Human locomotion is a phenomenon of the most extraordinary complexity with a multitude of individual motions occuring simultaneously in the sagittal, frontal and the transverse planes of space. A concept adopted in several studies assumes that locomotion is the translation of the center of gravity of the body through space along a pathway requiring the least expenditure of energy. The pathway described by the center of gravity in the plane of progression is a smooth, undulating, almost sinusoidal curve. In a single cycle of locomotion from the right heel-strike to the next right heel-strike, the center of gravity of the body rises smoothly to a summit at 25% of the cycle and at the same time deviates to the right. As the center begins to descend it smoothly deviates toward the left to continue this deviation as it once more

begins to rise to a second summit at 75% of the cycle.

When the second summit is reached and the center of mass proceeds to fall, it begins to return gradually to the right and has reached the central axis of the forward motion as the cycle is completed. A sensitive balance on each foot exists as the upper body goes through the undulating motion. A complete gait cycle is the period from heel-strike on one leg to the next heel-strike on the same leg. The cycle is broadly divided into two phases; the stance phase and the swing phase. Stance phase begins at the heel-strike on one leg and ends at toe-off on the same leg. Swing phase begins when the stance phase ends and represents the period between toe-off (T.O.) on one foot and heel contact (H.C.) on the same foot.

A complete gait cycle is explained with reference to Fig. 2. Stance phase is characterised by six key events. It begins at the instant the heel touches the floor - 'Heel contact' (H.C.). Shortly thereafter, the sole makes contact with the ground - 'Foot flat' (F.F.). Next the body weight is swung directly over the supporting extremity - 'mid stance' (M.S.) and continues to rotate over the foot. As the body mass above the ankle continues to rotate forward, the heel lifts off the ground - 'Heel off' (H.O.). Shortly after this, the body is propelled forward by the forceful action of the calf muscles - 'push-off'. The push-off phase terminates when the entire foot rises from the ground - 'Toe off' (T.O.). Swing phase, as represented in Fig. 2, is divided into three main periods. Just at the end of toe-off, a phase of rapid acceleration (as high as 4g at the ankle) begins. The leg must be accelerated in order to catch up to and get in front of the body in preparation for the next heel-contact. The leg is in 'mid-swing' position when the swinging leg has caught up and

passes directly beneath the body. It is also the instant at which the fore and aft shear forces registered on the ground are zero. The deceleration phase begins after mid-swing when the forward motion of the leg is restrained by the stretching of the hamstring muscles to control the position and velocity of the foot immediately before heel-contact. As the body alternates from swing to stance on each leg, there is a period when both feet are in contact with the ground simultaneously. This period, termed 'double support', occurs between push-off and toe-off on one foot and heel-contact and foot-flat on the other. The duration of double support is inversely related to cadence. Figure 2 also shows temporal components of walking cycle. At ordinary speeds, the single leg stance phase period is approximately 60% of the cycle and the swing phase approximately 40%. The period of double support occupies about 25% of the gait cycle time and includes a portion of the stance-phase time for each leg.

The continous process of rise and fall of the upper body can be seen by monitoring the time varying ground-reaction force. A typical tracing of these force curves for a double step, as obtained by Balakrishnan and Thornton-Trump(11) is shown in Fig. 3. The vertical component of the reaction force has a double-peak shape and two smaller peaks; this is due to vertical upward and downward accelerations of the body. The difference between the vertical component of floor reaction and the body weight is proportional to the vertical acceleration of the body. The smaller peak occurs shortly after heel strike, when the body rolls over the supporting leg and the second peak occurs when the leg 'pushes' the body just before the other leg strikes the floor. The lateral component of the ground

reaction has a very small magnitude but plays a vital part in the lateral stability in walking. As the body weight is shifted from one leg to the other, the lateral reaction force must be directed inward with respect to the body in order to prevent the subject from falling sidewise. The magnitude of this force will depend largely upon the amount of lateral hip motion. The posterior-anterior (fore-aft) component of floor reaction force has a typical shape approximating a saw tooth during the stance phase. The temporal variation in this force is due to the fact that upon heel strike the force first must retard the forward motion of the body and then a fraction of a second later must provide the push-off or forward acceleration necessary to continue the forward motion of the body.

Many departures from these simple features are present in a pathological gait, the most frequent being the lack of force and time symmetry, reduced and non-uniform rates of loading and unloading on the foot, reduced peaks and valleys and lengthened phases, particularly those of double support. The asymmetry of force traces may extend over one or more features such as differences during the left and right limb support phases, maximum forces or the general appearance of the trace.

2.3 Force Plates Used in Gait Study

Force plates are dynamometric platforms designed to measure the forces exerted by the foot on the ground during walking or other activities. They are essentially flat plates supported by a base frame. The base frame or, in certain cases, linkages between the base frame and the force plate carry transducers to detect the exchanged loads. Reaction forces between the foot and the ground during walking have been of

considerable interest to orthopaedic surgeons for a long time. From the literature available to the researchers in gait study, measurement of the ground reaction force was attempted as early as 1872. This is evident from the works published by Carlet[12] and Marey[13]. The vertical component of the ground reaction was measured by them with a pneumatic cell fixed in the sole of the shoe. Other ingenious methods like relating the impressions of the foot to the forces exerted on a floor made of plaster of paris - Beely[14], have also been reported. Abrahamson[15] studied the impressions left on a lead plate when the subject walked upon it with steel shots fixed to the shoe. While the above studies would help in understanding the load distribution under the feet in static conditions, the applicability of such methods for a continuous monitoring of forces on a dynamic state as would be encountered in human locomotion is limited.

With the advent of photography as a means of recording measurements, Elftman[16] filmed the underside of a corrugated mat placed on a glass plate. The deformations produced due to the forces when the mat was walked upon were taken to represent the load distribution. Barnett[17] devised a box of vertical perspex rods whose vertical displacement into a rubber support could be filmed from the side when the subject walked on the upper surface. Thus with the introduction of photography, the recordings of pressure distribution under the feet in a dynamic state was presented as a possibility.

The first device capable of measuring the three components of the floor reaction on the feet was reported by Amar[18] and Elftman[19]. Vertical deflections of four springs supporting a level plate were

measured and compared to a calibration chart for determining the vertical load. The horizontal loads were measured as a function of bending of the springs in the horizontal plane. Both the devices of Elftman and Amar were entirely mechanical and a permanent record of the measurement was not possible. Elftman's force plate was perhaps the most direct and accurate device reported up to that time. However, the large deflections of the walking surface, inertia of the force plate and friction in the linkages were found to produce large errors. While efforts were being made to measure forces using a supported platform, Schwartz and Heath[20] and Baumen and Brand[21] investigated the use of electronic transducers for measuring forces. In their studies pressure sensitive discs were attached to the foot for measuring forces. This principle is used even today by several researchers. Instrumented shoes have a tendency to alter the gait of the subject and measure the force only at a specific point on the feet.

The advent of an electronically instrumented force plate developed by Cunningham and Brown[6] allowed the addition of new dimension to force measurements. This is demonstrated by the works of Bresler and Frankel[22] who, using Cunningham's force plate, obtained the three components of moments at the lower limb joints. Cunningham's force plate was a rectangular flat plate 15" x 20", and rigidly supported at each corner by tubular columns. Vertical load and its position was determined by means of three pairs of axially placed strain gauges. Shear force on the top plate in each of the coordinate directions was measured by a combination of eight gauges, responsive to the bending strain in the columns. Torque about a vertical axis of the force plate was measured by the same set of eight gauges switched in a different combination. The

linearity in calibration of such a force plate is claimed to have a maximum deviation of less than 3 pounds in the vertical direction. The average deviation was one pound in the shear measurement and seven inch pounds in torque values. Damping of the force plate was found necessary and was achieved by a thin layer of fluid between the top force plate and a parallel bottom plate. A leaf spring was interposed between the two plates for additional damping. The available publications on the force plate do not report the cross-talk between the various transducers. A rigidly supported force plate with each support carrying several transducers will generally produce large cross-talk. Since the horizontal components of force produced in walking are considerably smaller in magnitude when compared to the vertical component, any large errors introduced in their measurement due to cross-talk would reduce the usefulness of force measurement.

McLeish and Arnold[23] improved the sensitivity of ground reaction force measurement by supporting the force plate on vertical and horizontal steel strips. Several support strips with strain gauges mounted on them measured the forces in the respective axes. The suspension system adopted in their design improved the sensitivity in force measurements by nearly five times when compared to the column supported design of Cunningham. Grundy et al[24] adopted the same design of support systems and the force plate had a glass walkway set in the middle for synchronized photography of the sole of the foot. From the film and force measurement, plots of center of pressure along with the force curves were obtained for several normal subjects. Other investigators - Paul and McGrouther[25], Paul[26] have used similar force plates in their studies. It is difficult to

compare the performance of the different force plates discussed so far, on the basis of force tracing obtained from different subjects. The characteristics of the force place such as natural frequency, resolution, cross-talk are not generally well documented.

The introduction of minicomputers and microprocessors has given rise to the development of computer based force platforms in recent years. Data processing of force information, modelling, simulation and prediction of human gait analysis are all feasible for the experimentalist without having to spend many man hours. It took Bresler and Frankel[22] nearly 500 man hours to analyse one stride of force data.

A study related to analysing the moving pattern of point of application of the vertical resultant force during level walking resulted in the development of a triangular force plate by Yamashita and Katoh[27]. The force plate was right isosceles triangle in shape, supported at its three vertices by load cells of high rigidity. The load cell was sensitive to forces in the vertical direction only. The unknown coordinates of the vertical force acting on the platform were determined by measuring the reactive components at the three vertices. The accuracy of this geometry with just three supports at corners depends mainly on the accuracy of the load cell. For a static calibration the error was less than 5% except for a few points around the vertex where a maximum error of 10% was found. A satisfactory (no figures available) dynamic response has been reported. By using a triangular element, the number of supports were reduced and thus the structure becomes statically determinate. Since Yamashita's force plate can measure the vertical components only, its application is limited.

Gola[28] applied the concept of a statically determinate system for the design and development of a new kind of force plate. It was again a triangular element force plate suspended at each corner by two strips. A set of strain gauges glued to these strips measured the force. Each suspension element was hinged at both ends and their position in space will not be affected by deformation of the plate, nor will they be subjected to any bending. The cross-talk between the transducers with this arrangement was expected to be a minimum. The natural frequency of vibration as obtained by them was 190 Hz. Sensitivity was reported to be 1/2 Newton at the plate center in the x-direction, and 1/6 Newton in the y-direction.

A newer approach to ground-force visualization is being attempted by several researchers. Whilst the information from force plates have been providing valuable information regarding kinetic factors influencing gait, the difficulty of relating the three separate force components and positional components (coordinates of center of pressure) was always a problem for use as a clinical evaluation. Cook et al[29, 30] have overcome this problem by superimposing a vector of ground reaction force on a film of the subject ambulating. The system uses the relevant force plate outputs for the plane of interest to produce Lissajous figures by deflecting a laser beam with galvonometer mirrors driven through analog circuits. The resulting 'line' is optically combined with the view of the subject and recorded on film. Stallard et. al[31] used the same principle but instead of recording the images on film they devised a technique by which the force vector was instantaneously superimposed on a television picture of the subject, by electronically processing the video signal.

Using the vector display approach Pedotti[32] created on - line butterfly diagrams for a spatial-temporal representation of evolution of ground reaction during each stride. The above principle was investigated further by Boccardi et al[33,35]. The images of the vector representing the ground-reaction are superimposed on-line to the images showing the positions of the hip, knee and ankle joint axis. Muscular moments during stance phase were obtained by multiplying the vector amplitude by its distance from the joints in each image. All the above investigations on force-vector visualization can be adapted for any force plate design using supplementary hardware. The vector visualization approach has great potential to help the clinician perform a rapid diagnosis of gait abnormalities.

From the review of force plates, it can be seen that, in general, force plates are of two types. In the first category of force plates, instrumented supports in the form of columns, cantilevers or some kind of solid supports were used as base structure and the instrumented support act as tranducers. A single support may carry more than one transducer as seen in Cunningham's[6] force plate. In the second category, the force plate was suspended by strips of metal and tension changes in the elements were used as load sensing devices. Gola's[28] force plate is one such example. In the case of force plates having supports carrying more than one set of transducers the cross-talk between various signals is bound to be large. With a rigid support system the problem is magnified. The rigid support system will also have a reduced sensitivity. In the case of the suspended type of force platforms, the alignment of various transducers is quite critical, especially to minimise cross-talk error.

Provision for fine balancing of the force platform has to be provided. It is not clear from the publications whether such a provision is available in the majority of force plates. The force plates investigated so far have the disadvantage of being small in size and suitable for single step gait analysis. Only that of Yamashita[27] could be calibrated by direct loading of the transducers, but his force plate was capable of measuring only the vertical forces. Following the development of force plates reported in this thesis, the only other accurate force plate allowing direct calibration is the one reported by Gola[28]. All others require either solution of statically indeterminant systems based on several transducer readings from the force plate or need further signal processing.

2.4 Kinematic Measurement Techniques

The methods and variety of kinematic measurement of limb segments are almost endless being limited only by the ingenuity of the researcher and the facilities available to him. Among the many devices used in understanding human motion are goniometers, interrupted light photography, still cameras, normal and high speed motion cameras, TV cameras and x- rays. The majority of studies have used limb displacement measurement for a detailed kinematical analysis. Velocity and acceleration can be deduced from a series of instantaneous displacement measurements. The accuracy with which the latter can be measured and the inherent characteristics of the required process of differentiation have given rise to a number of difficulties. A brief review on the use of motion film cameras and video systems for collecting kinematic information will be

presented in this section.

Chronophotography or interrupted light photography was developed by Marey[13] in 1873. Marey's method utilized a rotating disk with a variable number of apertures placed in front of the shutter of a camera to take successive exposures on a single fixed piece of film. The walking subject wore shiny reflecting buttons and reflecting bands on various segments of the body. A series of pictures were taken of the subject walking and deductions were made about the way the different segments of the body moved. Indirect deduction of forces acting on the body by measuring the three-dimensional space-time relationships of various segments of the body was attempted in 1895 by Fisher[3,36]. A thorough analysis of one subject was made by means of still photographs. Geisler tubes fastened to the body segments flashed intermittently providing markers on the still photographs. The investigation was devoted to the graphic representation of the pathways of human gait. From the pathways, velocities were calculated and by using the velocity information, acceleration and floor pressures were also determined. This procedure, with refinements in analysis, is being followed by several investigators even today. About 20 years after Fisher, Bernstein[37] extended his work and analysed the gait of several normal subjects. Bresler and Frankel[22] in their study of kinematics and kinetics of walking subjects used continously lighted opthalmoscope bulbs as body markers instead of shiny buttons. By exposing a film in a darkened room to the light 30 times a second, they obtained a photograph containing many points of light. With these data points they were able to calculate displacement, velocity, and acceleration of various segments of the leg using graphic

and arithmetic techniques. The disadvantage of the chronophotography was the overlapping images of the body markers at the boundaries of the range of motion.

All of the earlier studies were done assuming coplanar motion and three-dimensional motion studies were not attempted. The techniques described thus far would introduce a large number of constraints on the way in which a subject walked, due to the darkness and the bulky reflectors.

The first major measurement of displacements of the extremities of the human limb was performed by Saunders et. al[38]. A technique different from those reported so far was employed to determine the kinematic information. They used a glass walkway to permit displacement measurement in three planes. An interrupted-light technique similar to that employed by Marey[13] was used. Transverse rotation of limb segments were determined by the use of bone markers. The goal of their study was to relate six major determinants in locomotion. Using the interrupted light technique and an overhead mirror, Murray et. al[39] and Murray[40] listed the range of normal values for 20 simultaneous gait components including the serial displacement patterns of the head, neck, trunk, upper and lower limbs. Examples of abnormal movement patterns of disabled subjects were also investigated.

Cinematography with both normal and high speed motion picture cameras has been one of the most widely used systems of kinematic analysis of motion. After establishment of motion photography as a medium of recording the phases of gait, quantitative investigations on velocity, acceleration and moving forces could be done more easily. Frame-by-frame

analysis of the motion picture film yielded results in the form of composite tracings and stick figures showing the position of body segments at subsequent times in the gait cycle. Using a computer based system, Kasvand et. al[41,42] were able to draw 'stick diagrams' for hip, knee and ankle positions. They employed high speed photography of subjects and limbs were marked with black dots on a white area for each dot. The co-ordinates (x,y) of the various points with reference to a background marker were converted to voltages by reading the output of a photomultiplier with an analogue-to-digital converter. A real-time computer was used for processing the film data. Background markers were not exactly in the same plane as the spots on the subject and whenever the spots were not moving at the same speed as the camera, parallax caused position errors. Following this work a televion-computer system was employed by Winter et. al[43,44] based on an interface developed by Dinn et. al[45]. Some of the difficulties reported by Kasvand et. al[41,42] were corrected. The subject was tracked along the walkway at a range of about 4 meters from the track by a television camera mounted on a tracking cart. Larger markers were chosen to increase the accuracy of their calculated centres. By calculating absolute coordinates of the body markers from determining their positions relative to the background markers, the problem of having to synchronize the speed of camera cart with that of the subject was eliminated. Using this system, a statistical study on the kinematics of normal locomotion was reported. The study reported measurements on a group of normal subjects walking at slow, comfortable and fast candences.

A commercially available system, 'Selspot'[46], uses silicon photosensors capable of transducing the coordinates (in a plane) of light emitting diodes. Multiple locations are tracked by sequentially switching the l.e.d. markers. A computer system is needed for processing the data, and must provide for data storage as well. A somewhat different approach described by Güth et. al[47] operates with photodetectors located on pertinent parts of the body while a v-shaped light pattern scans the object. Information read from the photodiodes enabled the determination of their planar coordinates with the aid of a PDP-8 computer. Andrews and Jarrett[48] developed a multiple camera system interfaced with a PDP-12 computer. The interface stored horizontal and vertical information in a buffer memory. The line synchronised signal then transfers the data into the core memory of the computer. For systems such as the selspot using switched light sources, cable connections to the subject pose problems and are somewhat cumbersome. Brugger and Milner[49] exploited the use of a c.c.d. (charge coupled device) for image sensing in locomotion. The digital nature of c.c.d. devices considerably simplifies the design of the required computer-interface since no analogue-to digital conversion was required for extraction of the data coordinates. A wide range of frame rates, extending from 10 to 300 Hz was possible. The labels or markers attached to the subject need not be point sources and an averaging over the field of the marker is claimed to improve the resolution and hence careful focussing of the camera is not needed. Using the current state-of-the art in the field of microprocessor technology, a microprogrammed processor for locomotion data extraction was built by Slonosky and Shwedyk[50]. A standard, 60 frames/sec., 525 line interlaced Sony video

camera is used as an opitical sensor to obtain data points. The system has a sampler which collects and stores a frame of sampled data and the processor processes the sampled data to compute the marker coordinates. The system is capable of storing data for up to 25 markers (body or reference). There are two sample memories, each 1K x 16 bits in size. The system has not yet been interfaced for use in locomotion data acquisition.

As is evident from the review, the basic ideas concerning capture of motions of the body is by no means a product of this decade, even though advances have hinged upon several technological developments and innovations particularly over the last century. The practicalities and economics of particular situations have dictated the method of data capture. Digital processing would be of considerable help in the analysis of various complex aspects associated with human gait. Most of the studies reported so far have assumed symmetry in motion and measurements in the sagittal plane have proved to be adequate. In the case of pathological gait studies, three-dimensional kinematic measurements will be needed to describe the complete motion and the recording system must be able to perceive the marked body locations in three dimensions at all times. The systems used to analyse the motions must monitor certain assumptions usually made, such as: a) plane of photography sufficiently approximates or models the spatial motion b) the spatial orientation of the plane of photography must be able to be known at all times.

In the case of disrupted gait with unsymmetrical motions in space, multiple cameras have to be used for tracking the motions. The optical axes of the cameras may be perpendicular and must intersect at a common point. An additional difficulty of most multiple camera techniques is the

requirement of the filming of the landmarks or targets by all cameras for determining the three coordinates. Because of the solid, irregular and opaque nature of the human body segments, the same landmark or target may not be seen at all times by both the cameras. Solutions for such problems will have to be developed.

2.5 Joint Model

According to the physiological functions and anatomical constraints of human limb joints, different types of mechanical joint analogs have been assumed by different investigators. The mechanical equivalents for each joint, its degree of freedom and the associated unknown constraint forces and moments have resulted in different kinds of joint models. In each articulating human joint, a total of six degrees of freedom exist to some extent. However, the anatomists have a different understanding of 'degrees of freedom'; Steindler[72] and MacConaill[73] imply that three degrees of freedom is the maximum number required for anatomical motion. The following classification is made according to the order of increasing complexity.

A hinge or revolute joint is probably the most widely used articulating joint model and has a single degree of freedom. The motion between two articulated body segments is assumed to be a hinge type, when the motion is characterized by rotation about a single axis fixed in one of the segments. Thus, only one independent coordinate, i.e. the angle formed between two reference lines inscribed on the segments, is sufficient to determine the position of one segment with reference to the other one. Some representative publications assuming hinge joint models

have been written by Saunders et. al[38] and Beckett and Chang[74].

A spherical model is the next widely used joint approximation in investigations reported in the literature. There are two versions of the spherical joint and both have two degrees of freedom. In the first version of the model marked I in Fig. 4, the limbs are rotated about origin O. The motion is determined by two independent angles ϕ and θ and the axial rotation ψ is assumed to be zero. In the second version of a spherical joint, marked II in Fig. 4, the axial rotation is allowed but the motion is restricted to a plane passing through the center of the sphere. In Fig. 4 the slot defined by angle 'ϕ' refers to the plane in which motion is restricted.

The first version of the spherical joint model was used by Paul[56] for the hip. The knee joint was modelled in this way by Bresler and Frankel[22], Eberhart and Inman[75] and Morrison[76]. The second version of spherical joint has been primarily used for the elbow by Taylor and Blaschke[77], Dempster[78] and for the knee by Dempster[78].

The socket joint has three degrees of freedom and is most frequently used for modelling hip and shoulder joints. The motion is characterized as shown in Fig. 4 (marked III) by the independent coordinates ψ, θ and ϕ. Dempster [78], Chao[79] have used this type of joint in their investigations.

A planar joint has been used less widely. Such a type of joint permits motion of the instantaneous axes which are always normal to the plane of motion. The primary application for planar joint models has been in modelling the knee joint, Radcliffe[81], Smidt[82] and Burstein and Frankel[83].

A rather complicated joint model possessing six degrees of freedom is the general joint. This joint model allows all possible motions between the segments of the body. A good application for this joint is the shoulder joint. Thompson[84] developed a mechanical linkage system capable of monitoring the lengths of six links connected via ball and socket joints to the femur and the tibia for the purpose of studying motion of the human knee.

The joint models with one degree of freedom are restricted in applicability to single plane motion studies. The three degree of freedom joint models allow a more general representation of the movements involved in human locomotion. The six degree of freedom models are probably very specialised and the complexity involved in designing the special instrumentation needed for tracking the motions generally prohibits their application to clinical studies. A good joint model must permit analysis of the dynamic motions and the selection must be such as to allow the quantification of the articulated total body motion at the given joint.

2.6 Human Locomotion Models

The data gathering techniques reviewed in the previous sections resulted in the development of mathematical models of various degrees of complexity to explain the complex motions associated with human gait. The study of locomotion has gone through a long and colorful history of fitful development. As contrasted to experimental investigation, the rational approach entails the development of dynamic models with varying degrees of detail and sophistication. Locomotion models described in the literature can be broadly classified into two categories. The basis behind all the

models was to visualize the human body as being composed of several segments (or links) to represent the various limbs. The links are joined together at joints having specified degrees of freedom ranging up to six. In the first category of models, the applied forces and moments at limb joints were computed from known limb kinematics (obtained from laboratory measurements). In the second category, the model gives a solution for the motion (system response) from joint moments (system inputs). The first category of models are sometimes referred to as representing the Inverse dynamic problem and the second type, the Direct dynamic problem.

Mathematical and anatomical analysis of human body motion started as early as 1898. Fischer, (a mathematician) in cooperation with Braune an anatomist, investigated the kinetic properties of different segments of the human body[51,52]. Using the chronophotographic methods developed by Marey[13], Fischer and Braune used classical approaches of mechanics in deriving their analysis. Bernstein[37] extended Fischer's work and concluded that the complexity of locomotion would preclude the smoothing out of any data (raw data as obtained from filming the subject's movement). Much of this pioneering work was aimed at locating the centers of gravity of the various segments, their radii of gyration and the relative masses. Elftman[53,54] proposed a methodology for determining instantaneous values of the forces and torques at the joints in lower limb. The transfer of energy within the leg and between the leg and the rest of the body was followed by means of activity of these forces and torques. Elftman improved Fischer's work by determining the reaction forces at the foot through the use of his force plate[19]. He, however could not solve the hip joint forces. Elftman's analytical work was

largely dormant until 1952 when Bresler and Frankel[22] reported their investigation on the joint forces and moments in the leg during level walking. The principle of dynamic equilibrium of bodies while in motion was used for the analysis. The internal forces or moments at the joints were expressed directly in terms of reaction forces, gravity forces and inertial forces. The mass moment of inertia of the lower extremity for each subject analysed was determined experimentally. Calculations of the mass, centroid location and moment of inertia of the combined shank and foot were made using methods outlined by Fischer[51] and Weinbach[55]. Cunningham's force plate[6] provided the necessary ground-reaction forces measurement. The kinematics of limb segments was obtained by biplane photography. Bresler's work was probably the most exhaustive up to that time and was the first to combine the three dimensional kinetics and kinematics for human locomotion modelling.

A technique for assessment of magnitude and direction of the resultant forces transmitted at joints in the human body was investigated by Paul[56]. Assuming mass properties, as reported in Braune and Fischer's[52] work, Paul proposed equilibrium equations at each joint. The moment actions at each joint were assumed to be transmitted by the development of tension in muscular or ligamentous connections crossing each joint and the corresponding reaction at that joint. The ground reaction force measured by a force plate and photographic records provided the kinetic and kinematic input for his model. The number of muscular or ligamentous connections at any joint in the human body exceeds the number of available equilibrium equations and a guide to the muscles which are acting at any instant of time has to be obtained by electro-myography.

Even with this information an explicit solution is generally not possible. Only resultant actions can be analysed by making use of approximations.

The various developments in image analysis briefly described in section 2.4 provided a plethora of kinematic information to be applied to many aspects of biomechanics of walking. These data range from investigations of the trajectories of limb segments, which are fairly straightforward, to considerations of segment energies and energy transfers across joints. An analysis of the energy components of human gait in the sagittal plane was investigated by Quanbury et. al[57] and Winter et. al[58]. The trajectory in absolute coordinates of anatomical markers fixed to the body was obtained using a TV-computer system[42]. From the coordinate data, angles between various limb segments were computed along with the velocity and accelerations. The location of the center of mass of each segment was determined from anthropometric tables developed by Contini[59]. Inter-segment forces and floor reaction forces in the sagittal plane, as well as the instantaneous energy of the shank foot combination, were determined from kinematic and anthropometric information.

A computer analysis of gait data to predict floor reaction forces from the translational and angular accelerations during normal locomotion was performed by Thornton-Trump and Daher[60]. It was shown that the phase of the head-arms-trunk system with respect to the hip-thigh-shank system was important in determining hip moments.

With the developement of load carrying tripod walkers and robots, models developed for biped machines are being applied to the study of locomotion. An approach to the design of a biped machine was investigated

by Frank[61]. The design criteria was to achieve minimum energy while maintaining stability, which is similar to the energy efficient motion that the human body tries to achieve in any kind of locomotion. Frank modelled his system with a rigid upper body mass having three principle axes of inertia. The upper body was attached to two legs of zero mass. The leg was capable of supplying a force between the body attachment point and the contact point on the ground. A ball joint, capable of supplying torques about three independent axes, connected the body and the leg. The object of the investigation was to evolve control strategies for attaining stable, straight-line motion without any lateral sway. Rotation about three angular axes and propulsion distance in the forward direction were used as control parameters. Synchronous switching between the two legs was assumed as against an asynchronous system. Man's decision to switch load from one leg to another is probably dependent upon his body state and would have to be treated as an asynchronous system. Being synchronous, Frank's model will be limited to the analysis of biped synchronous machines.

Many living organisms which move with legs exhibit a property of movement repeatability during different forms of locomotion[62]. This is especially noticeable for locomotion at a constant velocity over a level surface, e.g. jogging. Some kind of regulation mechanisms must exist in these living organisms to maintain these conditions of repeatability. Vukobratovic et. al[63] described a method for the analysis of such systems in dynamic equilibrium. They assumed that the dynamic equilibrium in a legged locomotion system coincides with the conditions of repeatability and hence conditions of repeatability were assumed to

represent a set of necessary conditions for dynamic equilibrium. A control system comprising of a force controller and a position controller was used by Vukabratovic et. al to maintain the conditions of repeatability of the system. In brief, the force controller supplies the force, independent of the position of the controlled element, while the position controller holds a position independent of the force applied to the controlled element. A set of differential equations for motion of the system with the imposed regime of repeatability was proposed by Vukobratovic et. al.

A general theory for the analysis and synthesis of bipedal locomotion was the object of a study by Townsend and Seireg[64]. Their model consisted of a rigid upper body with massless, extensible legs. General equations of motion for the biped machine were proposed by Townsend. The model was subjected to motion criteria such as maximised stability and minimum energy expenditure. Stability was defined in terms of foot print size (obtained by calculating the center of pressure under the feet). Relationships for calculating machine work and physiological work were proposed and were used for calculating an efficiency factor. The efficiency factor indirectly quantifies energy expenditure. Various body trajectories were analysed for optimum performance of the model. The model does not take into account pelvic rotation with respect to upper body and upper body rotation was assumed to represent the total body rotation. In human locomotion the rotations of various segments of the body are not synchronized and overall stability of the body is brought about by the synthesis of motions in the various segments of the body.

In recent years, human locomotion is being analysed using various disciplines of science. The basic principle of energy efficient motion has prompted optimization techniques as a tool for analysing the motions. Chow and Kim[65] used the principle of optimization and, in their analysis, the joint moments were iteratively varied until the theoretical displacements matched those measured in the laboratory. The model was only capable of motion in the sagittal plane, with the upper body mass lumped at the hip and the lower limb modelled as a stick with pin joints at the various joint locations.

A simpler approach to the control of upper body in a biped locomotion system was proposed by Yamashita and Yamada[66]. The model was analysed by taking into consideration the frictional force between the ground and foot. The body force and moment vectors in the leg supporting phase were related to the control force and moments defined in the leg coordinate system. The variability in step length together with the hip moments, defined in leg coordinates were used, as control parameters for producing a rotation free upper body. An upper body which was free of rotation was assumed to have maximum stability. The analysis in their work was modified to include an extensible leg[67,68]. A prescribed motion in the form of a sinusoidal displacement at the hip joint was used as the model input in all their analyses.

In sports, dance or rehabilitation work it is important to know which appropriate combination of body-segment movements would accomplish a desired function. The models reviewed so far have used three segments to represent the human body. With the ever increasing application of high speed computers to movement analysis, researchers are attempting the

application of more complex models for human locomotion. Yamashita and Tagawa[69] have investigated a multi-segment model with two body elements (upper and lower torso) and three segments to represent a massless thigh, shank and foot. The body was permitted movement in three dimensional space. By applying principles of mechanics, the balancing equations for moments and forces have been derived for each element. Since the number of unknown variables exceeds the number of equations, a predetermined motion was applied to the lower torso to simulate the motion of the pelvis. The forward speed of the hip was assumed constant and the lower torso was subjected to sinusoidal oscillation in the vertical and lateral planes. The computer simulation allowed variation of parameters associated with human movement and the response of the system was determined in terms of joint moments and forces. The analysis uses the body fixed coordinate system for defining rotations of the segments. The rotation angles have been assumed to be small and the transformation matrices use the small angle approximation to determine the rotation matrix.

A seven segment model to represent a human body has been proposed by Onyshko and Winter[70]. The head, arms and trunk [HAT] are represented as one segment and six joints - one at each of the hip; knee and ankle characterised their model. Using limb angles as the variables, the Lagrangian equations of motion for the body were determined. The stance and swing phase were analysed using two different mathematical representations. To ease the complexity of the constraint equations, a spring and damper coupling was used to represent the connection between the right thigh, left thigh and upper body. The response of the proposed

model was studied for a prescribed initial condition in the form of angular displacements and velocities of the limbs and joint moments were used as system input. The model was tested with several existing records on such variables. In comparison to other segment models, the above analysis did not assume any prescribed trajectory for motion of various limbs. The model would permit investigator interaction to predict the trajectories resulting from any pattern of joint muscle moments. In the present form the model can be used for motions in the sagittal plane only.

A nine segment model was developed by Ramey and Yang[71]. The segments consisted of a head and torso, upper arm, lower arm on each side and the leg and foot in each lower limb. The upper arm and thigh were connected to the main body by ball and socket joints and the lower arm and leg were connected to their respective upper limbs by simple hinge joints. The equations of motions associated with a torque-free motion were developed along with the necessary transformation technique to define the known quantities in their appropriate frame of reference. The model was used to simulate hitch-kick and somersault and long jump motions.

The multi-dimensional, multi-directional movement device, namely the human body has been modelled as being a collection of interconnected rigid-body segments for developing appropriate equations of motion. The function of the body may be to walk in a normal pattern and, in the case of certain sports activity, it might mean to jump higher while maintaining a striking pose. The wide spectrum of studies reviewed show the various approaches used in gait studies. Some of the models impose a predetermined trajectory, mostly a sinusoidal displacement pattern at the

hip level. This input trajectory was based on the pattern observed in normal locomotion. Such an imposition, however, may not be valid for pathological gait studies. The aspect of symmetry is also not likely to be present in abnormal gait as pointed out earlier, and asymmetry in gait can be observed in motions in the frontal plane as well as the sagittal plane. A model for abnormal gait movements should have no trajectory constraints and should permit analysis of even undesired locomotion patterns. Use of optimization techniques in computing moments at joints alters the problem from one of pure synthesis to one of curve fitting the limb displacement histories.

Description of quantities associated with gait in the appropriate frame of reference would be closer to the physiological conditions of limb movements and muscle activity. Even though the use of body coordinates for defining movements has been attempted by a few, the assumption of small angle theory and vectorial addition of rotation angles to obtain the necessary rotation matrices is only valid for the analysis of biped machines which meet those assumptions. The human body exibits large rotations of the body segments, especially in pathological gait conditions, thus theory must be modified.

As a result of reviewing the literature on force plates, it was determined that a large force plate with good accuracy in the measurement of shear force was needed. Ideally, such a plate would be statically determinate and directly calibratable in each direction. The size of such a plate is desired to be large enough to allow subjects with pathological gait and/or aids to be wholly on the plate during a full gait cycle. The development of such a plate is one of the objectives of the current

investigation and is described in the following chapters.

The mere measurement of forces, however, does not add greatly to the ability of a clinician to quantify gait characteristics in terms of normal gait. As is apparent in the survey of the literature, much researched effort has gone into mathematical models describing the motions of limbs during locomotion. However, none of the models appear general enough to accept the large asymetrical motions of pathological gait. In general, parameters of symmetry which would relate reaction forces as measured by force plates and asymetrical characteristics of pathological gait appear undeveloped. It is the purpose of this work to relate the measured reaction force patterns to the upper body motions using the principles of impulse and momentum and also to express force and moment equilibrium in body coordinates, thereby developing simple parameters to allow a clinician greater ease in quantifying pathological gait. To accomplish this relationship, large angle transformation matrices to convert data into body coordinate systems are applied to models of the body motions. These transformed results are related to the simultaneously measured force traces and the appropriate parameters developed. The meaning of the parameters is thus explained in terms of the net body segment geometry changes necessary to produce the reaction force parameters measured.

CHAPTER 3

DESCRIPTION OF DEVELOPED FORCE PLATE

3.1 Introduction

The role of force plates in the study of human locomotion has been described in the previous chapter. It was noted that in the act of walking the magnitude and direction of the force exerted on the ground by each foot varies with time. When this force is resolved into three mutually perpendicular components, the variations in each of these components may be represented by time functions. This force pattern, peculiar to each individual, is characteristic of the gait. One device that would help record such information on force patterns is a force plate.

3.2 Design Criteria for a Force Plate

From the review of force plates described in section 2.3, various force plates have used the principle of instrumented supports for detecting the ground-reaction components and this seems to be the most practical way from the viewpoint of instrumentation. The statical determinacy or indeterminacy of a structure is dependent on the number of unknown support reaction forces or moments. A statically determinate structure is preferable in view of the reduced algorithms needed in order to obtain the total reaction forces in the structure. By monitoring the individual components of support reactions, the non-linearity and cross-talk among the various signals if any, (as could happen in the case of

rigidly supported platforms carrying more than one set of transducers) could be checked and corrected.

A majority of investigators have used their force plates for the analysis of normal locomotion in the sagittal plane only. The variations in medio-lateral force components have been assumed to be very small and an accurate measurement of this component was not considered. In the case of abnormal gait, the movements in the other planes of motion are bound to be larger than what is normally present. Hence an accurate measurement of all the components of ground reactions should be obtained for a proper understanding of abnormal gait. The force platforms described in the literature are also very small and the subjects have to adjust their cadence in order to step on the force plate. This would impose a constraint on the subject's gait.

The present design is an attempt at the development of a force plate large enough to accommodate the cadence of many types of abnormal gait normally encountered by the clinician. The design would also aim at the accurate measurement of all the components of ground-reactions with a reduced level of cross-talk. From the dynamic point of view, a larger force plate would tend to reduce the fundamental natural frequency of the system and the measurements obtained will be affected. Hence the present design would attempt to keep the fundamental natural frequency well above the measurement range.

3.2.1 Layout of the Force Plate

The force plate developed is right isosceles triangle in shape (Fig. 5) and has a base length of 7'11" and a width from vertex to

hypotenuse of 3' 11 1/2". The force plate weights 110 lbs. The base structure of the force plate is made of several lengths of 2" x 1" x 1/4" mild steel channels welded together to form an open steel truss. A 3/4" particle board sheet, cut to the dimensions of the truss, is bolted to the top of the truss and forms a smooth walking surface. The truss provides flexural rigidity for the force plate. The walkway has approach walkways, 20 feet long on either side of the force platform[Fig. 5].

3.2.2 Suspension System

The force plate developed belongs to the class of the suspended type, where the force plate is hung from a solid support instead of resting on solid support. The suspended type was preferred because it is possible to use as transducers thin steel sections on which strain gauges are mounted. By using this method, it is possible to get comparatively large output signals and this improves the sensitivity. The force plate uses a unique suspension system and the description of the various elements will be presented in this section.

The three corners of the triangular truss of the force plate have steel blocks fixed to them. A threaded hole 5/8" in dia. runs through the center line of the block from top to bottom. The spatial orientation of the suspension elements will be defined with respect to a coordinate axis fixed to the center line of the force plate[Fig. 5]. The force plate has five suspension elements, one at the apex 'B' of the triangular frame, two at the leading corner 'A' of the triangle and two at the trailing corner, 'C'. All the suspension elements to be described in detail, have one end rigidly fixed to the force plate.

The three vertical suspension elements (A, B and C in Fig. 5) are machined to specific dimensions and are identical in all dimensions. The narrow central section of each vertical suspension (Fig. 6) element was machined to precision (± 0.001mms). One end of the vertical suspension element has threads to match the threaded hole in the steel block and the other end is provided with a adjustable suspension hook. Each vertical suspension element is screwed to the corresponding steel block and acts as a solid connector between the force plate and the solid support. Three vertical steel pipes of 2 1/16" inside diameter, 1/8" wall thickness and 29" long are used as solid supports for suspending the force plate. The pipes at corners A and C are fixed to a frame work and the frame is rigidly connected to the floor. The vertical pipe at corner B is fixed to a rigid solid base. All the three pipes are capable of fine rotations about their vertical axis for very fine alignment of the force plate. The alignment procedure will be discussed in a later section. A short length (approx. 4 1/2") of horizontal tubing welded to the top end of each support pipe carries a suspension system as well. The force plate is hung from the horizontal pipes by means of a short length of high tensile steel wire (0.06" dia.). One end of the wire loops over the anchor bolts provided in the vertical suspension elements and the other end is connected to the pipe through the suspension hook in the pipe. The weight of the force plate is distributed equally among the three vertical supports due to the geometrical symmetry of the suspension.
The suspension arrangement in all the vertical elements allows finer control of the length of the wire and this enables proper levelling of the force plate.

The stability of the force plate in the hortizontal plane was provided by the suspension elements 'd' and 'e'. The suspension elements 'd' and 'e' are square in section (0.5" x 0.5") and 2" long. One end is threaded into the steel blocks at corners A and C respectively. The vertical axis of suspension element 'a' and 'd' and that of 'c' and 'e' coincide and project on opposite sides of the force plate. The free end of suspension element'd' has a short threaded section and a grip nut (Fig. 6). Just at the top end of the threaded section two small holes are drilled. The holes intersect each other at right angles and run through the body of the horizontal suspension element. High strength tensile wires similar to those used in the vertical support system pass through these holes and are connected to tension devices provided on the support frame on each side of the element. A photograph of the force plate and the suspension systems is shown in Fig. 8. The grip nut on the two horizontal suspension elements fastens the horizontal tension wires to the suspension element. The two horizontal wires at corner 'A' are parallel to the x and y axes respectively of the force plate. The tension devices on the support frame can be moved up and down for proper levelling of the horizontal tension wires. The tension in the wires is also adjustable, and the tension controls the sensitivity and cross-talk. This will be described under calibration procedure. The suspension element 'e' at corner 'c' is exactly identical to the suspension element 'd' except it has only one tension wire running through it along the y axis.

The structural action of the various suspension elements can be modelled as follows. The three vertical suspension elements will act as point ball joints at the point of connection of the support frame to the

high tensile wire and any vertical load will be transmitted as axial load to the suspension elements. Changes in the axial strain can be taken as directly proportional to the changes in the vertical load. The three vertical suspension elements give rise to three measureable forces in the vertical direction. The suspension element 'd' at corner 'A' is held in space at its lower end by means of the tension wires. This anchored end structurally behaves as a bi-directional hinge joint and the two reaction forces in the X and Y directions will contribute to two more unknown but measurable forces in the system. The forces will be proportional to the appropriate bending strain in the suspension system. The suspension element 'e' can also be modelled as a hinge in the y direction and the force in that direction will constitute the sixth unknown but measureable force. The unknowns in this mechanical system are the magnitudes of the forces in the six hinge joints described above and their number equals the degrees of freedom of the force plate. Thus, the force plate is reduced to a statically determinate structure.

3.2.3 Force Detection

In order to measure the forces exerted by the subject walking on the force platform, strain gauges positioned in the suspension elements were utilized. The strain gauges in the vertical suspension elements respond only to the axial strains produced during load changes while the strain gauges in the horizontal suspension elements respond only to the bending strain produced about the appropriate axis during load changes.

The two opposite faces of the vertical suspension element [Fig. 6] have carefully machined flat surfaces and carry a resistance type wire

strain gauge on each of the vertical faces. The longitudinal axis of the strain gauge lies parallel to the axis of the suspension element. Thus the two strain gauges will respond to changes in axial strain. The substrate carries two more gauges which are inactive to strains and are used for temperature compensation. The compensation gauges are orientated in the lateral direction and, hence, will be insensitive to axial strains. The four gauges used in each vertical suspension element are connected to the four arms of a wheatstone bridge. Due to the point ball, joint action of the suspension wire, the vertical suspension elements will not be subjected to any measureable bending moment for the displacements caused by anticipated forces. As an extra measure to improve the sensitivity of the vertical force transducer, the two active gauges are connected to the diagonally opposite arms of the wheatstone's network and this improves the sensitivity of the transducer to axial strain and, at the same time, renders it insensitive to any bending strain. The strain bridge configuration is shown in Fig. 9.

The horizontal force component detection transducer works on the principle of measuring the strain produced due to bending on the suspension elements 'd' and 'e'. Suspension element 'd' carries four gauges, one on each of the vertical faces [Fig. 7]. Each set of gauges on opposite faces are perpendicular to the tension wires and any lateral shear force applied to the force plate, results in a bending of the suspension element. The gauges in the YZ plane measure the bending strain produced due to longitudinal shear force (X-component) and gauges in the XZ plane measure the bending strain produced due to lateral force along the Y-axis (Y-component). Suspension element 'e' carries just two active

gauges on faces in the XZ plane and is constrained in the Y-direction only. Thus the bending strain produced due to lateral force in element 'e' is measured by these two gauges. The gauges in elements 'd' and 'e' are connected to the arms of a wheatstone bridge with two compensation gauges in each network. The elements are made insensitive to axial strains by connecting the two active gauges to the upper arms of the bridge. The horizontal strain bridge configuration is shown in Fig. 10.

3.2.4 Force Detection Instrumentation

A simple representation of the ground-reaction force resulting from a subject stepping on the force plate is shown in Fig. 11. The ground-reaction force vector is resolved into components in the three orthogonal directions by the force transducers described previously. These components are: i) F_X (referred to as longitudinal or posterior-anterior or fore-aft shear force), ii) F_Y (lateral or medio-lateral or right-left shear force) and iii) F_Z (the vertical force component). The instrumentation to be described will measure these three reaction components as the subject traverses the force plate. For this purpose, each of the suspension elements of the force plate with strain gauges mounted to their substrate was designed to function as a transducer. The total vertical reaction force distributes itself among the three vertical suspension elements 'a', 'b' and 'c'. The distribution of these reaction forces depends on the position or point of application of the external force on the force plate. If the external force is applied at the centroid of the force plate, the three vertical suspension element

reaction forces will be equal in magnitude. In a similar way, the horizontal force component F_Y is distributed between the two suspension elements 'd' and 'e' and the horizontal force component F_X is carried wholly by the suspension element 'd'. The strain gauge networks on each suspension element is connected to six individual strain bridge amplifiers. A regulated D.C. supply (5 Volts) is used for excitation of strain bridges. Each bridge amplifier has a balancing potentiometer and built in instrumentation amplifiers with variable gain controls. The six analog amplifiers containing the circuitary for bridge excitation, balancing, calibration and scaling are shown in Fig. 12. The analog amplifiers convert the strain level in each bridge to proportional electrical outputs and, by proper calibration, the electrical outputs will represent the force of each suspension element. The procedure for calibration of force plate is explained in a subsequent section. Each transducer measures the force applied to the corresponding suspension element in one of the coordinate axes and further processing of the signals is needed to get the total reaction-force component. If V_a, V_b and V_c represent the outputs of transducers 'a', 'b' and 'c', proportional to loads F_{Za}, F_{Zb} and F_{Zc} carried by each vertical transducer respectively, the total output for the resultant vertical load will be a sum of these three outputs.

$$V_{Total} = V_a + V_b + V_c \qquad - \quad 3.2.4.1.$$

The V_{Total} is proportional to the resultant vertical load on the force plate. In the same way, if M_1 represents the output of horizontal

transducer 'd' corresponding to a lateral load F_{Ya} at corner A and M_3, the output of transducer 'e' corresponding to a lateral load F_{Yc} at corner 'c' the resultant output will give the total lateral force on the force plate.

$$M_{Total} = M_1 + M_3 \qquad - \ 3.2.4.2$$

Hence, M_{Total} is proportional to the resultant mediolateral force F_Y.

The longitudinal load (X-direction) on the force plate is entirely carried by the suspension element 'd'. This element will give a signal proportional to the total fore-aft shear force on the plate.

$$H_{longitudinal} \ (H_x) = H_{x_c} \qquad - \ 3.2.4.3$$

A set of operational amplifiers are used for processing the individual outputs and the schematic diagram in Fig. 13 represents the scheme followed.

3.2.5 Alignment and Calibration of Force Plate

The force plate developed uses a suspension system that is unique in force plate design. The three dimensional hinge behaviour of each suspension system allows the function of each transducer to be independent of one another and structurally connected to the force plate through the suspension wires. After trying several types of suspension devices, the present hinge system was evolved. The geometrical arrangement of suspension systems allow them to be sensitive to force actions in one direction only. The flexible coupling in the form of a wire suspension provides a frictionless joint between the force plate and the supporting structure. This allowed the transducers to be very sensitive to small variations in the loads. In the case of vertical suspension elements, the

pin coupling between the wires and the suspension elements provide a pin joint. In the case of horizontal suspension elements, the pre-tension in the wires always keeps the wires on either side of the suspension element in tension and does not permit any displacement of the elements in that direction. The long length of wire allows free deflection of the suspension elements for loads in the vertical direction in the measurement range. The suspension system with the various transducers separated from one another was expected to reduce the cross-talk considerably. The structural action of each transducer would also permit direct interpretation of outputs of each transducer in terms of forces. Above all, the force plate could be easily calibrated by monitoring the individual support reactions. This was a direct advantage of making the structure statically determinate.

The geometrical arrangement of each suspension element being important for the performance of the force plate necessitates a precise alignment of the various elements of the force plate. The basic requirement for alignment of the force plate is the accurate orientation of each transducer in the respective direction of load action. The axes of the transducers should coincide with the line of action of the support reaction in the case of a vertical transducer and should be perpendicular in the case of horizontal load sensors. The plane of the substrates containing the strain gauges should be parallel to the reference XZ or YZ plane depending on the force component they are measuring. A systematic alignment procedure was carried out as follows; the force plate was relieved of its horizontal suspension wires by loosening the grip nut provided at the tip of suspension elements 'd' and 'e'. This way the

force plate is free to move horizontally in space and hangs from the three vertical transducers. The force plate is in perfect alignment in the vertical plane if the axes of the three transducers a, b and c coincide with the point of suspension on the respective vertical supports. In order to avoid a very large mismatch in the vertical alignment, precaution was taken at the fabrication stage to transfer the point of suspension on to the laboratory floor and orientate the support frame close to a final alignment. The smaller deviations in the vertical alignment were then corrected by rotating each vertical support about its vertical axis. The second step involved alignment of the X and Y reference axes fixed to the force plate. When aligned, they should be parallel to the floor. In order to achieve this requirement, levelling of the top surface of the force plate is carried out similar to the three point levelling procedure commonly adopted in survey instruments. The length of the three vertical suspension wires can be varied to lift the force plate at any of the three corners. The balancing procedures outlined above bring about a proper alignment of the reference coordinate system fixed to the centroid of the force plate along with the vertical suspension elements. Finally the alignment of the two horizontal suspension elements 'd' and 'e' with respect to the reference frame is carried out as follows. The three axes of the suspension elements 'd' and 'e' should be made parallel to the reference axes and the three horizontal suspension wires attached to the suspension elements should also be in a horizontal plane and parallel to the measurement axes. The horizontal suspension elements can be rotated about their vertical axes and this would enable orientation of the axes of the suspension elements. The tension wires are also brought into proper

orientation by moving the anchor blocks provided in the support frame, to which, they are attached. At the completion of the alignment procedure, the various suspension elements are firmly secured to the respective support structures and the force plate can be calibrated for force measurements.

A predetermined tension (arrived at on the basis of maximum expected load) is applied to the horizontal tension wires prior to calibration. To calibrate the force plate in the vertical direction, the calibration rig shown in Fig. 8 is used. The vertical calibration rig (A in Fig. 8) is a horizontal beam pivoted at one end to a rigid support and carries a movable collar. The movable collar transfers the load to the force plate. The other end of the beam has a hook from which known static loads can be hung. Graduations on the beam would give the position of the collar and hence the load transferred to the force plate can be calculated. The collar is moved over the centroid of the force plate and known loads are applied to the end of the beam. The reaction load at the centroid distributes itself equally among the three vertical supports. The gain control on each vertical bridge amplifier is adjusted to a predetermined output. The individual vertical amplifiers should have the same output for any load applied at the centroid. For the present study, the gain factor was set at 10 millivolts/lbf. Since the weight of the force plate distributes itself equally among the three vertical transducers, the d.c. offset on each vertical amplifier is adjusted to produce a null output for zero external load on the force plate. The calibration curve for the vertical transducer is shown in Fig. 14 and 15.

The principle involved in calibrating the horizontal transducers is very similar to the calibration in the vertical direction. Loads to represent lateral shear and longitudinal shear are applied to the X and Y direction of the force plate using a calibration frame (B in Fig. 8). Variable gain controls on each strain bridge amplifier can be adjusted to set desired output in both the horizontal directions. The calibration curve is shown in Fig. 16.

3.2.6 Dynamic Response of the Force Plate

The natural frequency of the force plate was obtained experimentally. A vertical load of 250 lbs was applied to the centroid of the force plate using the calibration rig 'A' in Fig. 8. The calibration rig was modified to enable a quick release of this load from the force plate. The sudden release of the load (achieved by cutting a string attached to the calibration arm) would represent a step load on the force plate. The output from the force transducers was recorded on a storage scope and Fig. 17 represents one such trace. The abscissa represents time and the ordinate corresponds to the vertical load on the force plate. From an initial load of 250 lbs, the plate response to the step load was recorded by releasing the load. From the response trace shown in Fig. 17, the fundamental natural frequency was calculated by obtaining the mean period for ten consecutive peaks in the trace shown in Fig. 17. A fundamental natural frequency of 17.22 HZ was obtained using this method. A similar procedure was adopted for determining the dynamic response in the horizontal direction. The plate was loaded in the horizontal direction using the calibration frame 'B', shown in Fig. 8. The plate

response was obtained by suddenly releasing the load. The fundamental natural frequency in the lateral direction was measured and found to be 16.1 HZ. A further check was done by applying oscillatory loads for frequencies of up to 5 HZ at the centroid of the force plate. The output from a load cell interposed between the loading frame and force plate output was recorded simultaneously. The output from the two followed closely.

3.2.7 Center of Force Detection

The concept of center of pressure has been used in the studies of locomotion to describe normal and pathological gait (Cunningham [6], Grundy et. al[24], Yamashita et. al[27]). The center of force at any instant during foot-ground contact is the projection of the centroid of the vertical force distribution on the ground plane. In effect, it is the location where the resultant force vector would act if it could be considered to have a single point of application. The present study does not use the center of force as a major determinant in the analysis, rather the coordinates of the point of application of the ground to foot vector as measured by the force plate, were used in conjunction with the foot-ground contact point established from biplane motion pictures for determining the lower limb displacement.

To locate the center of force application requires that the force be located in the longitudinal and lateral direction of the force plate with respect to a reference point. With reference to Fig. 18, using the apex of the triangular plate as an origin and assuming a known force acting at an unknown point (x,y) on the force plate (Fig. 18), the unknown coordinates 'x' and 'y' can be determined by measuring the reactive

components at the three vertices of the force plate. The following procedure could then be employed.

$$F = F_{Z_a} + F_{Z_b} + F_{Z_c} \quad - \quad 3.2.7.1$$

where F_{Z_a}, F_{Z_b} and F_{Z_c} are the three vertical forces at the plate vertices obtained from the three vertical transducers.

Taking moments about the sides BC and BA (Fig. 18) of the force plate,

$$x = \frac{F_{Z_a}}{F} \cdot L \quad - \quad 3.2.7.2$$

$$y = \frac{F_{Z_c}}{F} \cdot L \quad - \quad 3.2.7.3$$

where L is the length of side AB of the force plate.

By measuring the reactive force components at the corners of the force plate, as described in previous sections of this chapter, the point of force application during walking can be determined as a function of time. The point of application of force was used only to a limited extent in the study reported in this thesis. The center of force obtained for a single step and double step stride is also represented by dots in Fig. 18. Fig. 19 represents the trace of center of the force as determined by the force plate for a roller skater executing a 'spin' while on the force plate. Figure 19 also shows the center of force for a load rolled along the sides of the force plate. The center of force was used in a study pertaining to forces generated for different maneuvers in roller skating, Balakrishnan and Thornton-Trump[34]. The performance characteristics of the force plate developed is presented in Table 1. The performance evaluation of the force plate developed in comparison to other force plates reported in literature will be discussed in Chapter 6.

CHAPTER 4

THERETICAL CONSIDERATIONS AND MATHEMATICAL MODELLING

4.1 Background to Modelling

Having developed a force plate capable of accurate measurement of the ground reaction force in the space coordinate axes, a mathematical model relating reaction force information to body segment position in three dimensional space is required if the reaction forces are to be given reasonable interpretation. Such a three dimensional model was not available and the development of one such model is described in this Chapter.

The model must have general parameters to allow reaction force data to be related to the upper body posture. It is the common procedure to define motions and related physical quantities about a general Newtonian reference frame. It would be more appropriate for human locomotion to relate the motions to the joint structure of the body. The joint angulation represents in some way the pain-free posture of the various body segments and would also retain a constant relationship to the point of origin and insertion of muscle groups. One method of representing the joint angulation would be to define a body centered co-ordinate system that moves with the segment. The mathematical model developed in this chapter has the above required feature as well as features similar to those encompassed by other models developed previously.

One of the valuable biomechanical variables to consider for the assessment of any human movement is the history of the moments and forces at each joint. The net effect of all agonist and antagonist muscle

activity of the body is shown by these kinetic patterns. The mechanisms involved in movement control and the efficiency of the therapies adopted in orthopaedics, rehabilitation and in general clinical practice can be investigated and, perhaps, evaluated by knowing the moment history of the joints. Several mathematical models ranging from a simple one-body model to complex multi-body models have been investigated [26, 64, 70, 71]. The complex analytical procedure required to apply some of the locomotion models to gait study reduces their clinical usefulness. This study presents a simplified three dimensional mathematical model that is conceptually simple, employs a relatively small number of parameters and uses the experimentally determinable, ground-reaction forces and displacements of limb segments as input. The model may then be used to interpret reaction force data without the need for displacement data.

The spatial kinematics of the limb segments is determined by displacement analysis using cinematography and the reactive force between the foot and ground is measured by the force plate described earlier. Traditional clinical measurements of the joint motion usually uses motion in three independent planes and the measurements are generally referred back to the neutral position of the limb. All the computed moments are defined in the present study with respect to the rotating body axes by using classical rigid-body mechanics. A method to simultaneously compute all three coupled angular motions (Eulerian angles) has been developed. This method enables continuous joint motion analysis. The rigid-body representation of angular motion has the added advantage of matching the definition of joint angulation commonly used by clinicians.

4.2.1 Basis for the Model

Human ambulation involves a series of co-ordinated movements of the body segments employing an interplay of muscular forces and external forces (inertial, gravitational and, ultimately, reaction forces). The metabolic energy expended by muscular actions is used efficiently by iteratively learned, optimal orientation and phasic activity of the body segments and these learned relationships result in an optimized individualistic gait. The skeletal structure, can be modelled due to its configuration, as a system of links hinged to one another. The muscular forces acting on these links rotate them about their hinge points by generating moments. Since more than one muscle action is involved, the total action of all the muscles has to be taken into account in order to quantify the resultant action. The muscular moment at a joint is defined as the product of the force exerted by each muscle crossing the joint and the distance from its articular axis. The vector sum of the moments produced by each muscle acting at a joint provides the total moment at the joint.

The total moment at any specific joint may be computed mathematically by developing a free body model at that joint and writing the dynamic equilibrium equations for that joint. The dynamic equilibrium of a joint is a function of $\mathbf{M, d, \dot{d}, \ddot{d}, R}$ and $\mathbf{p}$ where $\mathbf{M}$ is the net moment produced by the musculature at the joint under consideration. Remaining variables are defined as:

$\mathbf{d}$ - is the coordinate of the point which is used to define the mechanical parameters of the system;

$\dot{d}$ - and $\ddot{d}$ are the first and second derivative with respect to time of 'd' ;

R - is the ground reaction vector of the external force acting on the system; and

p - is a mechanical parameter of the system such as mass, length, distance to the center of mass or moment of inertia.

The total moment at any joint is given by the sum of three different moments due to the inertial, gravitational and reactive components of the limbs below that joint. The moments produced by the muscle action at the joint are those moments required for dynamic equilibrium as a result of external and dynamic forces acting on the limb. If we represent M_j as the total moment at the jth joint due to muscular forces

$$M_j = M_{j_i} + M_{j_g} + M_{j_r} \qquad - \ 4.2.1.1$$

where

M_{j_r} - moment produced by the ground-reaction force at the jth joint.

M_{j_g} - moment due to gravity forces of leg segments below the jth joint.

M_{j_i} - moment at the jth joint due to inertial forces of the leg segments below the jth joint.

The foot exerts a pressure and a shear force on the ground during locomotion. The resultant force of this pressure and shear is compensated exactly by the ground reaction. The ground reaction can be represented by a vector whose amplitude, inclination and point of application varies as the body progresses during motion. The spatial-

temporal evolution of this vector provides an integrated representation of the body segment movement dynamics. From the review in section 2.2, the body alternates support between the two feet as it progresses and is in single support approximately 70 to 75% of a gait cycle, while the double stance period is approximately 10 to 25% of the gait cycle. During the double support period, the load is distributed between the two feet and the proportion in which the force is distributed varies during the gait cycle. The position of the resultant reaction vector during double stance period can be found easily. For the load on each foot, the magnitude of ground-forces on each of the two feet should be measured simultaneously by using two separate sensing devices. However, this work is primarily concerned with the single support phase, thus only one force plate is required.

Considering the single stance period, the foot supporting the body rests firmly on the floor while the other foot goes through the acceleration and deceleration process associated with the swinging forward of the leg. The dynamics of the upper limbs of the body as well as the moving lower limb produce the resultant time varying ground-reaction force on the supporting limb. The sum of inertial and gravity forces acting on each element of the body will be in equilibrium with the ground reaction force. The moment produced by this reactive force at any particular joint of the lower limb is represented by M_{j_r} in equation 4.2.1.1 and would be the most dominant component of the total moment at the joint during the single stance-phase. The validity of this assumption has been investigated by Bresler et. al[22] who had complete dynamic data from

the Univ. of Calif. prosthetics research group[90]. Recently Boccardi et. al[33, 35, 87] and Redotti[32] have also verified its validity. All their findings indicate that ground forces have a paramount effect on the dynamics of the lower limb during stance and the gravitational and inertial components have relatively minor influences.

The model in the present study makes use of the above assumption along with other assumptions which will be briefly stated in the following paragraph. The human body is visualised as having a rigid upper body connected at the hip joint to two massless legs by means of a spherical joint described in section 2.5. The upper body represents the body mass with the center of gravity located at a known distance with respect to the hip joint. Fig. 20 indicates the model considered. The motion of the upper body is described by the translation and rotation of a body centered coordinate system $X^b\ Y^b\ Z^b$ with respect to a reference frame $X_1\ Y_1\ Z_1$, both the axes are assumed to be fixed at the center of gravity of the body. A typical relative position of the two coordinate systems is shown in Fig. 20. The overall motion is described with respect to the general Newtonian frame $X_E\ Y_E\ Z_E$ (Fig. 20). All coordinate systems are assumed to be right handed and the general direction of the motion is assumed to be in the forward direction of the X axis. The model has a $X_2\ Y_2\ Z_2$ reference axes fixed at the hip joint. As the body moves in space, the locomotion produces excursions of the body about a nominal trajectory determined by the propulsive force acting on the body. With reference to

Fig. 20, the body segments and the motions considered here are as follows:

(i) the upper body rotations in the three fundamental planes of motion (sagittal, transverse and frontal); and

(ii) the lower limb (the limb in stance phase only is considered) motions occur in the three fundamental planes of motion.

The supporting limb is considered massless in the present study. During the stance-phase of a stride, the motion of the center of mass of the supported limb is considerably smaller in comparison to the upper body motion. The inertial force of the supported limb as a result, would be negligible in comparison to the inertial and gravitational forces of the upper body. The static friction between the foot and ground keeps the leg in the supporting phase. In other words, there is no slip between the foot and the ground. The support on the floor is assumed to be a point contact for the present analysis and this assumption is made to simplify the analysis. The dynamics of the swinging leg and the upper body would result in time varying ground-reaction forces on the supported limb. The temporal ground-reaction force at the supported limb is available in the form of force records from the force plate developed. The geometrical orientation of the two segments-upper body and supported limb could be established using cinematography by following the position of a set of body markers fixed to the body at various locations. Details will be given in Chapter 5. With this method of measurement, the calculation of joint moments caused by the external ground reaction will be developed in the next section.

4.2.2 Computation of Moments due to Ground Reaction

Let **h** represent the position vector of the center of mass of the body with respect to the $X_2\ Y_2\ Z_2$ reference frame (Fig. 21) at the hip joint and further suppose that **'r'** is the position vector of the center of rotation at the hip joint defined with respect to the reference point $X_F\ Y_F\ Z_F$ (the point of contact of the lower limb with the floor). Then **'h'** and **'r'** can be obtained by finding the individual components h_{X_1}, h_{Y_1}, h_{Z_1}, r_{X_2}, r_{Y_2} and r_{Z_2}. The methods to obtain the components will be described in chapter 5. Assume for the present that they can be determined so that the reaction moment at the hip joint can be obtained as a cross-product of **r** and **R**, where **R** is the ground-reaction vector. If we represent the reaction moment at the hip joint as M_H, in the reference frame then

$$\mathbf{M_H} = \mathbf{r} \times \mathbf{R} \qquad - 4.2.2.1$$

Here M_H and **R** are defined in the earth parallel reference frames at the hip joint and point of contact at the floor, respectively.

Represent **r** and **R** in component form as:

$$\mathbf{r} = a_1\,\mathbf{i} + b_1\,\mathbf{j} + c_1\,\mathbf{k} \qquad - 4.2.2.2$$

$$\mathbf{R} = R_X\,\mathbf{i} + R_Y\,\mathbf{j} + R_Z\,\mathbf{k} \qquad - 4.2.2.3$$

$$\left.\begin{aligned} M_{H_X} &= (b_1 R_Z - C_1 R_Y) \\ M_{H_Y} &= -(a_1 R_Z - C_1 R_X) \\ M_{H_Z} &= (a_1 R_Y - b_1 R_X) \end{aligned}\right\} \qquad - 4.2.2.4$$

Having determined the moments due to the external reaction at the hip joint about the earth parallel reference frame, the next step involves

transforming the moment into the body coordinate system fixed to the hip joint. The present investigation aims to describe the motions of the body about the moving body coordinate system for reasons stated in the opening section of this chapter. The transformation can be achieved by knowing the rotation angles of the body coordinate axes with respect to the reference space coordinate axes. In order to determine the body coordinate system at various intervals of time, transformations based on Eulerian angles, similar to the transformations followed in rigid-body mechanics, were used. The methodology is presented in the following section.

4.2.3 Eulerian Angle Representation

If a rigid body is considered as a body, one of whose points is fixed at the origin of some X, Y, Z coordinate system and suppose, that coordinate system is assumed not fixed to the body. A sequence of rotations of the body within that general X, Y, Z system produces a sequence of displacements of every one of its points except those, lying on the axis of rotation. After the rotations are completed, every point is generally in a new position. The new position has components X, Y, Z in the coordinate system which is not fixed to the body. A new coordinate axes X^1, Y^1, Z^1, is fixed to the body so that a set of relations can be derived to get the components of the position change relative to this new frame. The relationships between the two coordinate systems can be obtained in the form of a transformation matrix whose elements are the direction cosines of the body-fixed axes with respect to the axis-system

which is not fixed in the body. These relationships have been derived already [86] and shown to have the following properties:

(i) the transformation matrix is orthogonal; and

(ii) the transformation matrix of a sequence of rotations is equal to the product of individual transformation matrices, multiplied in the inverse sequence of that in which the rotations were made.

Since rotations do not add like vectors, a different sequence results generally in a different transformation matrix. Data must be taken in a sequence compatible with the transformation.

The general displacement of a point on a rigid body is describable by three independent rotations because a rigid body with one point fixed has three degrees of freedom. The usual description of a displacement resulting from a rotation is that given in terms of the Euler angles. The sequence of rotations used by various researchers are not all the same and, as pointed out earlier, these differences result in different transformation matrices. The relationship to be derived in the next sections follows the sequence given by Goldstein[86].

Consider an X, Y, Z coordinate system not fixed to the body, and an X^1, Y^1, Z^1 system fixed to the body, as shown in Fig. 22. The two systems coincide before rotation. The first rotation is about the Z axis by an amount 'ψ' (right handed rotation). The body fixed axis moves to a new

position indicated by X_1', Y_1', Z_1'. For this rotation

$$\begin{bmatrix} X_1' \\ Y_1' \\ Z_1' \end{bmatrix} = D \begin{bmatrix} X \\ Y \\ Z \end{bmatrix} \qquad - \ 4.2.3.1$$

where D is the matrix of the direction cosines, the elements d_{ij}, i and j = 1, 2, 3, of which are :

$$d_{11} = \cos(X_1', X) = \cos \psi$$

$$d_{12} = \cos(X_1', Y) = \sin \psi$$

$$d_{13} = \cos(X_1', Z) = 0$$

$$d_{21} = \cos(Y_1', X) = - \sin \psi$$

$$d_{22} = \cos(Y_1', Y) = \cos \psi$$

$$d_{23} = \cos(Y_1', Z) = 0$$

$$d_{31} = \cos(Z_1', X) = 0$$

$$d_{32} = \cos(Z_1', Y) = 0$$

$$d_{33} = \cos(Z_1', Z) = 1.$$

Therefore

$$D = \begin{bmatrix} \cos \psi & \sin \psi & 0 \\ - \sin \psi & \cos \psi & 0 \\ 0 & 0 & 1 \end{bmatrix} \qquad - \ 4.2.3.2$$

Next consider X_1', Y_1', Z_1' as not fixed in the system and let the body fixed system be denoted as X_2', Y_2', Z_2' as shown in Fig. 22. Before rotation the

two systems coincide and the body fixed system is given a right handed rotation'θ' about the X_1' axis, as shown in Fig. 22. The X_1' axis lies in the 'line of nodes'. The transformation for the second rotation is given by:

$$\begin{bmatrix} X'_2 \\ Y_2' \\ Z_2' \end{bmatrix} = C \begin{bmatrix} X_1' \\ Y_1' \\ Z_1' \end{bmatrix} \qquad - \ 4.2.3.3$$

The transformation matrix C has the elements, C_{ij}, i and j = 1,2,3, given by

$$\begin{aligned} C_{11} &= \cos(X_2', X_1') = 1 \\ C_{12} &= \cos(X_2', Y_1') = 0 \\ C_{13} &= \cos(X_2', Z_1') = 0 \\ C_{21} &= \cos(Y_2', X_1') = 0 \\ C_{22} &= \cos(Y_2', Y_1') = \cos\theta \\ C_{23} &= \cos(Y_2', Z_1') = \sin\theta \\ C_{31} &= \cos(Z_2', X_1') = 0 \\ C_{32} &= \cos(Z_2', Y_1') = -\sin\theta \\ C_{33} &= \cos(Z_2', Z_1') = \cos\theta \end{aligned}$$

Therefore

$$C = \begin{bmatrix} 1 & 0 & 0 \\ 0 & \cos\theta & \sin\theta \\ 0 & -\sin\theta & \cos\theta \end{bmatrix} \qquad - \ 4.2.3.4$$

Finally, consider the X_2', Y_2', Z_2' system as not fixed in the body while X_3', Y_3', Z_3' is fixed to the body. As before the two systems coincide before a given rotation. A right handed rotation 'ϕ' about the Z_2' axis

brings the body-fixed coordinate axes to its final position X_3', Y_3', Z_3' as shown in Fig. 22. The transformation for this rotation is given by

$$\begin{bmatrix} X_3' \\ Y_3' \\ Z_3' \end{bmatrix} = B \begin{bmatrix} X_2' \\ Y_2' \\ Z_2' \end{bmatrix} \qquad - \ 4.2.3.5$$

The transformation matrix B has its elements given below:

$$b_{11} = \cos(X_3', X_2') = \cos\phi$$
$$b_{12} = \cos(X_3', Y_2') = \sin\phi$$
$$b_{13} = \cos(X_3', Z_2') = 0$$
$$b_{21} = \cos(Y_3', X_2') = -\sin\phi$$
$$b_{22} = \cos(Y_3', Y_2') = \cos\phi$$
$$b_{23} = \cos(Y_3', Z_2') = 0$$
$$b_{31} = \cos(Z_3', X_2') = 0$$
$$b_{32} = \cos(Z_3', Y_2') = 0$$
$$b_{33} = \cos(Z_3', Z_2') = 1$$

Therefore

$$B = \begin{bmatrix} \cos\phi & \sin\phi & 0 \\ -\sin\phi & \cos\phi & 0 \\ 0 & 0 & 1 \end{bmatrix} \qquad - \ 4.2.3.6.$$

By the rule of the composition of rotations, the transformation from (X,Y,Z)(to be denoted hereafter as the 'space frame') to the final body frame X_3' Y_3' Z_3' is

$$\begin{bmatrix} X_3' \\ Y_3' \\ Z_3' \end{bmatrix} = A \begin{bmatrix} X \\ Y \\ Z \end{bmatrix} \qquad - \ 4.2.3.7$$

where

$$A = B\ C\ D. \qquad - \ 4.2.3.8$$

The matrix multiplication in equation 4.2.3.8 results in the following form for A

$$A = \begin{bmatrix} \cos\psi\cos\phi - \cos\theta\sin\phi\sin\psi, & \cos\phi\sin\psi + \cos\theta\cos\psi\sin\phi, & \sin\phi\sin\theta \\ -\sin\phi\cos\psi - \cos\theta\sin\psi\cos\phi, & -\sin\phi\sin\psi + \cos\theta\cos\phi\cos\psi, & \cos\phi\sin\theta \\ \sin\theta\sin\psi, & -\sin\theta\cos\psi, & \cos\theta \end{bmatrix}$$

$$- \ 4.2.3.9$$

If we write

$X_3' = X'$, $Y_3' = Y'$, $Z_3' = Z'$, the components in the body axes are given as

$$X' = (\cos\psi\cos\phi - \cos\theta\sin\phi\sin\psi)\,X + (\cos\phi\sin\psi + \cos\theta\cos\psi\sin\phi)\,Y + (\sin\phi\sin\theta)Z \quad - \ 4.2.3.10$$

$$Y' = (-\sin\phi\cos\psi - \cos\theta\sin\psi\cos\phi)\,X\ (-\sin\phi\sin\psi + \cos\theta\cos\phi\cos\psi)\,Y + (\cos\phi\sin\theta)Z \quad - \ 4.2.3.11$$

and

$$Z' = (\sin\theta\sin\psi)\,X - (\sin\theta\cos\psi)\,Y + (\cos\theta)Z \quad - \ 4.2.3.12$$

Hence in order to transform from space coordinates X, Y, Z to body coordinates X', Y', Z', the transformation matrix given by equation 4.2.3.9 is used. The inverse transformation from body coordinates X', Y', Z' to space coordinate X, Y, Z is given by

$$\begin{bmatrix} X \\ Y \\ Z \end{bmatrix} = A^{-1} \begin{bmatrix} X' \\ Y' \\ Z' \end{bmatrix} \qquad - \ 4.2.3.13$$

where

$$A^{-1} = \begin{bmatrix} \cos\psi\cos\phi - \cos\theta\sin\phi\sin\psi, & -\sin\phi\cos\psi - \cos\theta\sin\psi\cos\phi, & \sin\theta\sin\psi \\ \cos\phi\sin\psi + \cos\theta\cos\psi\sin\phi, & -\sin\phi\sin\psi + \cos\theta\cos\phi\cos\psi, & -\sin\theta\cos\psi \\ \sin\phi\sin\theta, & \cos\phi\sin\theta, & \cos\theta \end{bmatrix}$$

- 4.2.3.14

As was pointed out earlier, several systems of Euler angles have been used in the literature and Table 2 shows three different systems used be various authors. The rotation followed in the present work is Type II in Table 2. The rotation sequence for Type I is shown in Fig. 23 but was not used for the transformations given here. Euler angles have the advantage that three ordered rotations would determine a unique orientation. But an orientation does not determine a unique set of Euler angles. Depending upon the order of rotations the various systems outlined in Table 2 would give rise to different set of values for the angles. Thus, in order to obtain a unique orientation of a segment in space the sequence of rotations and the corresponding Euler angles have to be used in the transformation matrix.

4.4 Determination of Reaction Moments in the body coordinate System

For the model considered, if $X^h\ Y^h\ Z^h$ and $X^b\ Y^b\ Z^b$ (Fig. 21) represent the body coordinate system attached to the hip joint and the center of gravity respectively, the desired transformation at the hip joint and at center of gravity may be performed, knowing the angular rotations ψ_ℓ, θ_ℓ, ϕ_ℓ and ψ_b, θ_b, ϕ_b at the respective joints. One such orientation of the axes is shown in Fig. 21. If the transformation matrix for the space to hip is represented as $[T_{S \rightarrow H}]$, the reaction moment in

the body coordinate system at the hip joint can be written as

$$M_H^b = [T_{S \rightarrow H}] \begin{bmatrix} M_{H_X} \\ M_{H_Y} \\ M_{H_Z} \end{bmatrix} \quad - 4.4.1$$

where M_H^b is the moment vector due to the ground reaction force in the body coordinate system at the hip joint and M_{H_X}, M_{H_Y}, M_{H_Z} are the components of moment vector M_H in the reference frame X_2 Y_2 Z_2. The component form of M_H^b is given by:

$$\begin{bmatrix} M_{H_X}^b \\ M_{H_Y}^b \\ M_{H_Z}^b \end{bmatrix} = [T_{S \rightarrow H}] \begin{bmatrix} M_{H_X} \\ M_{H_Y} \\ M_{H_Z} \end{bmatrix} \quad - 4.4.2$$

The transformation matrix $[T_{S \rightarrow H}]$ can be obtained from equation 4.2.3.9.

Having determined the reaction moments about the hip joint, the reaction moments about the upper body can be computed. If $[T_{S \rightarrow B}]$ represents the transformation matrix for the upper body and M_B^b represents the vector moment due to the external reaction in the body frame at the center of gravity,

$$\begin{bmatrix} M_{B_X}^b \\ M_{B_Y}^b \\ M_{B_Z}^b \end{bmatrix} = [T_{S \rightarrow B}][\mathbf{h} \times \mathbf{F}_H] - [T_{S \rightarrow B}][M_H] \quad - 4.4.3$$

where

$[T_{S \rightarrow B}]$ is the transformation matrix for space to upper body

$\mathbf{h}$ - is the position vector from hip to the center of gravity of the body,

$\mathbf{F}_H$ - is the reaction force about the space frame at the hip joint

If ψ_b and θ_b and ϕ_b are the Eulerian angles for the upper body, $[T_{S \rightarrow B}]$ can be obtained using the relations given in equation 4.2.3.9. $M^b_{B_X}$, $M^b_{B_Y}$, $M^b_{B_Z}$ in equation 4.4.3 represent the moment components about the respective X^b Y^b Z^b coordinate axes.

The methods to obtain the moment due to external reaction at the hip joint in the body coordinate system will be described in the following sections.

4.5 Determination of Transformation Matrix

The use of Eulerian angles to represent the limb rotations was illustrated in the previous two sections. Earlier in this chapter it was pointed out that several systems of Eulerian rotations are in common usage. Even though the symbols used are the same, the sequence of carrying out the Euler rotation is not always the same and, to date no standard sequence has been agreed upon. Methods to find the rotation angles for any arbitrary rotation of a body have not been illustrated clearly. Langrana[88] and Chao et.al[89] have tried to determine the rotation angles ψ, θ, ϕ by fixing triads to external bony markers for finger joints and upper limb extremity joints, respectively. For the sequence of rotations adopted in this study, methods to determine the elements of rotation matrix $[T_{S \rightarrow B}]$ and $[T_{S \rightarrow H}]$ will be developed and

various approaches will be employed to match with the anatomical motions possibly encountered in the lower limb and upper body.

The transformation techniques proposed in this study are the result of an examination of the factors which determine the pathway of the center of gravity. The details of the technique employed will be described after briefly summarising the determinants controlling the translation and rotation of the segments of the body.

For the purpose of analysis, a bipedal system is considered with lower extremities represented by levers without foot and articulated at the equivalent of a hip joint. Fig. 24 is one such system permitting flexion and extension of the lower limb. The movement of the lower limb in this system would be analogous to the process of stepping-off distances with a pair of compass or dividers. The pathway of the center of gravity during forward translation would be a series of intersecting arcs as shown in Figure 24 by dotted lines. The upper body, which is attached to the lower extremity at the hip joint, would go through a similar up and down motion without rotation. If a right handed coordinate system is fixed to the head of femur with X-axis in the direction of walking, the motion described can be observed by monitoring the orientation of the body fixed coordinate axes at the hip joint with respect to a reference frame. The body fixed X-axis moves up and down in a vertical plane and since there is no adduction or abduction* of the lower extremity, the body fixed Y-axis always remains in the XY plane.

*The terminology used to define movement of the limbs is represented in Fig. 40.

The body fixed Z-axis follows the movement of the lower extremity and goes through a forward and backward tilt alternately as the lower extremity steps off distances. The above described locomotion is a hypothetical gait and produces a very inefficient gait in terms of energy due to maximum excursions of the joint in the vertical direction.

The pelvis goes through a rotation during normal walking and when this is added to the hypothetical gait considered previously, a motion with the alternating pelvic rotation is achieved. Fig. 25 shows the resultant motion. The pelvis rotates alternately to the right and to the left relative to the line of progression and, at customary cadence and stride, the magnitude of this rotation is estimated to be approximately 4° on either side of the central axis. This rotation shows itself as alternating internal and external rotation of the pelvis and upper body about the hip joint during the stance phase because, the pelvis is a rigid structure. The resulting motion, viewed from the rotations of upper and lower limb coordinate axes, would be: rotation about the vertical axis for the upper body and reduced angular tilt of the body fixed X and Z axis for the lower extremity.

In the third category of motion, the pelvic tilt, present in normal locomotion, is added. There is a listing downward relative to the horizontal plane on the side of the non weight-bearing limb. This tilt produces an average of 5° angular displacement at the hip joint. The result of the pelvic tilt is an outward deflection of the hip joint supporting the limb in the stance phase. Thus, there is an adduction of the extremity in the stance phase and a relative abduction of the extremity in the swing phase. The knee joint of the non-weight bearing

limb also flexes to allow clearance for swing-through of that member. Such a motion is represented in Fig. 26. The motion of this category produces a rotation about the vertical axis and a tilt in the horizontal plane of the upper body. The lower extremity in stance phase undergoes a tilt due to the relative adduction of the hip joint in the horizontal plane in addition to all the other rotations described in the first two categories of motion.

The motions described above would produce rotations of the upper body as well as of the lower extremity and would contribute directly to the rotations of the body fixed coordinate systems in both the segments of the body considered in this analysis. The transformation technique proposed is a result of close examination of these movement patterns and the motion described in Fig. 26 is considered as representative of several abnormal gaits.

The upper body, assumed rigid in this analysis, is attached to the lower limb by a ball and socket joint. When the upper body is subjected to propulsive forces as the whole body moves forward about the supporting limb, the pelvis is observed to twist in a counter-clockwise and clockwise direction alternately for normal locomotion[5, 38]. Assuming a left heel strike, the pelvis begins to twist in a counter-clockwise direction. At the time of the right heel strike, the left side of the thorax is advanced and the remainder of the cycle is characterised by thoracic rotation similar to that described for the left heel strike. This kind of phasic behaviour probably contributes to the smoothness in translation of the body. In the case of abnormal gait, the smooth and symmetric movements described above may not be present and compensatory motions in the form of

reduced motions in one plane and more than normal motions in other planes may result in overall stability of the body. The transformation techniques to be outlined in this thesis would determine all the rotation angles of the upper body coordinate axes.

4.6 Upper Body Transformations

This section describes the procedure for determining the transformation matrices developed in Section 4.2.2. The basic principle involved in the transformations is based on obtaining the Eulerian rotation angles for a specific position of the lower limb and upper body segments. The geometrical position of the lower extremity and upper body is given by the position vectors **'r'** and **'h'** defined in section 4.2.2. The rotations of the two body segments will be governed by the instantaneous positions of these two line vectors.

4.6.1 Upper Body Rotation Matrix

Figure 27 illustrates the upper body, with the geometrical position of center of gravity 'C', connected to the lower extremity by a spherical joint at hip center, 'B'. Thus the geometrical position of the center of gravity at any given time can be defined with respect to a reference axis fixed at the hip joint. The position vector 'BC', henceforth referred to as the 'hip vector', is assumed determinable from biplane measurements. The upper body is assumed rigid so that the orientation of the upper body in space would be defined uniquely by the hip vector, 'BC'. The rotation of the upper body is described by Eulerian angles ψ_b, θ_b and ϕ_b (defined in Section 4.2.3) of a body fixed coordinate system X^b Y^b Z^b with respect

to a reference frame $X_1 Y_1 Z_1$ located at the center of gravity. The reference frame X_1 Y_1 Z_1 always remains parallel to the earth reference frame X_E Y_E Z_E. The neutral position of the center of gravity of the body is assumed to be located in the frontal plane passing through the hip joint with the Y and Z coordinates 0.15 and 0.30 times the length of the leg, respectively, defined as in Fig. 21 with respect to the X_2 Y_2 Z_2 coordinate axes at the hip joint. This assumption agrees with the values given in anatomical tables[59]. If the position vector 'BC' in the body neutral -standing erect position is represented as $\mathbf{h}_S$, then

$$\mathbf{h}_S = (0.00\ \mathbf{i} + 0.15\ell\ \mathbf{j} - 0.30\ell\ \mathbf{k}) - \quad 4.6.1$$

where 'ℓ' is the length of the leg and the components are measured with respect to the X_1 Y_1 Z_1 coordinate system. The relative movement of 'C' with respect to 'B' changes the components of 'BC' as the body moves in space. If the position vector of 'BC' at any instant other than that coinciding with the neutral position is denoted as '**h**', then

$$\mathbf{h} = a_2\ \mathbf{i} + b_2\ \mathbf{j} + c_2\ \mathbf{k} \quad - \quad 4.6.2$$

The a_2, b_2 and c_2 are the components of BC defined with respect to the space parallel reference system X_1 Y_1 Z_1. Also $\hat{\mathbf{h}}$, the unit vector along BC, can be expressed as

$$\mathbf{h} = \frac{a_2\ \mathbf{i} + b_2\ \mathbf{j} + c_2\ \mathbf{k}}{\sqrt{(a_2^2 + b_2^2 + c_2^2)}} \quad - \quad 4.6.3$$

Referring to Fig. 27, C' indicates the new position of the center of gravity of the body relative to the hip. This new position vector is

represented by B'C'. Since the rotation is described relative to a reference frame fixed to the hip joint, B'C represents the neutral limb position of the center of gravity of the body in the new position relative to the hip. If 'ν' represents the angle between the reference axis Z_1 and 'h_s' the direction cosine '$\cos\nu$' is given as

$$\cos \nu = \frac{\hat{Z}_1 \cdot \hat{h}_s}{| \hat{Z}_1 | | \hat{h}_s |} \qquad - \qquad 4.6.4$$

If X^b, Y^b, Z^b refers to the new position of the body axes fixed at center of gravity, the rotation angles ψ_b, θ_b and ϕ_b can be determined as follows. The upper body is assumed rigid so that the body coordinate system would maintain the same initial angular orientation with respect to the new position vector '**h**'.

The vector operations outlined below are performed in order to define the motion of the body axes with respect to the initial position vector 'h_s'.

$$\mathbf{T} = \hat{Z}_1 \times \hat{h}_s \qquad - \qquad 4.6.5$$

where $\hat{T}$ defines a unit vector, normal to the plane containing $\hat{Z}_1$ and $\hat{h}_s$. Forming a cross product between $\hat{T}$ and the new position vector '$\hat{h}$' would define the vector $\hat{P}$ normal to the plane containing $\hat{T}$ and $\hat{h}$, or

$$\hat{P} = \hat{h} \times \hat{T}. \qquad - \qquad 4.6.6$$

The body axis Z^b would be in the plane containing $\hat{P}$ and $\hat{h}$ and would maintain the same angular orientation 'ν', defined by eqn. 4.6.4, with respect $\hat{h}$. The components of $\hat{Z}^b$ contributed by $\hat{h}$ and

$\hat{P}$, are given by

$$\hat{Z}^b = \hat{h} \cos\nu + \hat{P} \sin\nu \quad - \quad 4.6.7$$

or, from equation 4.2.3.12,

$$\hat{Z}^b = (\sin\theta_b \sin\psi_b)\ \hat{X} - (\sin\theta_b \cos\psi_b)\ \hat{Y} + (\cos\theta_b)\ \hat{Z} \quad - \quad 4.6.8$$

The ψ_b and θ_b can be obtained by equating corresponding components in equation 4.6.7 and 4.6.8.

To obtain X^b and Y^b with respect to Z^b , the coordinate axes Y_1, Y^b , X_1 and X^b are expressed as a function of $\hat{T}$, $\hat{T}_1$, $\hat{h}_s$, $\hat{h}$, $\hat{Z}$, and $\hat{Z}^b$, as given below

$$\hat{Y}_1 = a\ \hat{T} + b\ \hat{h}_s + d\ \hat{Z}_1 \quad - \quad 4.6.9$$

and

$$\hat{Y}^b = a\ \hat{T}_1 + b\ \hat{h} + d\ \hat{Z}^b \quad - \quad 4.6.10$$

where $\hat{T}_1 = \hat{Z}^b \times \hat{h}$. - 4.6.11

The a, b and d are constants representing the angular orientation of the body coordinate axes with respect to the position vector 'BC'.

The constants a, b and d are obtained from the known initial position of vector BC. The program flow chart to obtain a, b and d is outlined in Appendix B. When substituted into equation 4.6.10 these constants will define the position of Y^b . Since the body coordinate system is orthogonal, X^b can be obtained through the cross-product

$$\hat{X}^b = \hat{Y}^b \times \hat{Z}^b . \quad - \quad 4.6.12$$

The next chapter describes the method used to determine the limb positions as a function of time. From the limb positions determined from the biplane views of body markers, the variables in the transformation techniques discussed can be computed.

4.6.2 Lower Limb Transformation

The rotation angles for the body coordinate system located at the hip joint cannot be determined uniquely without imposing certain conditions on the articulation of the lower limb. A method to obtain the lower limb transformations with the current body marker systems is proposed in Appendix A. As will be pointed out in the next section, the net muscle moment at the hip joint can be computed without knowledge of rotation angles for the lower limb. The next section will outline the method to calculate the net upper body moment which is also the net muscle moment at the hip joint.

4.7 Net Muscle Moment at the Hip Joint in Upper Body Coordinate System

The moment produced by the ground reaction at the hip joint and center of gravity is given by M_{j_r}, the last term in equation 4.2.1.1. This could be obtained directly from the measured ground reaction **R** and its distance from the articular axis. The reaction moment about the hip joint is obtained using equation 4.2.2.1. Equation 4.4.3 gives the net reaction moments about center of gravity in the upper body coordinate system. The conditions for the dynamic equilibrium of the model under consideration can be expressed in a reference frame fixed to upper body [96, 97] as follows: The vector summation of forces

$$\sum_i \mathbf{f}_i + \mathbf{mg} + (-\mathbf{ma}_c) = 0 \quad - \quad 4.7.1$$

and the vector summation of moments about any segment joint

$$\sum_i \mathbf{M}_{ci} + (-\dot{\mathbf{H}}_c) = 0 \quad - \quad 4.7.2.$$

where

m = total mass of the body

f_i = the force vectors acting on the body at the hip(hip forces)

mg = the weight of the body

$-ma_c$ = the inertia force vector

a_c = the acceleration vector of the center of mass

M_{ci} = the moment vectors acting on the body at the hips (hip moments)

$(-\dot{H}_c)$ = the rate of change of the inertial moment of momentum vector about the center of mass.

The forces f_i and moments M_{ci} are the active controls which cause the body to move. The right hand side of equation 4.4.3 represents the external reaction moment about CG. During the stance phase, as pointed out earlier, the resultant ground reaction force is the sum of inertia and gravity forces of each element of the body. In the present model the lower limb, assumed massless during the stance phase does not contribute to the inertial and gravity forces and, hence, the net moment at the hip joint would be the result of gravitational and inertia forces of the upper body alone. The net dynamic muscle moment given by equation 4.7.2. is found directly from equation 4.4.3. Equation 4.4.3 expresses the moment due to external reaction in the body coordinate system from which the net moment at the hip joint can be computed in the body coordinate system .

The scope of the present study is to monitor the ground reaction forces for several cases of abnormal locomotion resulting from injury to any one of the load bearing extremities and relate the asymmetry in locomotion to a set of indices derived from reaction force records. To keep the body in dynamic equilibrium it may then be shown that the compensatory movements brought about by the upper body could be monitored by a similar set of indices for the upper body. A discussion on the various indices along with the results obtained is presented in Chapter 6.

CHAPTER 5

EXPERIMENTAL PROCEDURE

5.1 General Layout of Experimental Set up

This chapter describes briefly the general procedure for gathering data in the present study. A schematic illustration of the experimental layout is shown in Fig. 28. The force platform 'e', is located in the center of walkway 'f' which is 48 feet long. The long walkway allows the subject to reach a normal ambulation before reaching the force platform. As the subject strides over the force plate, signals proportional to the ground reaction components are amplified by a set of strain bridge amplifiers 'h' and then are recorded on magnetic tape. A Philips FM tape recorder, 'g', with 10 channel capability was used for this purpose. The order of the recorded signals is shown in Table 5. The subject, appropriately lighted by spot lights 'c', traverses the force plate several times from either direction. Bi-plane photography was used to capture the positions of various segments of the body as the subject traverses the force plate. The common problem with three dimensional motion studies has been the inability of several cameras to perceive the marked body locations at all times. Two 16mm movie cameras (Action Master 500 and Arriflex ST) were used in the present study. Camera 'a' was located in line with the centroid of the force plate and perpendicular to the long side of the force platform. Camera 'b' was located with its axis perpendicular to the lens axis of camera 'a' and in line with the centroid of the force plate. The two camera axes intersect at the centroid of the force plate. Camera 'a' views the motion of the subject in the sagittal plane and frontal plane motions are recorded by camera 'b'. A series of

cross-hatched circular markers, 'd', which are 2" in diameter are used as background markers. The movements of the markers are measured with respect to the cross-hatched set of fixed reference markers. The position of the background markers with respect to the force plate geometry is known accurately. In addition to the background markers, the three support pipes carry markers and appear in the field of view of both cameras. Body segments are identified by several markers and bony prominences close to the joints were chosen as marker sites. The subject's preparation involved fixing adhesive markers on these bony prominences. Strips of adhesive tape (1" in width and 2" long) carrying a black circular patch 3/4" diameter constituted the body markers and identified the points of interest on the body segments. Markers 1, 2 and 3 in Fig. 29 represent the lateral side of the toe, tarsal bone and heel as viewed in the sagittal plane. Marker '4' represents the lateral malleolus and 5 and 6 represent the lateral tibial head and lateral epicondyle of the femur. The greater trochanter was identified by marker 7 and marker '8' corresponds to the center of gravity of the body as viewed from the lateral or frontal camera. The center of gravity of the body was established by using equation 4.6.1. The accurate determination of the location of the center of gravity is beyond the scope of the present work. All eight marker points described above appear in the field of view of the sagittal camera. Markers of size and shape similar to those used on the two lateral sides of the limbs were also fixed on the medial sides of the limbs. The dorsal and ventral sides of the subject was identified by a similar set of markers which identified the location of the heel, knee joint and center of gravity. Care was taken to align

the markers as accurately as possible.

The movie cameras were operated at a constant speed of 50 frames/sec. The practicalities and economics of the situation determined the operating speed. Various measurements have to be synchronized to correlate the kinematic and kinetic measurements. This was achieved using a comparator circuit. The signal from the vertical summing amplifier was fed through a comparator circuit. Any changes with reference to the balanced null output of the vertical summing amplifier when there is no external load on the force plate would trigger the comparator circuit. The threshold was adjusted to correspond to an increase of 5 pounds in external load on the force plate. Thus, as the vertical load on the force plate starts increasing, when the heel strikes the force plate, the comparator will be triggered for vertical reactions greater than 5 pounds. The comparator output was recorded on analog recorders with the force signals. It was also amplified to operate a relay which, in turn, controls two flash lights pointed in the field of view of the two cameras. The flash lights would come on at the instance of heel strike on the force plate so that complete synchronization of the force output and the kinematic data was achieved. The comparator output recorded on the magnetic tape in the form of a pulse is shown in Fig. 42.

The locomotion analysis involved the kinetic and kinematic measurements of the subject's gait. The first step involved preparation of the subject as outlined in this section. The subject was familiarised with the general procedure and subsequently traversed the force plate several times prior to the actual data collection. The static weight of the subject when in an erect or neutral position was recorded along with

the neutral position of the markers. A complete motion analysis, as the subject traversed the force plate several times, was then obtained.

5.2 Data Reduction

Data reduction comprised an analysis of the cine the film and the force signals. The reduction from the film was done on a P.C.D. Digital reader system and a Hewlett Packard (HP) 9874A digitizer interfaced to a 9835A minicomputer. The HP system available at the School of Physical Education, University of Manitoba is used for analysing sports motions. Both the units are used for converting data on paper charts or graphs and film material to computer compatible digital form. Both the systems essentially consist of an XY reader head and the recording process is initiated by a push switch mounted on the reader head. The P.C.D. system uses a well proven potentiometer system for measurement. The optical sight is positioned over the point to be digitized and the analog signals derived from manual positioning of the optical sight are converted to X and Y digital displays with the help of built-in analog to digital converters. The HP system has a platen on which the graphs or films to be digitized are projected. The platen is a sheet of laminated glass with the X and Y conductors placed between the layers of glass. When the cursor is moved over the point to be digitized, the digitized X and Y co-ordinate values of the point are fed automatically to the minicomputer at the press of a button. The HP digitizing system is fully programmable.

To digitize the force curves from the force plate, analog force signals stored on magnetic tape were transferred to traces on paper by using a strip chart recorder. Transparencies made from the strip chart

output were then projected on the digitizer platen for an enlarged image of the traces. Both the P.C.D. and HP systems have facilities for scaling the ordinates. The HP system was programmed to read into memory only those Y ordinate values corresponding to a X increment of 0.02 sec (scaled to proper units). Since the cine film data was taken at 50 frames/sec every frame corresponds to an interval of 0.02 sec. The active digitizing area (315 x 435 mms) of the HP unit is divided into 25 micrometer units. The accuracy of the cursor unit is ± 125 micrometers (0.00492").

For measurement and analysis of various types of film material, the P.C.D. system is fitted with a compact rear projection unit. The 16 mm cine film of the subject walking across the force plate was projected on the translucent screen of the digitising pad. The projector was a Lafayette motion analyser which has controls for projecting frame by frame. The film was wound up to the frame corresponding to the first heel strike on the force plate which was recognised by the instant at which a flash light comes on. The cursor is moved sequentially over the markers fixed to the body and the digitized X and Y coordinate values of every marker point was transferred to the minicomputer. The digitizer was programmed to read the values initialised with reference to a spatial origin corresponding to one of the background markers fixed to the force plate. Since the vertical and horizontal distances of the markers are fixed, the scaling was done with respect to these markers. A similar procedure was adopted for digitizing the frontal displacement measurements. Every alternate frame from the first heel strike was digitized and, hence, a complete force-displacement time history was obtained. The digitised values of marker points were

then used for calculating the X, Y and Z positions as described below. Fig. 30 shows the projected view of the human body on the digipad as seen by camera 'a' from the sagittal plane. The digitiser axis is represented by OX and OY and O' is the background reference point. The program developed for digitization, initialises point O' with respect to O for every frame and all further measurements are made relative to O'. This way any errors introduced due to a shift in origin O' between frames were minimised. From the measurement of marker positions at floor, hip joint and center of gravity, the components are computed in space reference frame by using:

$$a_1 = X_{hip} - X_{floor}$$
$$c_1 = Y_{hip} - Y_{floor}$$

and 5.2.1

$$a_2 = X_{cg} - X_{hip}$$
$$c_2 = Y_{cg} - Y_{hip}.$$

The a_1, a_2, c_1 and c_2 are the components of the position vectors AB and BC defined in section 4.2.2. Proper signs were assigned to the components depending upon the position of the hip and center of gravity with respect to the floor marker. The 'b_1' and 'b_2' are the components of its position vector in the body and hip reference frames which were obtained from the frontal view of the subject as seen by camera 'b'. OX and OY represent the digitiser axis in Fig. 31 and, as in the previous case, the measurements were with respect to a permanent background marker O'. In the frontal view, the location of hip joint was established by

interpolation. It is difficult to establish the hip joint in the posterior view due to the vast musculature.

The methods described above provide a discrete mapping of the body positions at 0.04 second intervals. The analysis of the data as applied to the model was carried out according to the procedure shown in Fig. 32

5.3 Experimental Set up for Verification of the Transformation Model

An experimental jig was constructed to verify the mathematical model for transformations from the space to body systems or vice versa. Even though the specific transformation for the upper body could not be verified in view of the complexities involved in constructing a physical model of the hip joint, the general principle involved in the transformation could be verified. The jig (Fig. 33) consisted of a mild steel tube 'A' 40" long, 1 3/8" internal diameter and 1/8" wall thickness and carried a universal joint 'B' at its lower end. A flat plate, 'C', 3" x 3" x 1/4" and welded to the free end of the universal joint allowed the fixture to be anchored to the force plate. The universal joint permitted rotations of the tube about the X and Y axis of the force plate. Any rotations about the Z axis was prevented by fixing 'C' rigidly to the force plate. A collar, 'D', machined to the outer dimensions of the tube, was arranged to slide freely on the tube 'A'. The collar was supported by a specially designed suspension system, 'E', and the two together provided a hinge joint with three degrees of freedom for the upper end of the tube. This suspension system was free to move to any position along the length of the tube and was fixed in space to two rigid horizontal beams, 'F', running either side of the suspension system, 'E'. The two horizontal

beams, joined at their ends, are supported in turn by two beams, 'G', running on either side of the force plate. The structural arrangement permitted tube 'A' to be set to any inclination in space. The length of the tube from the point of support at the force plate to the point of suspension at collar 'D' represents the position vector of the limb segment in the human model. The position vector of its components is determined accurately by measurements from two perpendicular directions using precision theodolites.

The top end of the tube carries two loading arms fixed to a collar 'H'. These arms were set at right angles to each other and their longitudinal axis remained perpendicular to the length of the tube. Thus, the loading arm represents the moving body axis and the angular orientation could be changed by rotating collar 'H'. In order to verify the transformation techniques, tube 'A' was set to any position and the position vector was determined from theodolite measurements. The loading arm was rotated to the angular position determined from the transformation techniques. The two theodilites enabled accurate setting of the loading arm. Loads applied to the arm produced moments about the respective body axis fixed to the collar and the reactions at the lower end of the pipe were measured using the force plate transducers. The reaction values determined by using the transducers are with respect to the space frame. The accuracy of the model could then be checked by comparing the theoretical reactions with those obtained by experimental measurements. The results of the experimental investigation are presented in the following section.

5.3.1 Results of the Analysis

The experimental rig described in section 5.3 was set to various inclinations of tube 'A'. The two theodolites were used to measure the projected angle of the tube in the XZ and YZ planes respectively. The loading arm was rotated to the corresponding angle determined from the transformation technique for each setting of the tube. Ground reactions were measured for different loadings of tube 'A' up to a maximum bending moment of 840 in lbs. about the body fixed axes. The difference in the reaction components as measured by the force plate transducers and the reaction component calculated from the transformation technique was computed for various settings. Fig. 34 represents the percentage error obtained for various inclinations of the tube. The plot in Fig. 34 represents a typical case where the tube was set to the same inclination in the XZ and YZ planes and the various symbols represent the percentage error for different values of bending moment applied to the tube.

Values plotted in Fig. 34 indicate a maximum difference of 7% between the ground reactions obtained experimentally, and theoretically. Theoretical values tend to be the highest. For inclinations of the tube closer to 25° or greater tilt, there was an increase in experimental values. The Fig. 34 also shows the percentage error to be higher for reduced moment values on the loading beam. Even though a detailed analysis of the results will not be attempted at the present time, the increased differences for lower ranges of loading of the beam could be attributed to the slight slackness in the various joints of the rig. It was felt that the error values obtained are quite low and do not warrant any further analysis. As pointed out earlier, the rig cannot be used for checking the upper body transformation without further modification.

CHAPTER 6

RESULTS AND DISCUSSION

6.1 General Points Considered in Presentation of Results

The large number of gait studies performed by several investigators have all resulted in a current understanding of primarily normal locomotion. Most of the studies come from largely descriptive and qualitative kinematical evaluations. It has been the general conclusion of various researchers, as observed by Townsend[95], that the motions of various body segments cooperate to facilitate a specific gait, minimize forces and/or energy expenditure, or ensure adequate stability or some combination of these parameters. Results from various studies undertaken in the present investigation will be presented in the form of general ground reaction forces for various subjects along with a set of net muscle moments computed in the translating body-fixed coordinate system, fixed at the hip joint. Since the model developed idealises the human body as two segments, a rigid upper body capable of motion in three dimensional space about the hip joint and massless legs, the net postural compensation, if any, should be seen in the net dynamic muscle moment at the hip joint. The mechanical behaviour of the upper part of the human body has never been studied in detail in relation to the lower limb. As part of the results, the performance of the developed force plate will be discussed first, followed by the definition of various parameters used to present an integrated view of the various motions.

6.2 General Performance of the Force Plate

The force plate developed has been used for nearly two and a half years. It is larger than those reported in the literature having a surface area of 16 sq. ft. Cunningham's[6] force plate measured 15" x 20" and Gola's[28], approx 1.73 sq. ft. Some investigators have used two plates set on the walkway in order to accommodate the normal cadence. In the present design, the long length of the platform (approximately 6' at the long side when the subject walks at approximately 8" from the base of the platform) allowed capture of more than one stride. No constraint was imposed on the subject and no pacing was required. The width of the platform (4' at the center of the triangle) permitted easier subject manoeuvrability and allowed locomotion studies on subjects with large motions in the frontal plane[10]. The size of the force plate therefore allowed pathological or abnormal gait and permitted certain specialised sports motions [34].

The current force plate with its unique suspension system (evolved while considering various possibilities to make the structure statically determinate) was classified as a 'suspended force platform' in an earlier chapter. However, the structural behaviour of the suspension system is similar in certain respects to the 'rigidly supported' type of force platforms. The three vertical suspension elements fixed at one end to the force platform, are held by a short length of wire attached at the free end as described in Chapter 3. This allowed free horizontal movement of the suspension element although the elements were constrained downwards in the vertical direction only. The vertical load or body weight always acts downward on the force plate and, in the present design, the vertical

suspension elements will be subjected to axial tension irrespective of the position of the load on the force plate. The majority of previous investigators used a rectangular force plate as indicated in the review of force plates. In the case of a four-cornered support system, there is an area at the center of the force plate known as a 'kern or core'[91] within which a load must be placed in order for the four supports to experience compression. Loads placed outside the core or kern would produce tension in one or more of the supports. Output from such plates which employ unidirectional force transducers may be questionable. An engineering analysis relating plate stiffness, support stiffness and load weight to kern shape has been investigated by Harris et. al[92]. The current design using the three point support system eliminates the problem of kern areas.

The horizontal suspension elements were constrained by tension wires from moving in the direction in which they are supported. The tension in the horizontal wires is adjusted to a predetermined value and the wires allowed movement in other directions of load application. This freedom of motion results in the transducer being insensitive to load application in other directions. Thus every sensing element in the current force platform measures a force component either parallel or perpendicular to its axis and the six components of reactions constitute a statically determinate structure. The reaction load of the force platform can be determined completely by measuring the six reactions without any further complicated processing of the primary signals. Some of the force plates reviewed with more than one set of sensing gauges on the same support would need more complicated processing of the signals in order to define

the desired statically indeterminant quantities. The determination of the center of pressure using the current force platform was relatively simple when compared to other force plates.

The force plate developed has a range of 300 pounds and ± 60 pounds for force measurement in the vertical and horizontal directions respectively. Other force plates reviewed earlier have very similar load ranges and this has been found adequate for normal locomotion studies on subjects weighing up to 250 lbs. The load calibration curves shown in Fig. 14 through 16 indicated the response to be highly linear. The linearity in the vertical direction was found to be 1% and ± 0.5% in the two horizontal directions. These values were measured for an accurately aligned and balanced force platform. In Cunningham's force plate the maximum deviation from the mean for the vertical load was found to be less than 4 lbs. No figures are reported for calibration in the horizontal directions. The repeatability in calibration was less than 1% for the current force plate. Any deviations from the general characteristics were recognised as misalignement of the suspension element. The suspension, with all the provisions for fine balancing, was checked before every test and the calibration procedures described in section 3.2.5 were carried out as a general routine.

In spite of its largeness, the force plate showed good sensitivity for force measurement in all the three directions. The sensitivity was ± 1 pound at the plate center for vertical loading and ± 1/2 pound for loads in the two horizontal directions. Gola's force plate[28] which was about 1/10th in size of the force plate developed, was claimed to have a sensitivity of 0.1 lb for vertical load and 0.03 lbs for load measurement

in the horizontal directions. Figures for several other force plates reviewed earlier are not available for comparison.

Since strain gauge systems are sensitive to temperature changes, the various sensing elements were provided with temperature compensation gauges as outlined in section 3.2.3. The effectiveness of temperature compensation was checked by monitoring the signal output from the transducers for several hours. The drifts in the vertical and horizontal directions were 2% and 1% respectively. On further investigation the drifts were found to be the result of drifts in the custom built amplifiers. This was checked further by connecting each strain bridge network to a high quality Brüel and Kjaer strain indicator model No. 1526. The resulting drift in this case was measured at less than 0.1%. Figures on drift have not been reported by other investigators. The drift from the strain bridge amplifiers was nullified by adjusting each bridge individually before every test.

The cross-talk and its influence on the force measurement was emphasized in Section 3.2.5. Cross-talk would be present in any multi-component measurement system and the cross-talk error would depend on the relative magnitude of all the input forces and moments. An accurate estimate of the cross-talk should involve different combinations of the multi-component load. Since one of the design criteria was to keep the cross-talk at a low level, an experiment was designed to attempt to monitor the cross-talk for different load ranges.

The calibration jig described in section 3.2.5 was loaded with different combinations of loads. It was found that the upper bound on cross-talk occured when the force plate was loaded to 75% of the load range in the

vertical direction and approximately 85% of the load range horizontally. The upper bound on the cross-talk error was 0.15% in the vertical and 0.2% in the horizontal direction. Cross-talk could not be fitted into any definite mathematical relationship. The rather complex suspension elements with tensioning wires attached, permit movements in all directions except in the direction of load sensing. The low cross-talk error might be a result of the multi-directional hinge system. More detailed study on cross-talk errors was beyond the scope of the present work. Cross-talk errors have not been reported for any of the other force plates. Gola[28] has proposed plots of the cross-talk errors based on certain theoretical analysis for his force plate.

The fundamental natural frequency of the force plate was determined experimentally as outlined in Section 3.2.6. Even though one would desire a much higher frequency than that which was determined (17 HZ in the vertical direction and 16 HZ in the lateral direction), the largeness of the force plate puts a limitation on the upper bound. The current design has been adopted in the development of a force plate now in use at the Manitoba Rehabilitation Hospital for Children. The top plate is made of light weight alloy and is approximately two thirds the size of the force plate developed in this thesis. The fundamental natural frequency of the modified plate is approximately 75 HZ. The fundamental frequency of a walking cycle is of the order of 1.5 to 2HZ, and is below the fundamental natural grequency of the force plate. Future modifications will improve the resonant frequency of the system. For ease of reference, Table 1 lists the characteristics of the force plate developed.

6.3 Force Records Obtained for Normal Locomotion

Experimental measurements were taken on several subjects (predominantly male) in level walking on the force plate to understand normal locomotion. Figure 35 shows the tracing of the three components of force as measured on the force plate for a subject who does not show any abnormality (assessed visually) in walking. The individual traces A, B and C in Fig. 35 represent the vertical, medio-lateral and posterior-anterior force components for the same subject obtained over six months. All traces show a very consistent pattern in ground-reaction components and the small phase shifts in the various groups of curves are a result of slight differences in the speed of walking, each time the subject traversed the force plate. A normal procedure adopted in several studies involved pacing the subjects to a predetermined speed with the help of a metronome. In the present study, it was concluded after a preliminary investigation that any imposition on the subjects normal gait is bound to alter the normal locomotion patterns and would reduce the usefulness of the study. During the various locomotion studies reported in this work the subject always walked at his normal cadence.

With reference to the complete description of normal gait (presented in section 2.2) the vertical component traces in Fig. 35 have a typical shape with a double-peak and two smaller peaks. The peaks represent the vertical upward and downward acceleration of the body. The first small peak occurs shortly after heel strike, when the body rolls over the supporting leg, and the second peak occurs when the leg pushes the body up, just before the other leg strikes the floor. The X-component

(posterior-anterior) and Y-component of forces (medio-lateral) also exhibit typical shapes, approximating a full smooth wave during the stance phase in the respective directions. The sign convention for forces is based on the reference coordinate system shown in Fig. 5. Walking is always assumed to be along the X-axis and force components are expressed with reference to a right handed coordinate axes. Thus, negative posterior-anterior and medio-lateral ground reactions are obtained when the subject hits the force plate with his left heel while approaching the force plate from the right direction. A negative ground reaction in the posterior anterior direction indicates an external force tending to retard the forward motion of the body and a negative medio-lateral reaction represents an external component acting inwards to the body. Since the Y-direction changes in accordance with the right handed system when the subject traverses the force plate approaching from the left side, a positive posterior-anterior component indicates an external force tending to retard the forward motion and a positive medio-lateral component indicates an external force acting inwards to the body. The vertical component of ground reaction always acts in the positive Z-direction irrespective of direction of traverse. Since all the signals were recorded by using an analog tape recorder, it was not possible to switch the polarity of signals for various strides. This aspect has to be considered when analysing the force records. Force records in Fig. 35 represent a double step or complete gait cycle for the subject. During several data collection runs, the subject was not presented with any predetermined pathway. Individual force records were analysed one by one and the multiple force records presented are the result of individual

analysis of each force pattern. Several tests were obtained over a time interval for several normal subjects and the consistency in force tracings were present in all the tracings to such an extent it was possible to identify a subject by looking at the force curves. The single foot force traces showed the characteristic two peaks and a valley. Variations peculiar to each individual subject were observed and could be attributed to different mannerisms in walking.

In order to compare the force records obtained for normal subjects in this study with those of existing records from other studies, the ground reaction components obtained by Cunningham et. al[6] are reproduced in Fig. 36. The original records, replotted on a larger time scale, were digitised and reduced to a smaller scale for proper comparison with the records obtained in the present study. Even though Cunningham's vertical component shows a similar pattern, with a double peak seen in normal gait, a rather large valley between the two peaks with a force about 0.4 times the body weight prior to the push off phase was never obtained in any of the normal gait records in the present study. Such a large valley could be attributed either to the poor resolution of the force plate or to the subject being paced at a speed well above his normal cadence.
The posterior-anterior component compares well with the general force pattern obtained in the present study. The medio-lateral component shows an unusual double peak never seen in any of the records obtained in the present study. The unusual double peak seems to indicate a large stiffness in one direction of the force measurement. The magnitude of forces could not be compared because the scales are not indicated in the original records of Cunningham[6]. Fig. 36 also shows the average data

obtained from sixty healthy subjects by Seliktar et. al[93]. Only the vertical and posterior-anterior component have been reported and hence the medio-lateral forces could not be compared. Seliktar's force pattern compares well with the records obtained in the present study both in shape and magnitude. Greater, in-depth comparisons other than what has been stated above is difficult. The different nature of each researcher's system for acquiring data and defining the individual parameters has not been well documented.

In order to assess the effect of the large mass of the force plate and its influence on the force signals, the recordings of force components of a subject with an additional plate weight of 80 lbs was obtained. In Fig. 37 the continuous lines represent the force signals obtained when the subject traversed the force plate with an additional 80 lbs added to the centroid of the plate and the dotted lines represent the force signals without the extra weight. The left hand corner of Fig. 37 represents the two vertical components for a single step and the tracing on the upper right for a double step on the force plate. The posterior-anterior component is shown at the bottom of the Figure 37. The tracings have been shifted in time to see the closeness of the two profiles. As can be seen from the Figure 37 there is a close match between the two traces even though a few finer details appear to be filtered in the force records obtained with the increased weight. Due to malfunction of one of the medio-lateral strain bridge amplifier at the time of this study, the medio-lateral tracings could not be obtained.

6.4 Synthesis of Force and Moment Records

Like inanimate machines, one human body varies greatly from another in build, musculature and mannerisms in walking. The combined action of internal muscle forces and the external forces results in a different pattern of ground reaction forces for different subjects. During the single support phase of the leg the resultant force exerted by the foot on the ground at each instant of time is equilibrated by the sum of inertia and gravity forces acting on each segment of the body. In order to express this variation in ground forces generated for various individuals quantitatively, a set of physical parameters could be used. Numerous parameters of gait are interrelated but none is probably capable of providing a total description of gait. The feasibility of measurement and analysis generally reduces the choice of parameters to two groups: (i) kinematical and (ii) dynamical. If the anthropometric information for various parts of the body are known, either of the two groups can be deduced from each other. To date no simple method has been presented except Contini's anatomical tables[59] wherein the numerical values of mass and inertia are measured accurately from living subjects. In view of this, the ground reaction force at the foot was chosen as the working parameter. Although several relevant force representations could be used to quantify gait, not all can be measured with the same ease as the ground reaction force. The majority of studies have assumed that the main effects of locomotion are apparent in the plane of progression only. This assumption has been made to simplify the analysis, but the results from the present study indicate that the assumption is not justified. The first step towards obtaining a synthesised picture of locomotion resulted

in the development of a set of symmetry indices described in the next section. The validity of these indices is confirmed by relating them to other indices developed from moment parameters associated with the upper body motion.

6.4.1 Symmmetry Indices for Ground Reaction Forces

Examining the force curves obtained for normal locomotion (Fig. 3), one can observe a high degree of symmetry as the body alternates in support on the two lower limbs. The medio-lateral and posterior-anterior force curves swing symmetrically about the mean zero line and there is a complete repetition in the vertical trace between cycles, even though the force exerted on the ground did not necessarily conform to a pure sine wave. A parameter having the dimension of time was considered to quantify the symmetry in motion. If one considers the area under the force curve, the area represents the momentum or impulse for the gait cycle. In a perfectly regular gait we would have complete similarity from cycle to cycle and the body would return exactly to the original state after one cycle of walking. Exactly similar motions would be present on either side of the body with a half-cycle phase shift. If we consider such a perfect gait cycle, there is no net change in velocity of the body in one cycle and therefore the net momentum does not change. In effect, the impulse over one cycle must be zero. The impulse can be obtained by integrating the force curves. If we consider the medio-lateral (side to side) and posterior-anterior (forward-backward) forces, the net impulse obtained by integrating the force curves on either side of the base line should be zero for a perfectly symmetrical motion. In the vertical direction, the

body goes through an upward and downward movement(reviewed in section 2.2) and the dynamic vertical reaction component represented in Fig. 35 has peaks and valleys. Since the body would return to the same state for a perfectly symmetrical gait cycle, the net impulse in the vertical direction must be zero. The net impulse can be found by vectorially adding the integral of the vertical reaction curve and the integral of body weight for the given gait cycle. In the present study the relative integrals of force curves in the three directions were expressed as symmetry indices in the respective directions. The symmetry index in the vertical direction hereafter denoted as vertical impulse ratio 'VI' was determined from the following relation:

$$VI = \frac{\text{Intergral of vertical reaction}}{\text{Integral of body weight}} \qquad - \qquad 6.4.1.1$$

The integrals in relation 6.4.1.1 were evaluated from the vertical force traces obtained for different subjects. The vertical impulse ratio should be unity for level walking in any type of gait.

The symmetry indices in the two horizontal directions were determined by integrating the force curves in the respective directions. As explained in the review of normal locomotion (Section 2.2), the two components alternate from side to side in the case of the medio-lateral component and forward to backward in the case of the posterior-anterior component. The symmetry indices could be determined by comparing the integral of the force curves generated by the two lower limbs. The MLI

(medio-lateral index) was determined by using the following expression:

$$MLI = \frac{\int_{o}^{t_1} R_{Y_\ell} \, dt}{\int_{o}^{t_2} R_{Y_r} \, dt} \qquad - \qquad 6.4.1.2$$

where

R_{Y_ℓ} - medio-lateral reaction force in left limb support phase

R_{Y_r} - medio-lateral reaction force in right limb support phase

t_1 - left limb support time

t_2 - right limb support time

Similarly,

$$PAI = \frac{\int_{o}^{t_1} R_{X_\ell} \, dt}{\int_{o}^{t_2} R_{X_r} \, dt} \qquad - \qquad 6.4.1.3$$

where

R_{X_ℓ} - posterior-anterior reaction force in left limb support phase

R_{X_r} - posterior-anterior reaction force in right limb support phase

t_1, t_2 are as defined in eqn. 6.4.1.2

6.4.2 Symmetry Indices Applied to Normal Gait

A group of normal subjects were analysed with a view to establishing the usefulness of symmetry indices for characterising locomotion. Only ground-reaction forces were recorded for the subjects. Since the subjects were available for several force records, a statistical analysis on the results was obtained. The integration of the force

records were performed using an analog computer (model EAI 180) and a planimeter. The results are presented in Table 3. The normal subjects show a high degree of symmetry as is evident in the symmetry indices reported. In the case of irregularity in gait, the uneveness in the force records should be expected to show the asymmetry in the force patterns. The symmetry indices for the several subjects with abnormal locomotion analysed as part of this study will be discussed in a subsequent section.

6.4.3 Symmetry Indices for Upper Body Dynamics

The upper body motions in normal human movement involve small excursions about a nominal trajectory defined by a mean forward velocity and zero mean values for other motions and velocities. The entire body center of mass moves forward at a mean velocity with a small sinusoidal variation and can oscillate laterally and vertically. But in the event of dysfunction of any of the lower extremities, the movement of the upper body would try to compensate to keep the whole body in dynamic equilibrium. The net dynamic moment vector at the hip joint is obtained in the present study using equation 4.4.3. The equation represents the total dynamic muscle moment about the hip joint defined in the upper body coordinate system. The integral of the moment curves divided by the time of support (total single support) for each limb would be proportional to the work done by the muscular forces on the upper body. The total work done by the muscular forces at the hip joint on the upper body during the single support of each limb would then show compensatory movements brought about by other limbs not in support with the ground. The work performed

about each support limb as the body alternates its support between the two lower limbs should be equal in the case of a symmetrical gait. Consequently a set of symmetry indices similar to the ones derived for ground reaction-force (Section 6.4.1) were used for upper body locomotion. As will be shown when presenting the results on upper body moments, the moment about the Z-axis in the body coordinate system is considerably small when compared to the moments about the X and Y axes. Hence symmetry indices for Z-axis moments are not considered. The symmetry indices for the upper body are defined about the two principal planes of motion (sagittal and frontal) as follows:

Symmetry index in sagittal plane referred to as 'SSP' is given by

$$SSP = \frac{\int_0^{t_1} M^b_{B_Y}{}_{right}}{\int_0^{t_2} M^b_{B_Y}{}_{left}} \cdot \frac{t_2}{t_1} \qquad - \qquad 6.4.3.1$$

where, $M^b_{B_Y}$ - muscle moment about the body Y-axis for the right and left limbs

t_1 - total single support time for right limb

t_2 - total single support time for left limb

Similarly, the symmetry index in the frontal plane or 'SFP' is given by

$$SFP = \frac{\int_0^{t_1} M^b_{B_X}{}_{right}}{\int_0^{t_2} M^b_{B_X}{}_{left}} \cdot \frac{t_2}{t_1} \qquad - \qquad 6.4.3.2$$

where

$M^{b}_{B_X}$ - muscle moment about the body X-axis for the right and left limb

t_1 and t_2 are as defined before

In comparison to equation 6.4.1.2 and 6.4.1.3, the symmetry indices for the upper body are defined with the order of limbs reversed in the expression. The reason for reversing the order will be clear when the results are presented. The results to be presented in the next few sections will qualitatively and quantitatively analyse the force patterns obtained for various subjects and discuss the various symmetry indices obtained for each subject and their relation to the character of gait abnormality.

6.5 Analysis of Force and Moment Records Obtained for a Normal Gait

Several investigators have studied normal locomotion using different approaches and a few have attempted to synthesise abnormal locomotion by measuring the displacement patterns of limbs in the plane of progression[38,40]. Since locomotion involves a very sensitive balance on one foot when the body is in single support phase, the continuous process of fall and recovery of the body as it alternates between the two feet can be seen by the undulating pattern in ground reaction forces. Some of the fine balance and symmetry seen in normal locomotion need not be present in the case of abnormal gait. Injury to any one of the limb joints or

musculature associated with the joint will shift the fine balance that would be present otherwise. Since an overall balance has to be achieved to keep the body in equilibrium, compensatory forces and moments in some joints of the body must come into play as a result of reduced or increased displacements at other segments of the body. Such a characteristic of abnormal locomotion can be observed easily in an amputee's gait. The ground reaction forces and displacement patterns, as reviewed in chapter 5, were obtained on several subjects with gait impediment to understand abnormal gait. Before presenting these results, the following points should be brought into focus. The force records obtained for various subjects represent the ground reaction as measured by the force plate from the time of contact of the foot with the plate until the foot completely leaves the force plate. For a short period of time at the beginning and end of the record, the foot in contact with the force plate is in double support and provides a period of indeterminacy in force measurement. The force values obtained during these periods are not the total indication of the reaction force on the body segment. Even though this does not present a great problem in the understanding of force patterns, the use of force values for obtaining reaction moments about the joint segments is not valid. Thus, the analysis is confined in the present study only to the period of complete single support on the limb considered. The beginning and end of complete single support is designated 'BTS' or beginning of total support and ETS or end of total support. These instants are marked accordingly in all the moment plots. The 'BTS' and 'ETS' were established by carefully examining the biplane

photographic films and the corresponding force values obtained by proper synchronization of force and movie records.

To check the validity of the mathematical model proposed in Chapter 4, a complete locomotion analysis was performed on a normal subject. The subject, henceforth called subject A, does not present any gait abnormality as examined visually and has shown good total symmetry in force patterns over several trials. This subject's force records compare well with the one considered by Bresler et. al[22] in their investigation. Figure 38 represents the single foot force records obtained for subject A. The net upper body moments ($M^b_{B_X}$, $M^b_{B_Y}$, $M^b_{B_Z}$) about the translatory upper body axes at the hip joint and about the reference axes (M_{B_X}, M_{B_Y}, M_{B_Z}) are presented in Fig. 39. The net upper body moment, obtained from Equation 4.4.3., represents the net muscular moment at the hip joint and is primarily responsible for the movement of the upper body.

The transformation matrices described in Section 4.6.1 define the relationship of the net upper body moment in the upper body axes to the moment in the space frame axes. Although the time courses of the net upper body moments in Fig. 39 are typical of the subject 'A', they compare well qualitatively with those obtained by Bresler[22]. Bresler's moment traces are also shown in Fig. 39. These traces represent the moments for the full single support cycle. The moments have been obtained in the

the full single support cycle. The moments have been obtained in the general X and Y space coordinate system. The details at the beginning and end of Bresler's traces will not be seen in records of subject A because they are not considered in the present analysis. The moment values obtained by Bresler are somewhat higher. Cappozzo et. al[94] and Boccardi et. al[33,35] have also obtained net moments at the hip joint in the sagittal plane and the profiles are very similar to those shown by Bresler and their moment values are comparable. Examining the traces of net upper body moment in the body coordinate system for subject A, it can be observed that the moment curves about the X and Z axes in the reference and body frame have the same general pattern with almost the same moment values. The magnitude of the moments about the Y axes show the smallest differences and the general pattern is the same. This closeness is expected because upper body locomotion for normal gait involves only small excursions about the neutral position of the body.

Even though mathematical techniques for defining limb motions in a body coordinate system have been proposed by a few researchers[71,88], none have applied the models for locomotion analysis. Thus, the upper body moments defined in the body axes could not be compared with any available records. But the general nature of the various moment curves could be explained by the biomechanics of locomotion. Motions at the joints are a result of internal muscle forces and external forces represented principally by the influence of gravity and inertia of the body. While standing erect, the center of gravity of the body is anterior to the hip joint tending to flex it and anterior to the ankle joint, tending to dorsiflex it. Terminology used commonly to explain body

motions is illustrated in Fig. 40. The body stays in balance by the combined action of the plantar flexors of the ankle and extensors of the hip. To begin walking the plantar flexors of one leg are relaxed, allowing the body to fall forward on that side and the other leg is swaying forward at the hip. During the swing phase, forcible hip flexion in the swinging leg accelerates the swinging leg forward, producing a flexion at the knee during mid-stance and the leg begins to extend, reaching full extension at the time of the next heel contact. Immediately on heel-contact with the ground, the pelvis and the superincumbent mass remain approximately vertical. The hip is in flexion at this point. As the body weight is applied in this position, the ground reaction force causes flexion moment about the hip because its line of action passes behind the knee and ankle joint and just anterior to the hip joint. This initial flexion moment at the hip joint can be seen in the traces obtained by Bresler (Fig. 39). It will not be seen in the records obtained for subject A since only those force records that correspond to total single support period were considered in the present analysis. As the major mass of the body rotates over the ankle and knee joints between foot-flat and mid-stance, the ground reaction force passes through and then behind the hip joint. Thus, the hip moment starts swinging from a net flexion moment to a hip extension moment. An extension moment of nearly 350 inch pounds was obtained for subject A while Bresler's subject has generated close to 450 inch pounds extension moment. The normal hip motion has been observed to be approximately 40° to 45° relative to the vertical axis in the sagittal plane. It changes from approximately 25° to 30° of flexion at heel contact to approximately 15° to 20° of extension (hyper extension) at

toe off. The upper body attached to the lower limb at the hip joint is kept erect by the extensor muscles. They resist the flexion moment. Even though the upper body is assumed by many investigators to stay erect during normal locomotion, the upper body rotates in all the planes of motion even though the rotations are considerably smaller than those of the lower limb. As the lower limb rotates forward between foot flat and mid-stance, the hip extension moments in the sagittal plane bring about a tilt of the upper body (longitudinal trunk extension). The body maintains equilibrium by slightly leaning backwards to compensate the accelerating force generated. This explains the reduced sagittal plane moment values about the body coordinate system for subject A.

Angular rotations in the frontal plane are far less than those in the sagittal plane. The motion of the hip joint in the frontal plane was presented in Section 4.5. The lateral components of moment reflect the requirements of bipedal walking. In shifting from one leg to the other, the torso is pushed one way then the other and moments which are recorded will be somewhat proportional to the elevation of the joint above the ground. This points out the relatively large magnitude of the lateral component of moment at the hip as seen in Fig. 39 for subject A. Bresler's curves show similar variations. The lateral moment is a product of the vertical component, medio lateral component and the position of the joint considered in the XY and YZ plane. The side to side motion of the pelvis is approximately 3" for normal locomotion which is about 1/10th the length of leg. Using the general order of ground reaction values obtained in this study for normal locomotion, the contribution of medio-lateral forces to the lateral hip moment is found to be approximately twice

those due to the vertical reaction forces. Thus, any large changes in the medio-lateral reaction forces would result in large lateral hip moments. This aspect can best be explained when analysing several abnormal locomotion patterns. The moment about the body fixed coordinate axes in the Y direction did not show much variation for subject A. As pointed out in Chapter 4, the upper body rotates very little about the vertical axis and dips to about 4° or 5° in the frontal plane. One should not expect with this small motion to see large variations in the two moment values. The lateral hip moment reaches a maximum when the maximum vertical load is being applied. The pelvis on the swing side tends to drop when its supporting member leaves the ground to initiate swing. At this instant, substantial moments are generated which tend to adduct the hip joint. A peak adduction moment of about 600 in lbs was obtained for subject A. Only a few investigations[22,35] have precisely measured the lateral moments. The computation of lateral moment needs measurement of the lateral position of the various joints and the medio-lateral forces.

Rotation moments about the vertical axis have not been reported by any investigator. The moment values are generally very small with a maximum of 100 inch pounds for subject A and show very little variation in the body coordinate axes. This supports the general assumption that rotations about the vertical axis are generally small for normal locomotion. With this background the next section discusses the results obtained for several abnormal gaits.

6.6 Analysis of Force and Moment Records obtained from Studies of Abnormal Gait

Several subjects with gait impediment were studied to better understand the abnormal locomotion. It was felt that, by analysing subjects who have suffered injury to various joints responsible for locomotion, some aspects of abnormal gait could be understood more clearly. Consequently several subjects undergoing rehabilitation after surgery to the injured limbs were chosen for analysis. The locomotion measurements as outlined in Chaper 5 were performed. Wherever possible, the same subject was analysed at different stages of recovery in order to monitor whether changes could be detected in their gait. Before presenting the individual results, a brief background is presented on each subject. Amongst these subjects, the results on a few, each with a different gait impediment will be presented in this thesis. Subject B suffered multiple injuries in an automobile accident and underwent corrective surgery for a broken femur (thigh bone) in the right leg. Both ankles suffered multiple fractures. Figure 41 shows the ground-reaction force patterns for subject B approximately six months after discharge from hospital. The subject, who normally depended on crutches, could and did walk without the help of crutches. Figure 41 represents the ground reaction components.

Kinematic measurements were not obtained for the first trial. Figures 42 and 43 represent the force and moment records obtained for subject B, thirteen months from the first trial. The subject was able to walk without the help of crutches and a complete locomotion measurement was obtained at this time. Even though such measurements were obtained

for subject B with the subject walking with the help of crutches, the discussion of results is not attempted in this thesis. The crutch-locomotion presents more difficulty in view of multiple support phases when the subject strides over the force plate.

Subject C suffered injury to the right ankle. Figure 44 and 45 show the force and moment traces at the end of 5 weeks of rehabilitation treatment at St. Boniface hospital. The subject could not be monitored over a longer period due to his unavailability. The left side traces in Figures 44 and 45 represent the records for the left limb support and the ones on the right hand side are those obtained for right limb support.

Subject D, on whom gait records were obtained over time, had underwent lateral menisectomy in the left knee joint (surgical removal of cartilage at the knee joint) and the right leg was considered normal. Figure 46 shows the ground force records twenty one days after the subject was discharged from hospital. The left hand traces in Figure 46 represent the force records for left limb support and the right side traces, those of right limb support. The subject was available for a subsequent trial and Figure 48 represent the force records obtained three weeks after the first trial. As in previous records, the left and right limb records are shown on the left and right side of Figures 46, 48. The moment records for subject 'D' on his first trial are shown in Figure 47.

Subject 'E' has a permanent gait impediment due to osteo-arthritis. The subject underwent hip replacement surgery and has a femoral head prosthesis (Charnley's) inserted into the left hip bone. The subject also suffers pain in his right hip joint due to arthritis and walks with the help of a cane. Figure 49 represents those force records for subject 'E',

and was obtained when he walked on the force plate with the cane in his left hand. Difficulties in the analysis were experienced for subject E similar to those in the case of crutch walk for subject B. The cane enhances lateral stability for gait and the mathematical model has to be altered to take account of the load sharing between the cane and foot. Hence, at the present time, only the ground-reaction forces are considered for analysis of subject E's gait. Figure 50 represents the force records obtained for subject E on a day when he was experiencing more pain in his right hip joint. With this background on the various subjects, the anomalies in the force and moment records will be examined in the following paragraphs. The subjects may not be referred to in the same sequence, and this is done to make the presentation of results easier.

Subject D: Referring to the pattern of force curves obtained for subject 'D' (Figs. 46 and 48) the vertical component of the ground-reaction for the left leg during the first trial (Fig. 46) shows a more shallow valley between the two peaks and a smaller peak at the push-off phase in comparison to the right leg trace. The first peak in both vertical traces is similar in magnitude so that, as reviewed in Section 2.2, the maximum forces reached at heel strike are comparable. The peak heel strike forces are indicative of the action of plantar-flexors at the ankle joint. Any injury to the ankle would reduce the magnitude of these heel strike forces. As the swinging leg and the center of gravity of the body move forward, the ankle moves from maximum plantar flexion to maximum dorsiflexion just before heel-off. The gastrocnemius and soleus muscles whose eccentric contractions control the motion of the ankle in

dorsiflexion as well as providing the peak force during push-off (represented by the second peak in vertical component) have their origins around the knee joint. A subject with injury to the knee joint could be expected to avoid the powerful contraction of these muscles. The reduced second peak and shallower valley seen in the vertical force traces of the left limb is indicative of the subject suffering from injury to the left knee joint. Shifting attention to the two horizontal components of forces, the posterior-anterior components in Fig. 46 have a more or less similar pattern for both limbs. The variation in posterior anterior component of ground reaction represents the net acceleration and deceleration forces of the body about the point of support. Since the upper body is expected to go through the same vertical excursion during each half of the gait cycle (unless one of the lower limbs is shorter than the other) the net force needed to propel and retard the body in the forward-backward direction during the swing phase must be more or less equal for each limb. For subject 'D' the 'PAI' (defined in section 6.4.1) during the first trial was 0.91. The medio-lateral reaction curves in Fig. 46 for subject 'D' have shown by far the greatest variation in ground-reaction between left and right leg. The 'MLI' for trial 1 was 0.74. This asymmetry in traces could be easily seen by examining the records of medio-lateral components in Fig. 46. For normal locomotion, the angular rotations of various segments of the body in the frontal plane are considerably less than those in the sagittal plane. Even though the knee flexes to about 65° during the swing phase and a maximum of 15° during the stance phase, a 4° rotation about the knee occurs in the frontal plane. In the case of injury to the knee even this smaller

rotation would not be present (to avoid pain). As pointed out earlier in Chapter 1, compensatory forces and moments in order to maintain stability of the body may be brought about by the upper body, in the event of joint dysfunction in the lower limb. In the case of subject 'D', an examination of moment records in Fig. 47 reveals the increased moment values obtained when the left limb was in support. The moments about the reference and body X-axis are greater for the left limb support (the injured limb) than the right limb. The moment values about the Y-axis are comparable. To express the variations more quantitatively, the symmetry indices 'SSP' and 'SFP' were obtained from the moment records. For subject D, the 'SSP' and 'SFP' during the first trial were 1.04 and 0.66 respectively. As pointed out in section 6.3.3, the symmetry indices for the upper body were expressed with the ratios reversed. The compensatory movements from the upper body to maintain stability would be expected to be greater when the injured limb is in the support phase. The compensation could be seen from the symmetry indices obtained (ref. Table 4). The 'MLI' index corresponds to the variation in force obtained in the frontal plane of motion and the similar index for the upper body would be the moment symmetry or 'SFP' index in the frontal plane. The 'PAI' index or moment symmetry in the sagittal plane should correspond similarly with the 'SSP'. From the values in Table 4, the values of' MLI' and' SFP' are very nearly equal and 'PAI' and 'SSP' also show similar trends. Similar indices were obtained for upper body moments about the space frame and it should be pointed out that there is a better correlation in the index values obtained in the body frame system. The vertical impulse index 'VI' was not examined for abnormal locomotion. Since the net movement in the vertical direction is

a result of interplay between various groups of muscles responsible for motion in the sagittal and frontal planes, physiological interpretation of variations in 'VI' for abnormal locomotion is not attempted in this thesis.

The force records obtained for subject 'D' on his second trial are shown in Fig. 48. The moments are not presented due to a difficulty in data abstraction. However, in comparison to the first trial, the increased valley between the two peaks in the vertical trace could be noticed. The peak during the push-off period is higher too. The medio-lateral force traces show a reduction in asymmetry as is evident by the symmetry index value (Table 4) approaching unity. The posterior-anterior traces do not show any observable changes.

Subject C: Subject 'C' suffered an injury to the right ankle. Referring to Fig. 44, the vertical component for the left leg strike shows a higher first peak compared to the second peak (push-off). The first peak is indicative of a strong, above normal heel strike and suggests that the body is coming down more strongly as a result of reduced push-off forces from the injured limb (right leg). The reduced activity of gastrocnemius and soleus muscles will produce a less than normal push-off force as evident in the vertical trace for the right leg. Gastrocnemius, along with Soleus, forms the achilles tendon and has a commom insertion on the middle posterior surface of the ankle joint. Thus, an injury to the ankle joint could be expected to cause a reduced activity of this muscle group. In contrast to subject D, the posterior-anterior forces for subject 'C' show greater differences in the force generated in the support phases

of the two limbs. Since the body pivots about the ankle joint during the support phase, the large fore-aft shear forces would be avoided by the injured limb and, hence, the reduction in posterior-anterior ground reaction forces should be expected. The two-fold reduction seen in posterior-anterior reaction forces should produce a corresponding change in the compensatory movements of the upper body. The 'PAI' and 'SSP' for subject 'C' were 1.76 and 1.70, respectively. The medio-lateral forces are also smaller during the right limb support. Values of 1.55 and 1.70 were obtained for 'MLI' and 'SFP', respectively. It was also observed, that in the case of subject 'C', the stance phase for the injured limb is smaller when compared to the sound limb. In comparison to subject 'D', the symmetry indices in the upper body reference frame did not show as good a correlation with the 'MLI' and 'PAI' indices. The 'SFP' and 'SSP' indices were 2.23 and 0.69 respectively.

Subject B: Subject 'B' had a severe gait abnormality at the time the first locomotion records were obtained (Fig. 41). The subject has a slightly shortened right leg (approximately 1") as a result of the surgery to the right leg. The subject had a large upper body tilt, leaning to the left side, and this could be viewed as a compensatory maneuver by the upper body to maintain stability and equilibrium. The records in Fig. 41 were obtained at the early stages of recovery from injury. At the time of the records in Fig. 41, the subject was on crutches for ambulation. The records in Fig. 41 represent the ground-reaction components when the subject attempted to walk without the help of crutches. As could be seen from the force records in Fig. 41, the subject produced the most unusual

pattern of ground reactions. The force records represent a double step on the force plate starting with right heel strike. The vertical component of ground-reaction is characterised by below normal right heel strike forces followed by above normal push-off forces. The left leg forces are closer to normal. The posterior-anterior components show similar reductions during right leg support. The medio-lateral force reactions, in comparison to the other two components, were always on one side of the normally defined neutral position or zero line. Some anomalies in subject B's force records could be explained by considering the biomechanics of such an abnormal gait. Figure 51 shows the frontal plane view (viewed posteriorly) of a normal subject standing vertically and another standing with a tilted upper body posture (leaning to the left). In the case of the normal subject, the body weight acting downwards would be balanced by two equal reaction forces at the foot during normal standing. A static muscle moment would be produced at the hip joint to keep the body vertical. For a subject with a lean to one side, the lean could be viewed as a result of compensatory effort on the part of the neuro-muscular system to reduce the load (to avoid pain) transmitted to the injured hip joint (assumed to be the right in the case considered). To maintain stability as a result of the lean, the left hip joint would be shifted outwards in the frontal plane. The resultant movement (an adduction of the left lower extremity) would subject the hip muscles to a net abduction moment to keep the hip joint from collapsing sideways. The body stays in equilibrium under the action of these forces and moments. Considering the dynamic case when the body shown in the right side of Fig. 51 begins to move, the locomotion can be discussed as follows: commencing from the

time the right extremity leaves the ground, the pelvis on the swing side would drop down from its neutral position. Substantial moments are generated at this instant which tend to abduct the hip joint, resulting in a reduced hip moment. The upper body would move inwards (from a lateral hyper extension to lateral flexion) in the frontal plane to maintain equilibrium and a large angular momentum would be produced in the upper body. In the case of an injured or diseased hip joint, the hip rotation of the right limb would be restricted and the right lower limb would move medially as a result of upper body momentum. Hence the left limb would strike the floor at an oblique angle producing a resulting reaction force pointed medially. The degree of obliquity may be related to the limited joint motion, muscle rigidity or inability to tolerate the muscle forces. The resultant medio-lateral ground reaction forces will also depend on the above factors. The left limb movement follows the normal pattern but the limb abducts more than seen during the swing phase. The locomotion described is typical for the particular subject considered and, as discussed later, subject 'E' who had a similar upper body tilt produced similar medio-lateral force patterns.

Subject B was examined from time to time but, due to the difficulties encountered in analysing crutch locomotion (multiple supports on the force plate), interpretation of the statically indeterminant results is difficult at present. Figures 42 and 43 represent the force and moment records obtained for subject B thirteen months after the first trial. Figure 42 represents a double step stride on the force plate. The injury recovery can be seen easily by looking at the medio-lateral ground reactions and symmetry induced. The subject still has a slight lean on

the upper body. A complete gait study was conducted on the subject and Figure 43 represents the upper body moment curves for subject B. The moment curves show greater moment values for right limb strike and reduced moment values for the left. The symmetry indices in the corresponding force records were 1.61 and 2.33 for 'MLI' and 'PAI', respectively. The upper body symmetry indices, 'SFP' and 'SSP', were 1.56 and 2.6, respectively in the body frame and 1.42 and 1.9 in the space frame.

Subject E: Subject E has a permanent gait impediment due to osteo-arthritis. Although the subject underwent surgery on the left hip joint, the subject has considerable pain in the right hip due to arthritis of the right joint and hence, attempts to reduce certain modes of loading on the right limb. The force records in Fig. 50 represent ground reaction components when he walks with the cane and Fig. 51 shows locomotion without the cane. As with subject B, the medio-lateral forces vary only to one side of the neutral position (the subject has a upper body lean to the left similar to that of subject B). Symmetry indices, defined in section 6.4.1, could not be obtained, due to the swing being only to one side. In comparing the force records, however, one could see the right limb reaction force (medio-lateral) tending more towards the neutral position (Fig. 49) for cane walk when compared to unaided walk (Fig. 50). Due to difficulties pointed out earlier, the moment records for subject E (kinematic measurements were taken with the subject walking with the help of a cane) are statically indeterminant and thus not discussed at the present time.

6.7 Summary of Results on Normal and Abnormal Gait

The symmetry indices for normal and abnormal locomotion listed in Table 3 and 4 clearly indicate the asymmetry in ground-reaction force components during abnormal locomotion. Even though symmetry indices could not be computed for subject E, the total asymmetry in motion in the case of subject E could be seen easily by examining the medio-lateral components. The symmetry indices for normal locomotion are almost unity and they give an integrated picture of normal ground-reaction forces in the three coordinate directions. Displacements of the various segments of the body in the lateral and longitudinal directions have a definite function in the process of locomotion - such as stabilizing the body during support in the frontal plane and providing the propelling moment in the sagittal plane. Displacements in the vertical direction have a less apparent function. Hence, the symmetry indices of forces and moments in two principal planes of motion (sagittal and frontal) were considered most important and significant for quantifying abnormal locomotion. The significance of finding the symmetry index for the vertical component of ground-reaction is not clear at present and, hence, was not reported for the abnormal gaits, except to qualitatively explain abnormal locomotion. The force symmetry indices reported for abnormal locomotion clearly show the asymmetry in gait as a integrated parameter and could be used for monitoring recovery after injury as in the pattern of force records presented.

It is apparent from an examination of Table 4 that the symmetry indices computed from upper body moments about body coordinate axes show clearly the compensatory maneuver by the upper body. Values of upper body

moments are consistently higher when the injured limb is in the support phase. Even though such compensatory movements have been stated to take place, they have never been measured before as symmetry parameters. The good correlation between the symmetry indices in the ground force reactions and the moments in the body fixed axis clearly demonstrate the validity of using ground-force reaction components to quantify asymmetry in gait by using a force plate. In comparison, the symmetry indices computed from moments in the space reference frame do not seem to show consistent correlation. Since the body axes accurately represent the joint angulation at any instant, the present study shows that the variations in the parameters associated with human locomotion are better represented when viewed from the moving body coordinate reference frame. In the case of grosser pathological gait with much larger angular rotations than seen in the studies on Legg-perthes Braces[10], measurements in the body frame would provide greater insight into abnormal locomotion. It is also seen from the various moment records that the hip moment about the X-axis is considerably higher and probably most sensitive in indicating abnormalities in posture of the upper body. The lateral moment maintains the body stable in the frontal plane. The two reaction components, medio-lateral and vertical, contribute to the moment in the frontal plane. This moment would be more sensitive to changes in the medio-lateral forces in view of the larger moment arm of the force vector in the YZ plane. This sensitivity indicates the importance of measuring the medio-lateral forces in locomotion studies.

The validity of the simplification for approximating the total moment at the hip joint with the moment due to ground reaction depends on the

joint considered. The contribution of inertial and gravitational forces on the fore-and-aft and lateral moments at the ankle, knee and hip joints were found to be very small throughout most of the stance phase, Bresler et.al[22] and Boccardi et.al[35] used the same simplification to calculate reaction moments about the hip joint and compared their results using the analytical procedure presented by Cappozzo et. al[94]. Capozzo's model includes the values of the body parameters which are only known statistically. Boccardi found the results to be more or less the same when using the simplified model except during the first part of the stance-phase. In the present analysis, the beginning and end of the stance phase is not considered and only the period corresponding to the total single limb support was analysed. Boccardi's[35] results also indicate that the inertia and gravity components have lower values in the frontal plane compared to the sagittal plane values. From the present investigation, it is seen that gait abnormalities have a close correspondence between asymmetry in forces and asymmetry in moments in the frontal plane directions and, hence, the original assumption appears justified. More studies will have to be done to arrive at a statistical analysis of the variation of symmetry parameters and to better understand symmetry indices in other planes of motion. The good correlation obtained in the frontal plane symmetry indices also suggests that it is possible to use medio-lateral ground-reaction forces for measuring symmetry in gait and to detect even small abnormalities of locomotion.

CHAPTER 7

CONCLUSIONS

The problem studied in this dissertation can be divided broadly into three areas: i) the development of a force plate, ii) the application of a simple three dimensional mathematical model to analyse the upper body motions as well as the development of a set of parameters which allows assessment of asymmetry in gait, iii) the clinical applicability of the symmetry indices in locomotion studies to detect gait disorders.

The force plate developed showed good sensitivity for the measurement of ground-reaction forces in all three coordinate directions of motion. The sensitivity in the lateral and longitudinal directions was sufficient to show subtle changes in the reaction components to enable an injury to the supporting limbs to be identified. It was possible in two cases to monitor the injury recovery by using the force plate. The size of the force plate was large enough to allow subjects with pathological gait and/or walking aids to be wholly on the force plate during a full gait cycle. Subjects were allowed to walk without any constraints normally imposed by smaller force platforms. The statically determinate force platform allowed the force platform to be calibrated directly in each measurement direction and the total ground components did not need complicated signal processing.

The previous absence of a simple three dimensional mathematical model prompted the evolution of a locomotion model which would be easily used by a clinician. The model proposed has made it possible to describe motions in the body coordinate system. The space to body transformations proposed are general enough to accept the large angle rotations

characteristic of pathological gait and the accuracy of the transformations are evident in the close balances obtained between the forces and moments in the ground and upper body planes, respectively. The model also resulted in the development of a set of symmetry indices that would allow a clinician greater use in quantifying pathological gait from ground-reaction force components.

Finally, in the area of clinical application of the force plate and the mathematical model, it was shown that gait abnormalities at different lower limb joints could be identified by a qualitative and quantitative analysis of the three dimensional force and moment records. Even though the model may not determine the actual moment and force values at the various joints (it is difficult to obtain them in a non-traumatic way), it could be used for comparison of two different states of gait as shown in monitoring injury recovery. A large bank of data on the force and displacement patterns of several abnormal gait states (patients at the Rehabilitation Center, St. Boniface Hospital) has been generated as part of this work. With the availability of a computing system for future investigators, a greater understanding of gait abnormalities could be attempted.

The author recommends the following for future investigation:

(i) analysis of the remaining records to establish the validity of using the symmetry indices as a parameter for quantifying pathological gait.

(ii) use of digital video cameras for future locomotion studies in view of the enormous time needed for digitizing the motion pictures.

(iii) use of another force plate along with the existing force plate for simultaneous measurement of ground-reactions on both the supporting limbs. This would enable a better understanding of the mechanics of locomotion during the double stance period which is a critical period for certain severely disabled states of gait.

It is hoped that this work will be of use to the future researchers in human locomotion.

REFERENCES

1. Borelli., De Motu Animalium, 1682.

2. Wilhem and Edward Weber., 'Die Mechanik der Gehwerkzeuge', 1836.

3. Braune and Fischer., 'Der Gang des Menschen', 1895.

4. Murray, M.P., Kory, R.C., Clarkson, B.H. and Sepic, S.B., 'Comparison of free and fast speed walking patterns of normal men', American Journal of Phys. Medicine, Vol. 45, No. 1, pp. 8-24, 1966.

5. Murray, M.P., 'Gait as a total pattern of movement', American Journal of Phys. Medicine, Vol. 46, No. 1, pp. 290-333, 1967.

6. Cunningham, D.M. and Brown, G.W., 'Two devices for measuring the forces acting on the human body during walking', Proc. Soc. Exp. Stress Anal. IX, 2, 75, 1952.

7. Hughes, J. and McGechan, M.B. 'The objective assessment of amputee Gait', Human locomotor Engineering, An I Mech. E. book, The Institution of Mechanical Engineers, London, pp. 120-125, 1974.

8. Hughes, J., Lowe, P.J. and Paul, J.P., 'Dynamic assessment of above knee prosthesis', Symp. of External Control of human extremities, Dubrovnik, 1969.

9. Balakrishnan, S. and Thornton-Trump, A.B., 'Reaction parameter variation with Gait changes', Proc. of the special conference of the Canadian Society for Biomechanics, London, Ontario, pp. 100-101, 1980.

10. Quanbury, A.O., Bannon, M.A., Thornton-Trump, A.B. and Balakrishnan, S., 'Biomechanical analysis of Legg Perthes Braces'. Proc. of the special Conference of the Canadian Society for Biomechanics, pp. 74-75, 1980.

11. Balakrishnan, S. and Thornton-Trump, A.B., 'Measurement of reaction forces between foot and ground using a modified force plate', CANCAM, 1979.

12. Carlet, M.G. 'Essai Experimental sur la locomotion humain', Etude de la marche. Ann.d. Scien. mat., Zool. 16: pp. 1-92, 1872.

13. Marey, E.J. 'De la locomotion terrestre chez les bipedes et les quadrupedes', J. de L'Anat. et. de la Physiol. 9:42-80, 1973.

14. Beely, F. 'Zur Mechanik des Stehens', Arch. f. Klin. Chir. 27: pp. 457-471, 1882.

15. Abrahamson, E. 'Zur Kentnis der Mechanik des Mittlelfusses', Skandinav. Arch. F. Physiol. 51: pp. 175-234, 1927.

16. Elftman, H. 'A cinematic study of the distribution of pressure in the human foot', Anat. Rec. 59: pp. 481-490, 1934.

17. Barnett, C.H. 'A plastic pedograph', Lancet, 2, 273, 1954.

18. Amar, J. 'Trottior dynamographiqe', Compt. rend, Acad. d. Sc. 163: 130, 1916.

19. Elftman, H. 'The measurement of the external force in walking', Science 84, pp. 152-153, 1938.

20. Schwartz, R.P. and Heath, A.L., 'The oscillographic recording and quantitative definition of functional disabilities of human locomotion', Archives of Physical Medicine, 30, pp. 568-578, 1949.

21. Bauman, J.H. and Brand, P.W., 'Measurement of pressure between foot and shoe', Lancet, 1, pp. 629-632.

22. Bresler, B. and Frankel, J.P., 'Forces and moments in leg during level walking', Trans. of the American Society of Mechanical Engineering, 72, pp. 27-36, 1952.

23. McLeish, R.D. and Arnold, D.A., 'A foot-ground reaction force plate', Joint British Committee for Stress Analysis Proc. of Conf. on the recording and Interpretation of engineering measurements, pp. 75-80, London; Inst. of Marine Engineers.

24. Michael Grundy, Blackburn, Tosh, P.A., McLeish, R.D. and Smidt, L., 'An investigation of the centers of pressure under the foot while walking', The Journal of Bone and Joint Surgery, Vol. 57-B, pp. 98-103, 1975.

25. Paul, J.P. and McGrouthr, D.A., 'Forces transmitted at the hip and knee joint of normal and disabled persons during a range of activities', CIBO 3rd symposium on Bone Biomechanics.

26. Paul, J.P. 'Bio-engineering studies of the forces transmitted by joints', Engineering Analysis reprinted from Biomechanics and related Bio-engineering topics, Proc. of a symposium held in Glasgow, pp. 369-380, Sept. 1964.

27. Yamashita, T. and Katoh, R., 'Moving pattern of point of application of resultant force during level walking', J. Biomechanics, Vol. 9, pp. 93-99, 1976.

28. Gola, M.M., 'Mechanical design, constructional details and calibration of a new force plate', J. Biomechanics, Vol. 13, No. 2, pp. 113-128, 1980.

29. Cook, T.M., Cozzens, B.A. and Kenosian, H., 'A technique for force-line visualisation', a report from Rehabilitation Hospital, Philadelphia, Pa. 1979.

30. Cook, T.M., Cossens, B.A. and Kenosian, H., 'Real time force visualization', Bio-engineering applications, Trans. ASME (paper No: 77-WA/Bio-6).

31. Stallard, J., Tait, J.H., Rose, G.K., 'Video vector display of ground reaction forces during physical activity', Proc. of the special conference of the Canadian Society for Biomechanics, Human Locomotion-I, pp. 102-103, 1980.

32. Pedotti, A., 'Simple equipment used in clinical practice for evaluation of locomotion', IEEE Transactions on Biomedical engineering, Vol. BME. 24, No. 5, 1977.

33. Boccardi, S., Chiesa, G., Pedotti, A., 'A new procedure for the evaluation of normal and abnormal gait', Am. J. Phys. Med. 56, pp. 163-182, 1977.

34. Balakrishnan, S. and Thornton-Trump, A.B., 'Reaction forces in roller skating', Proc. of 33rd Annual conf. on Engineering in Medicine and Biology, Washington, D.C. Vol. 22, 1980.

35. Boccardi, S., Pedotti, A., Rodano, R. and Santambrogio, 'Evaluation of muscular moments at the lower limb joints by an on-line processing of kinematic data and ground-reaction', J. Biomechanics, Vol. 14, pp. 35-45, 1981.

36. Fisher, O. 'Der Gang des Menschen', II, Thiel: Die Bewegung des Gesammtschwer-punktes und die ausseren Krafte, Abhandlum der mathematisch-physischen classe der Kiniglich Sachsischen. Gesellschaft der Wissenschaften: classe 25, pp. 3-130, Leipzig, 1895.

37. Bernstein, N.A. Biodynamics of locomotion, Vol. 1, Moscow, 1935.

38. Saunders, J.B., Inman, V.T. and Howard, D.E., 'The major determinants in normal and pathological gait', Journal of Bone and joint surgery, Vol. 35-A, No. 3, pp. 543-558, 1953.

39. Murray, M.P., Drought, A.B. and Kory, R.C., 'Walking patterns of normal men', J. Bone and Joint surgery, 46-A, pp. 335-360, 1964.

40. Murray, M.P. 'Gait as a total pattern of movement', American Journal of Physical medicine, Vol. 46, No. 1, pp. 290-333, 1967.

41. Kasvand, T., Milner, M. and Rapley, L.F., 'A computer-based system for the analysis of some aspects of human locomotion', Human locomotor engineering, The Institution of Mechanical engineers, London, pp. 170-174, 1974.

42. Kavsand, T., Milner, M., Quanbury, A.O. and Winter, D.A., 'computers and the Kinesiology of gait', Comput, Biol. Med. Vol. 6, pp. 111-120, 1976.

43. Winter, D.A., Quanbury, A.O., Hobson, D.A., Sidwall, H.G., Reimer, G., Tranholm, B.G., Steinke and Shlosser, H., 'Kinematics of normal locomotion - a statistical study based on T.V. data', Journal of Biomechanics, Vol. 7, pp. 479-486, 1974.

44. Winter, D.A., Greenlaw, R.K. and Hobson, D.A., 'Television/computer analysis of kinematics of human gait', Computers and Biomedical research, No. 5, pp. 498-504, 1972.

45. Dinn, D., Winter, D.A. and Trenholm, B.G., 'Cintel-computer interface for television, IEEE Trans. on comp., 19, pp. 1091-1095, 1970.

46. Selcom, A.B. 'Trade literature on the Selspot system', 1976.

47. Güth, V. Abbink, T. and Heinrichs, W. 'Eine methode Zur chronozyklographischen Bewegungs auf Zeichung mit einem Prozessrechner' Int. Z. Angew Physiol, pp. 151-162, 1973.

48. Andrews, B.J. and Jarrett, M.O. 'On-line kinematic data acquisition' Univ. of Strathclyde, Glasgow, Scotland, Internal report, 1976.

49. Brugger, W., and Milner, M. 'Computer aided tracking of body motions using a c.c.d -image sensor', Med. and Biol. Engg. Comput., 16 pp. 207-210, 1978.

50. Slonosky, M.J. and Shwedyk, E 'Locomotion data Extraction using a micro-programmed processor', Proc. of the 4th congress of the International Society of Electrophysiological Kinesiology, Boston, MA. pp. 144-145, 1979.

51. Fischer, O. 'Der Gang Des Menschen' (Human gait), Abhandlung, Math-Phys. Classe d. Konigl. Sachs, Gesellschaft der Wissenschaft, pp. 21-28, 1898-1904.

52. Braune, W. and Fischer, O. 'Uber der Schwerpunkt des Mensclicher Koerpers....' Abh. d. Koenigl. Sachs, Gesellsch. Math. Phys. cl. 26, 1890.

53. Elftman, H. 'Forces and energy change in the leg during walking', Amer. J. Physiol., 125. pp. 339-356, 1939(a).

54. Elftman, H. 'The function of muscles in locomotion', Amer. J. Physiol., 125, pp. 357-366, 1939 (b).

55. Weinbach, A.P. 'Contour maps, center of gravity, moment of inertia and surface area of the human body', Humman Biology, Vol. 10, pp. 356-371. Sept. 1938.

56. Paul, J.P. 'Forces transmitted by joints in the human body', Proc. Instn. Mech. Engrs. Vol. 181 paper 8, pt 3J, pp. 8-15, 1966-67.

57. Quanbury, A.O., Winter, D.A. and Reimer, G.D., 'Instantaneous power and power flow in body segments during walking', Journal of human movement studies, 1, pp. 59-67, 1975.

58. Winter, D.A., Quanbury, A.O. and Reimer, G.D., 'Analysis of instantaneous energy of normal gait', J. Biomechanics, Vol. 9, pp. 253-257, 1976.

59. Contini, R. 'Body segment parameters', pt. II, Artificial limbs, pp. 1-19, 1972.

60. Thornton-Trump, A.B. and Daher, R. 'The prediction of reaction forces from gait data', J. Biomechanics, Vol. 8, pp. 173-178, 1975.

61. Frank, A.A. 'An approach to the dynamic analysis and synthesis of biped locomotion machines', Med. & Biol. engg. Vol. 8, pp. 465-476, 1970.

62. Vukobratovic, M. and Juricic, D. 'Contributions to the synthesis of biped gait', IEEE transactions on Biomedical engineering, Vol. BME-16, No. 1, pp. 1-6, Jan. 1969.

63. Vukobratovic, M., Juricic, D. and Frank, A.A., 'On the control and stability of one class of biped locomotion systems', Transactions of ASME, pp. 328-332, June 1970.

64. Townsend, M.A. and Seireg, A. 'The synthesis of bipedal locomotion', J. Biomechanics, Vol. 5. pp. 71-83, 1972.

65. Chao, E.Y. and Rim, K. 'Application of optimization principles in determining the applied moments in human leg joints during gait', J. Biomechanics, Vol. 6, pp. 479-510, 1973.

66. Yamashita, T. and Yamada, H. 'A study on stability of bipedal locomotion', Proc. of first CISM-IFTOMM symp. on Theory and practice of Robots and manipulators, Vol. 1 Springer-verlag, Wien-New york, pp. 41-53, 1974.

67. Yamashita, T. and Taniguchi, T. 'Simulation of human walking characteristics by simple model', Proc. of the fifth World Congress on Theory of machines and mechanisms, 1979.

68. Yamashita, T., Kabashima, K. and Sakatani, Y. 'Control of macro-model to simulate human level walking', 2nd CISM-IFTOMM Symp. on Theory and Practice of Robots and manipulators, Warsaw, Poland, pp. 183-192, Sept. 1976.

69. Tagawa, Y. and Yamashita, T. 'Characteristics simulated by two-body massless leg model for human level walking' (to be published).

70. Onyshko, S. and Winter, D.A. 'A mathematical model for the dynamics of human locomotion', J. Biomechanics, Vol. 13, pp. 361-368, 1980.

71. Ramey, M.R. amd Yang, A.T. 'A simulation procedure for human motion studies', J. Biomechanics, Vol. 14, No. 4, pp. 203-213, 1981.

72. Steindler, A. 'Kinesiology of the human body', Thomas, Springfield, 62, 1964.

73. MacConaill, M.A. 'Joint movement', Physiotherapy, Vol. 50, pp. 359-367, 1964.

74. Beckett, R. and Chang, K. 'An evaluation of the kinematics of gait by minimum energy', J. Biomechanics, Vol. 1, pp. 147-159, 1968.

75. Eberhart, H. and Inman, V. 'An evaluation of experimental procedures used in a fundamental study of human locomotion', Annals of New York Academy of Sciences (51), pp. 1213-1228, 1951.

76. Morrison, J.B. 'Functions of the knee joint in various activities', Biomedical Engineering (4), pp. 573-580, 1969.

77. Taylor, C.L. and Blaschke, A.C. 'A method for kinematic analysis of motions of the shoulder, arm, and hand complex', Annals of New York Academy of Sciences (51), pp. 1251-1265, 1951.

78. Dempster, S.T. 'The anthropometry of body action', Annals of New York Academy of Sciences (63), pp. 559-585, 1955.

79. Chao, E.Y.S., Kwan Rim., Smidt, G.L. and Johnston, R.C. 'The application of 4 x 4 matrix method to the correction of the measurements of hip joint rotations', J. Biomechanics, Vol. 3, pp. 459-471, 1970.

80. Lamoureux, L.W. ASME paper, No. 72. Mech-80, 1972.

81. Radcliffe, C.W. Transactions of the 6th conference on Mechanisms, Purdue University, 143, 1960.

82. Smidt, G.L. 'Biomechanical Analysis of knee flexion and extension', Journal of Biomechanics (6), pp. 79-92, 1973.

83. Burnstein, A. and Frankel, V.H. ASME paper No. 67-DE-38, 1967.

84. Thompson, C.T. 'A system for determining the spatial motions of arbitrary mechanisms-demonstrated on a human knee', Ph.d. Thesis, Stanford University, 1972.

85. Rosenburg, R.M. Analytical dynamics of discrete systems, Plenum press, New York, 1977.

86. Goldstein, H. Classical Dynamics, Addison-Wesley Publishing Co., Reading, Massachusetts (1950).

87. Boccardi, S., Chiesa, G. and Pedotti, A. 'A new procedure for the evaluation of normal and abnormal gait', Am. J. Phys. Med. 56, pp. 163-182, 1977 (b).

88. Langrana, N.A. 'Spatial kinematic analysis of the upper extremity using a biplanar video taping method', Journal of Biomechanical Engineering, Transactions of the ASME, Vol. 103, pp. 11-17, 1981.

89. Chao, E.Y., Opgrande, J.D. and Axmear, F.E. 'Three-dimensional force analysis of finger joints in selected isometric hand functions', J. Biomechanics, Vol. 9, pp. 387-396, 1976.

90. University of California, Berkeley, Prosthetic devices research project: 'Fundamental studies of human locomotion and other information relating to design of artificial limbs', Prosthetic research project, College of Engineering, University of California, Berkeley, 1947.

91. Shanley, F.R. 1967, Mechanics of materials, McGraw Hill Book company, New York.

92. Harris, G.F. Salamon, N.J., Weber, R.C. and Sances, A., 'The balance platform or force plate Kern', Proc. of 33rd Annual Conf. on Engineering in Medicine and Biology, pp. 187-188, Vol. 22, 1980.

93. Siegler, S. And Seliktar 'Simplified simulation of the kinetic features of human gait', Proc. of the special Conference of the Canadian Society for Biomechanics, pp. 130-131, 1980.

94. Cappozzo, A., Figura, F. and Marchetti, M., 'The interplay of muscular and External forces in human ambulation', J. Biomechanics, Vol. 9, pp. 35-43, 1976.

95. Townsend, M.A. 'Dynamics and coordination of Torso motions in human locomotion', J. Biomechanics, Vol. 14, pp. 727-738, 1981.

96. Greenwood, D.T. (1965) Principle of Dynamics, Prentice-Hall, Englewood cliffs, New Jersey.

97. Shames, I.H. (1966) Engineering Mechanics: Dynamics, Vol. 2, Prentice Hall Englewood Cliffs, New Jersey.

APPENDIX A

LOWER LIMB TRANSFORMATIONS

This section will outline a method for determining the lower limb rotations from displacement records. As pointed out in Section 4.6.2 the rotation angles of the body coordinate axes located at the hip joint cannot be determined completely with the present body marker system without imposing certain conditions on the articulation of the lower limb.

One approach for finding the transformation matrice is outlined in this section. The basic principle is to assume the body axes Z^h to be always pointed in the positive direction of the extremity in the support phase. This choice is not one of convenience but based on the fact that the force vector in the leg during single support phase (total support only) would always be in the direction of the leg supporting the body. Thus, when the body is not in motion and is erect, the leg axis Z^h and reference Z-axis will both be parallel.

During motion of the body about the supported leg, the leg goes through rotations in the three-dimensional space. If the lower limb is represented in the support phase by the position vector $\mathbf{r}$, a unit vector along the leg axis is given as:

$$\hat{r} = \frac{\mathbf{r}}{|\mathbf{r}|}. \qquad - \qquad \text{A. 1}$$

A unit vector along the positive direction of Z^h axis (the reference axes

is located at the hip joint) will be

$$\hat{Z}^h = - \hat{r} \quad . \qquad - \qquad \text{A. 2}$$

If $X^h\ Y^h\ Z^h$ represent the leg coordinate axes, fixed at the hip joint (Fig. 52), and $X_2\ Y_2\ Z_2$ is the reference axes at the hip joint, the angular orientation of the body fixed coordinate axes with reference to the earth parallel reference frame can be defined by the direction cosines of $X^h\ Y^h\ Z^h$ (with respect to $X_2\ Y_2 Z_2$). The direction cosines will represent the elements of the matrix $[T_{S \rightarrow H}]$, the space to hip rotation matrix. As the leg moves into various positions at different phases of the gait, the rotation matrix will define the leg coordinate system at each instant. The Z^h is always in the direction of the leg and $X^h\ Y^h\ Z^h$ form a orthogonal system. If a_1, b_1 and c_1 represent the components of $\mathbf{r}$ in the reference frame $X_2\ Y_2\ Z_2$, the component form of $\mathbf{r}$ is given as:

$$\mathbf{r} = a_1\ \mathbf{i} + b_1\ \mathbf{j} + c_1\ \mathbf{k} \quad . \qquad - \qquad \text{A. 3}$$

The a_1, b_1 and c_1 can be determined by knowing the position of B with respect to A. In Fig. 52, B represents the hip joint and A is the point of contact of the lower extremity with the ground. The following can be determined from motion photography in biplane:

$$\left.\begin{aligned} a_1 &= X_{hip} - X_{heel} \\ b_1 &= Y_{hip} - Y_{heel} \end{aligned}\right\} \qquad - \qquad \text{A. 4}$$

and

$$\left.\begin{aligned} c_1 &= Z_{hip} - Z_{heel} \end{aligned}\right\}$$

The biplane motion pictures of the adhesive markers, fixed at the

respective locations on the subject, would help solve equation A. 4. The leg axis Z^h can be found by using relation A. 2. The principle behind obtaining the leg transformation matrix is to obtain a set of values for the X^h and Y^h axes that would uniquely transform the position vector $\mathbf{r}$ defined in reference to the leg axis. Due to the difficulty of not being able to fix a location marker on the posterior or anterior side of the hip joint (even though one could obtain its position by employing some form of approximations on the images), the transformation procedure outlined below would make use of the projected angles of $\mathbf{r}$ on the different planes of motion to obtain a unique transformation.

If $\mathbf{V}^{I}$, $\mathbf{V}^{II}$, $\mathbf{V}^{III}$ and $\mathbf{V}^{IV}$ represent the projections of $\mathbf{r}$ on the X, Y and Z axis and XY plane respectively, the projected angles between $\mathbf{V}^{IV}$ and the axes can be obtained from the dot product of $\mathbf{V}^{IV}$ and $\mathbf{V}^{IV}$. If α' is the angle between $\mathbf{V}^{I}$ and $\mathbf{V}^{IV}$, then

$$\cos\alpha' = \frac{\hat{\mathbf{V}}^{I} \cdot \hat{\mathbf{V}}^{IV}}{|\hat{\mathbf{V}}^{I}||\hat{\mathbf{V}}^{IV}|} \qquad - \qquad \text{A. 5}$$

and

$$\sin\alpha' = \frac{|\hat{\mathbf{V}}^{I} \times \hat{\mathbf{V}}^{IV}|}{|\hat{\mathbf{V}}^{I}||\hat{\mathbf{V}}^{IV}|} \qquad - \qquad \text{A. 6}$$

Similarly if β' represents the angle between $\mathbf{V}^{III}$ and $\mathbf{r}$, then

$$\cos\beta' = \frac{\hat{\mathbf{V}}^{III} \cdot \hat{\mathbf{r}}}{|\hat{\mathbf{V}}^{III}||\hat{\mathbf{r}}|} \qquad - \qquad \text{A. 7}$$

and

$$\sin\beta' = \frac{|\hat{\mathbf{V}}^{III} \times \hat{\mathbf{r}}|}{|\hat{\mathbf{V}}^{III}||\hat{\mathbf{r}}|} \qquad - \qquad \text{A. 8}$$

The unit vectors $\hat{\mathbf{V}}^{I}$, $\hat{\mathbf{V}}^{II}$, $\hat{\mathbf{V}}^{III}$ and $\hat{\mathbf{V}}^{IV}$ are obtained by resolving the components of $\hat{\mathbf{r}}$ in the respective directions.

Thus

$$\hat{\mathbf{V}}^{I} = \frac{a_1\ \mathbf{i} + b_1\ \mathbf{j} + c_1\ \mathbf{k}}{\sqrt{(a_1^2 + b_1^2 + c_1^2)}} \begin{bmatrix} 1 \\ 0 \\ 0 \end{bmatrix} \quad - \quad \text{A. 9}$$

and

$$\hat{\mathbf{V}}^{II} = \frac{a_1\ \mathbf{i} + b_1\ \mathbf{j} + c_1\ \mathbf{k}}{\sqrt{(a_1^2 + b_1^2 + c_1^2)}} \begin{bmatrix} 0 \\ 1 \\ 0 \end{bmatrix} \quad - \quad \text{A. 10}$$

$$\hat{\mathbf{V}}^{III} = \frac{a_1\ \mathbf{i} + b_1\ \mathbf{j} + c_1\ \mathbf{k}}{\sqrt{(a_1^2 + b_1^2 + c_1^2)}} \begin{bmatrix} 0 \\ 1 \\ 0 \end{bmatrix} \quad - \quad \text{A. 11}$$

and finally

$$\hat{\mathbf{V}}^{IV} = \frac{a_1\ \mathbf{i} + b_1\ \mathbf{j} + c_1\ \mathbf{k}}{\sqrt{(a_1^2 + b_1^2 + c_1^2)}} \begin{bmatrix} 0 & 0 & 0 \\ 1 & 1 & 0 \\ 0 & 0 & 0 \end{bmatrix} - \quad \text{A. 12}$$

In the rotation described above, angle β' represents the rotation about the X-axis and α' represents the resultant rotation about the Z-axis (similar to the Eulerian ψ and ϕ rotations described in Chapter 4). The space to body transformation matrix could be solved with respect to the known quantities Z^h, α' and β' to obtain the various elements of the matrix $[T_{S \rightarrow H}]$.

The transformation outlined above would describe the rotation of lower limb leg axes X^h Y^h Z^h with respect to the reference axes X_2 Y_2 Z_2. In the locomotion model proposed, the moments in the upper body axes can be determined without knowledge of rotation angles for the lower limb. Even though the reaction moments at hip joint in the lower

limb coordinate axes are obtainable using the above procedure, the clinical significance of such an attempt is not clear at the present time and, hence, the corresponding results are not presented in this dissertation.

APPENDIX B

Program 'BALA12' was developed to compute the various quantities described in the mathematical model. The listing of the program for a 'HP41C' is presented in this section. The block diagram for the program is given below followed by the listing of the program.

Block Diagrm for 'BALA12'

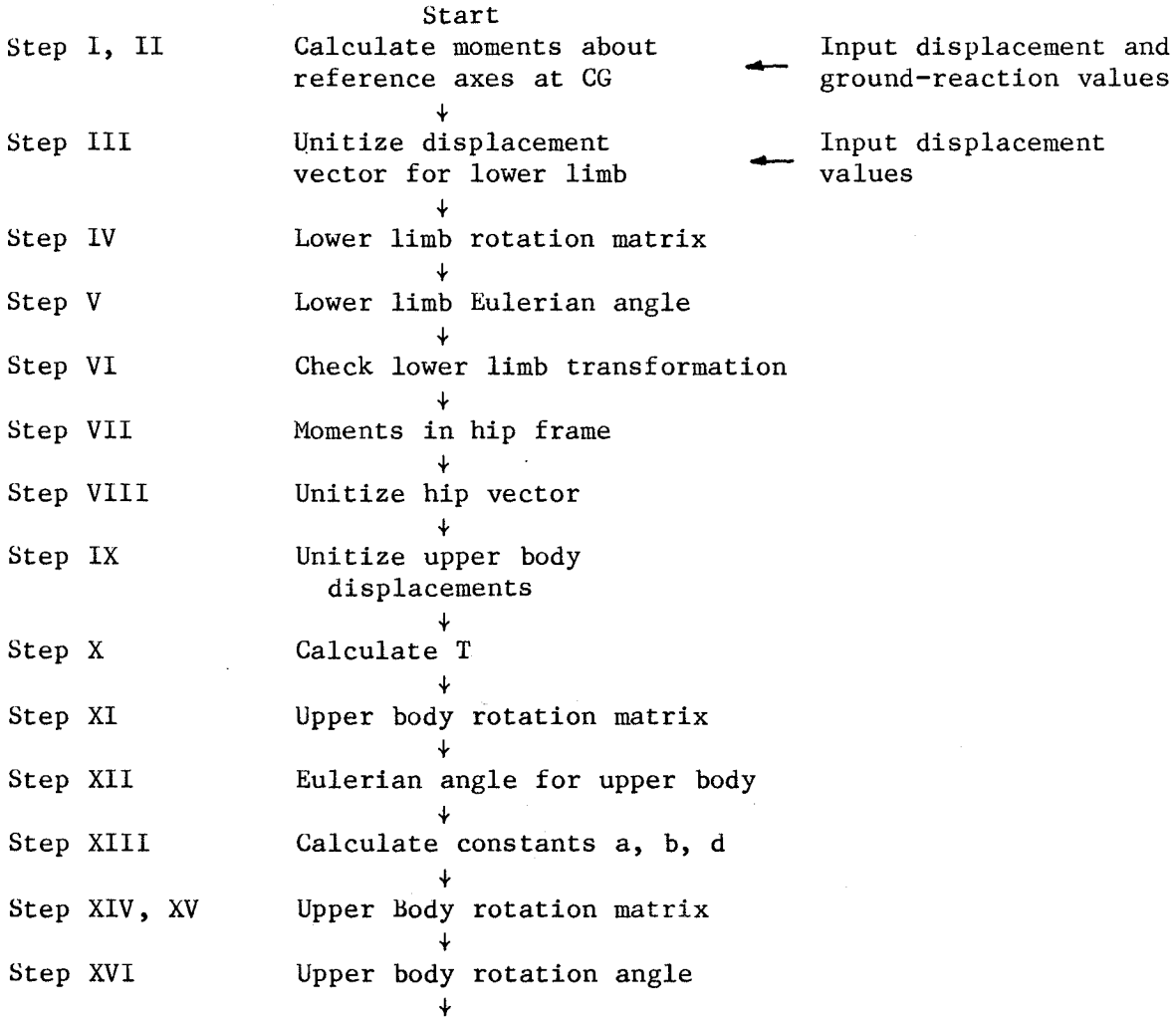

Step XVII,XVIII and XIX	Check upper body transformation for uniqueness
	↓
Step XX	Moments about CG in body frame
	↓
Step XXI, XXII and XXIII	Projected angles for the two segments
	↓
Step XXIV	Display and print results
	↓
'BALA13'	Run subroutine 'BALA13' for net moment in body frame, display and print results

I

```
01♦LBL "BALA12"
02♦LBL "BALA12"
03 RCL 46
04 RCL 53
05 *
06 RCL 47
07 RCL 52
08 *
09 -
10 STO 28
11 RCL 47
12 RCL 51
13 *
14 RCL 45
15 RCL 53
16 *
17 -
18 STO 29
19 RCL 45
20 RCL 52
21 *
22 RCL 46
23 RCL 51
24 *
25 -
26 STO 30
```

II

```
27 RCL 47
28 RCL 52
29 RCL 49
30 +
31 *
32 RCL 46
33 RCL 53
34 RCL 50
35 +
36 *
37 -
38 STO 18
39 RCL 45
40 RCL 53
41 RCL 50
42 +
43 *
44 RCL 47
45 RCL 51
46 RCL 48
47 +
48 *
49 -
50 STO 19
```

```
51 RCL 46
52 RCL 51
53 RCL 48
54 +
55 *
56 RCL 45
57 RCL 52
58 RCL 49
59 +
60 *
61 -
62 STO 20
```

III

```
63 RCL 51
64 X↑2
65 RCL 52
66 X↑2
67 +
68 RCL 53
69 X↑2
70 +
71 SQRT
72 STO 43
73 RCL 51
74 RCL 43
75 /
76 STO 51
77 RCL 52
78 RCL 43
79 /
80 STO 52
81 RCL 53
82 RCL 43
83 /
84 STO 53
```

IV

```
85♦LBL "EULER L"
86 RCL 52
87 RCL 51
88 *
89 CHS
90 STO 03
91 RCL 53
92 X↑2
93 RCL 51
94 X↑2
95 +
96 STO 04
97 RCL 53
98 RCL 52
99 *
100 CHS
101 STO 05
102 RCL 53
103 X↑2
104 RCL 51
105 X↑2
106 +
107 RCL 52
108 X↑2
109 +
110 RCL 53
111 *
112 STO 00
113 0
114 STO 01
115 RCL 51
116 X↑2
117 RCL 52
118 X↑2
119 +
120 RCL 53
121 X↑2
122 +
123 RCL 51
124 *
125 CHS
126 STO 02
127 RCL 51
128 STO 06
129 RCL 52
130 STO 07
131 RCL 53
132 STO 08
```

V

```
133 RCL 08
134 ACOS
135 STO 22
136 RCL 06
137 RCL 07
138 /
139 CHS
140 ATAN
141 STO 21
142 RCL 02
143 RCL 05
144 /
145 ATAN
146 STO 23
```

VI

```
147 RCL 00
148 RCL 51
149 *
150 RCL 01
151 RCL 52
152 *
153 +
154 RCL 02
155 RCL 53
156 *
157 +
158 .0001
159 X>Y?
160 GTO 01
161 BEEP
162 STOP
163♦LBL 01
164 RCL 03
165 RCL 51
166 *
167 RCL 04
168 RCL 52
169 *
170 +
171 RCL 05
172 RCL 53
173 *
174 +
175 .0001
176 X>Y?
177 GTO 02
178 BEEP
179 STOP
```

```
180♦LBL 02
181 RCL 06
182 RCL 51
183 *
184 RCL 07
185 RCL 52
186 *
187 +
188 RCL 08
189 RCL 53
190 *
191 +
192 1
193 -
194 .0001
195 X>Y?
196 GTO 03
197 BEEP
198 STOP
```

VII

```
199♦LBL 03
200 RCL 00
201 RCL 28
202 *
203 RCL 01
204 RCL 29
205 *
206 +
207 RCL 02
208 RCL 30
209 *
210 +
211 STO 31
212 RCL 03
213 RCL 28
214 *
215 RCL 04
216 RCL 29
217 *
218 +
219 RCL 05
220 RCL 30
221 *
222 +
223 STO 32
```

```
224 RCL 06
225 RCL 28
226 *
227 RCL 07
228 RCL 29
229 *
230 +
231 RCL 08
232 RCL 30
233 *
234 +
235 STO 33
```

VIII

```
236 RCL 44
237 .15
238 *
239 X↑2
240 RCL 44
241 .3
242 *
243 X↑2
244 +
245 SQRT
246 .3
247 RCL 44
248 *
249 /
250 1/X
251 CHS
252 ACOS
253 STO 54
```

IX

```
254♦LBL "EULER B"
255 RCL 48
256 X↑2
257 RCL 49
258 X↑2
259 +
260 RCL 50
261 X↑2
262 +
263 SQRT
264 STO 27
265 RCL 48
266 RCL 27
267 /
268 STO 48
269 RCL 49
270 RCL 27
271 /
272 STO 49
273 RCL 50
274 RCL 27
275 /
276 STO 50
```

X

```
277 RCL 49
278 CHS
279 RCL 48
280 X↑2
281 RCL 49
282 X↑2
283 +
284 SQRT
285 /
286 CHS
287 STO 55
288 LASTX
289 RCL 48
290 /
291 1/X
292 CHS
293 STO 56
```

XI

```
294 RCL 48
295 RCL 54
296 COS
297 *
298 RCL 56
299 RCL 50
300 *
301 RCL 54
302 SIN
303 *
304 -
305 CHS
306 STO 15
307 RCL 49
308 RCL 54
309 COS
310 *
311 RCL 55
312 RCL 50
313 *
314 RCL 54
315 SIN
316 *
317 +
318 CHS
319 STO 16
320 RCL 50
321 RCL 54
322 COS
323 *
324 RCL 48
325 RCL 56
326 *
327 RCL 54
328 SIN
329 *
330 +
331 RCL 55
332 RCL 49
333 *
334 RCL 54
335 SIN
336 *
337 -
338 CHS
339 STO 17
```

```
340 RCL 15
341 X↑2
342 RCL 16
343 X↑2
344 +
345 RCL 17
346 X↑2
347 +
348 SQRT
349 STO 57
350 RCL 15
351 RCL 57
352 /
353 STO 15
354 RCL 16
355 RCL 57
356 /
357 STO 16
358 RCL 17
359 RCL 57
360 /
361 STO 17
```

XII

```
362 RCL 17
363 ACOS
364 STO 25
365 RCL 15
366 RCL 16
367 /
368 CHS
369 ATAN
370 STO 24
```

XIII

```
371 .15
372 RCL 44
373 *
374 X↑2
375 .3
376 RCL 44
377 *
378 X↑2
379 +
380 SQRT
381 .15
382 RCL 44
383 *
384 /
385 STO 58
386 .3
387 RCL 44
388 *
389 *
390 .15
391 RCL 44
392 *
393 X↑2
394 RCL 44
395 .3
396 *
397 X↑2
398 +
399 SQRT
400 /
401 STO 59
```

XIV

```
402 RCL 48
403 CHS
404 RCL 58
405 *
406 RCL 15
407 RCL 59
408 *
409 +
410 STO 12
411 RCL 49
412 CHS
413 RCL 58
414 *
415 RCL 16
416 RCL 59
417 *
418 +
419 STO 13
```

```
420 RCL 50
421 CHS
422 RCL 58
423 *
424 RCL 17
425 RCL 59
426 *
427 +
428 STO 14
```

XV

```
429 RCL 13
430 RCL 17
431 *
432 RCL 16
433 RCL 14
434 *
435 -
436 STO 09
437 RCL 12
438 RCL 17
439 *
440 RCL 15
441 RCL 14
442 *
443 -
444 CHS
445 STO 10
446 RCL 12
447 RCL 16
448 *
449 RCL 15
450 RCL 13
451 *
452 -
453 STO 11
```

XVI

```
454 RCL 11
455 RCL 14
456 /
457 ATAN
458 STO 26
```

XVII

```
459 RCL 15
460 RCL 48
461 CHS
462 *
463 RCL 16
464 RCL 49
465 CHS
466 *
467 +
468 RCL 17
469 RCL 50
470 CHS
471 *
472 +
473 ACOS
474 RCL 54
475 -
476 .0001
477 X>Y?
478 GTO 04
479 BEEP
480 STOP
```

XVIII

```
481•LBL 04
482 RCL 09
483 RCL 48
484 CHS
485 *
486 RCL 10
487 RCL 49
488 CHS
489 *
490 +
491 RCL 11
492 RCL 50
493 CHS
494 *
495 +
496 ACOS
497 STO 60
498 90
499 -
500 .0001
501 X>Y?
502 GTO 05
503 BEEP
504 STOP
```

XIX

```
505♦LBL 05
506 RCL 12
507 RCL 48
508 CHS
509 *
510 RCL 13
511 RCL 49
512 CHS
513 *
514 +
515 RCL 14
516 RCL 50
517 CHS
518 *
519 +
520 ACOS
521 STO 61
522 .15
523 RCL 44
524 *
525 .15
526 RCL 44
527 *
528 X↑2
529 .3
530 RCL 44
531 *
532 X↑2
533 +
534 SQRT
535 /
536 ACOS
537 RCL 61
538 -
539 .0001
540 X>Y?
541 GTO 06
542 BEEP
543 STOP
```

XX

```
544♦LBL 06
545 RCL 09
546 RCL 18
547 *
548 RCL 10
549 RCL 19
550 *
551 +
552 RCL 11
553 RCL 20
554 *
555 +
556 STO 34
557 RCL 12
558 RCL 18
559 *
560 RCL 13
561 RCL 19
562 *
563 +
564 RCL 14
565 RCL 20
566 *
567 +
568 STO 35
569 RCL 15
570 RCL 18
571 *
572 RCL 16
573 RCL 19
574 *
575 +
576 RCL 17
577 RCL 20
578 *
579 +
580 STO 36
```

XXI

```
581 RCL 08
582 RCL 00
583 *
584 RCL 06
585 RCL 02
586 *
587 -
588 RCL 08
589 X↑2
590 RCL 06
591 X↑2
592 +
593 SQRT
594 RCL 00
595 X↑2
596 RCL 01
597 X↑2
598 +
599 RCL 02
600 X↑2
601 +
602 SQRT
603 *
604 /
605 ACOS
606 STO 37
607 RCL 04
608 RCL 04
609 X↑2
610 RCL 05
611 X↑2
612 +
613 SQRT
614 /
615 ACOS
616 STO 38
617 RCL 08
618 RCL 07
619 X↑2
620 RCL 08
621 X↑2
622 +
623 SQRT
624 /
625 ACOS
626 STO 39
```

XXII

```
627 RCL 17
628 RCL 09
629 *
630 RCL 15
631 RCL 11
632 *
633 -
634 RCL 17
635 X↑2
636 RCL 15
637 X↑2
638 +
639 SQRT
640 RCL 09
641 X↑2
642 RCL 10
643 X↑2
644 +
645 RCL 11
646 X↑2
647 +
648 SQRT
649 *
650 /
651 ACOS
652 STO 40
```

```
653 RCL 13
654 RCL 13
655 X↑2
656 RCL 14
657 X↑2
658 +
659 SQRT
660 /
661 ACOS
662 STO 41
663 RCL 17
664 RCL 16
665 X↑2
666 RCL 17
667 X↑2
668 +
669 SQRT
670 /
671 ACOS
672 STO 42
```

XXIII

```
673 RCL 00
674 RCL 00
675 X↑2
676 RCL 01
677 X↑2
678 +
679 RCL 02
680 X↑2
681 +
682 SQRT
683 /
684 ACOS
685 STO 62
```

XXIV

```
686 TONE 5
687 "BALA12 SUB RUN"
688 PRA
689 "STEP  FRAME  "
690 PRA
691 RCL 28
692 "MHIPX="
693 ARCL X
694 AVIEW
695 RCL 29
696 "MHIPY="
697 ARCL X
698 AVIEW
699 RCL 30
700 "MHIPZ="
701 ARCL X
702 AVIEW
703 RCL 31
704 "MHIP1X="
705 ARCL X
706 AVIEW
707 RCL 32
708 "MHIP1Y="
709 ARCL X
710 AVIEW
711 RCL 33
712 "MHIP1Z="
713 ARCL X
714 AVIEW
715 RCL 34
716 "MBODX="
717 ARCL X
718 AVIEW
719 RCL 35
720 "MBODY="
721 ARCL X
722 AVIEW
723 RCL 36
724 "MBODZ="
725 ARCL X
726 AVIEW
727 RCL 37
728 "ALPHAL="
729 ARCL X
730 AVIEW
731 RCL 38
732 "BETAL="
733 ARCL X
734 AVIEW
735 RCL 39
736 "GAMAL="
737 ARCL X
738 AVIEW
739 RCL 62
740 "DELTA="
741 ARCL X
742 AVIEW
743 RCL 40
744 "ALPHAB="
745 ARCL X
746 AVIEW
747 RCL 41
748 "BETAB="
749 ARCL X
750 AVIEW
751 RCL 42
752 "GAMAB="
753 ARCL X
754 AVIEW
755 00.026
756 PRREGX
757 44.054
758 PRREGX
759 ADV
760 ADV
761 ADV
762 .END.
```

Table 1

Performance Characteristic of the Force Plate Developed

	Vertical direction	Horizontal direction
RESOLUTION	1 pound	± 1/2 pound
RANGE	0-300 pounds	± 60 pounds
LINEARITY	1%	0.5%
CROSS-TALK	0.1%	0.2%
DRIFT	2%	1%
RESONANT FREQUENCY	17 Hz	16 Hz
CENTER OF PRESSURE RESOLUTION	± 1/2"	

Table 2

Types of Eulerian Rotations generally found in Literature

Type I	Type II	Type III
ψ about Z	ψ about Z	ϕ about Z
θ about Y	θ about X	θ about Y
ϕ about X	ϕ about Z	ψ about Z

Table 3

Values of Symmetry Index for Normal Locomotion

Subject	Body Weight (lbs)	'VI'		'MLI'		'PAI'	
		Mean	SDEV	Mean	SEDV	Mean	SDEV
1	125	1.008	0.005	1.100	0.024	1.055	0.021
2	154	1.005	0.018	1.200	0.011	1.041	0.027
3	175	0.994	0.006	1.118	0.004	1.038	0.032
4	205	1.010	0.020	1.006	0.017	1.125	0.042

Table 4

Symmetry Indices for Abnormal Locomotion

	'MLI'	'PLI'	BODY AXES		REFERENCE AXES	
			SFP	SSP	SFP	SSP
Subject B	1.61	2.33	1.56	2.6	1.42	1.9
Subject C	1.55	1.76	1.70	1.71	2.23	0.69
Subject D						
Trail I	0.74	0.91	0.66	1.04	0.60	0.80
Trail II	0.92	0.88	*	*	*	*

*Results are not presented due to some difficulties in data reduction.

Table 5

Scheme of Signals Recorded on Magnetic Tape

Channel	Signal Recorded
1	Sum of Vertical transducers
2	Vertical component at support A
3	Vertical component at support C
4	Comparator output
5	Center of force - x coordinate
6	Center of force - y coordinate
7	Sum of mediolateral forces
8	Mediolateral component at Corner A
9	Mediolateral component at Corner C
10	Posterior-anterior force

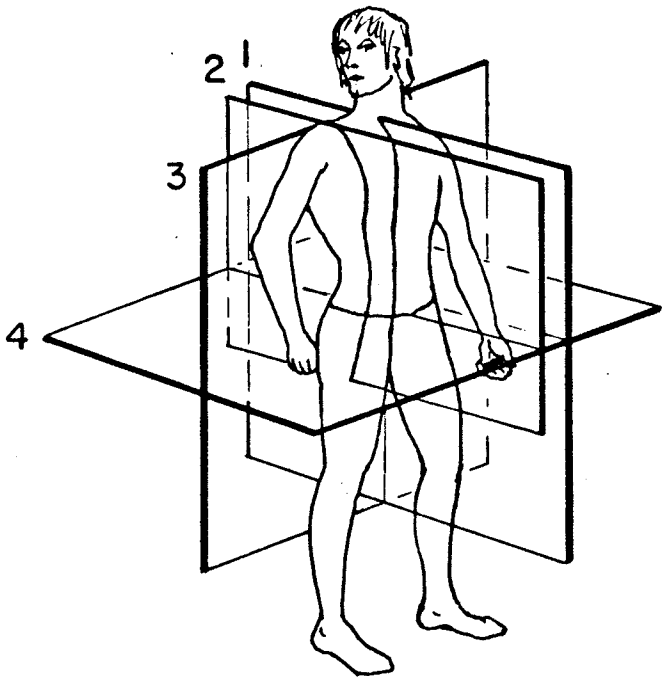

PLANES

1. Median Plane
2. Sagittal Plane
3. Frontal Plane
4. Transverse Plane

Figure 1 Planes normally considered in human locomotion

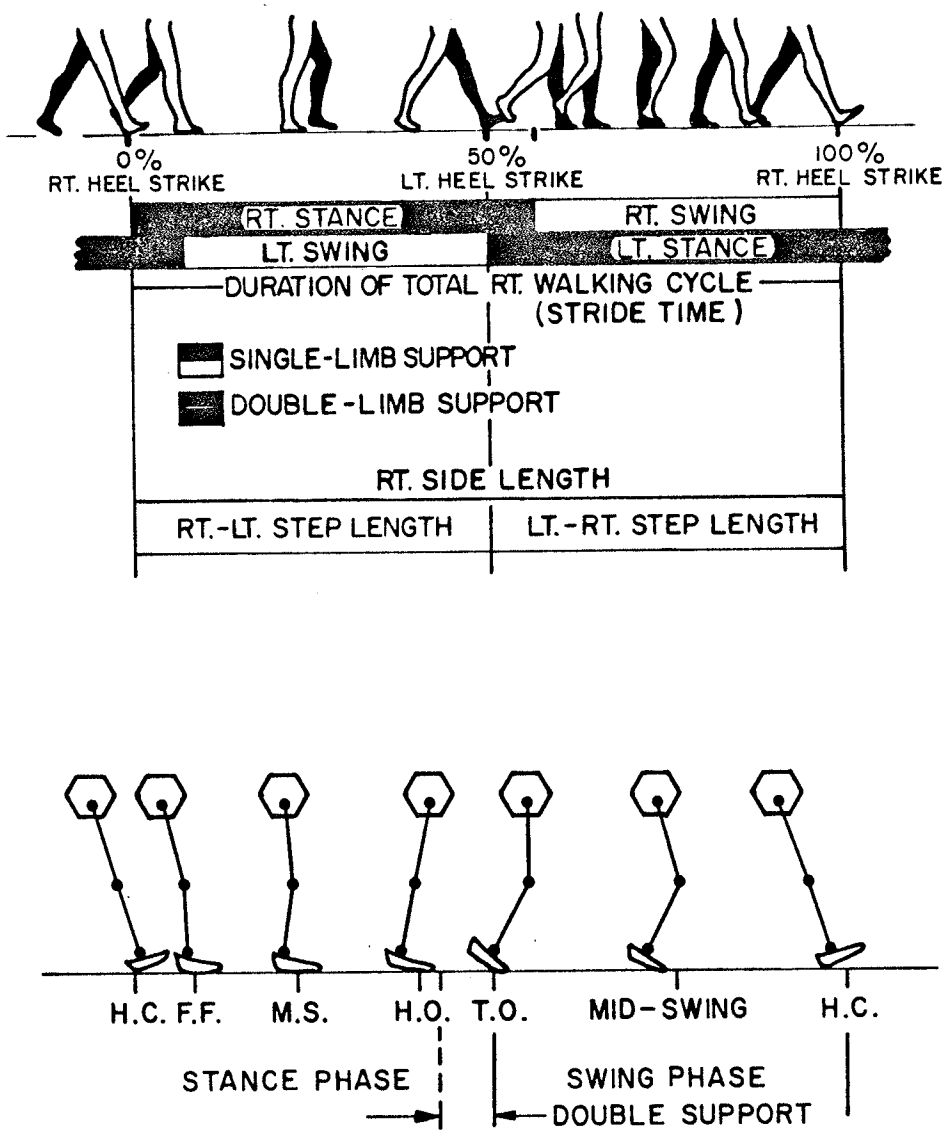

Figure 2 A normal gait cycle

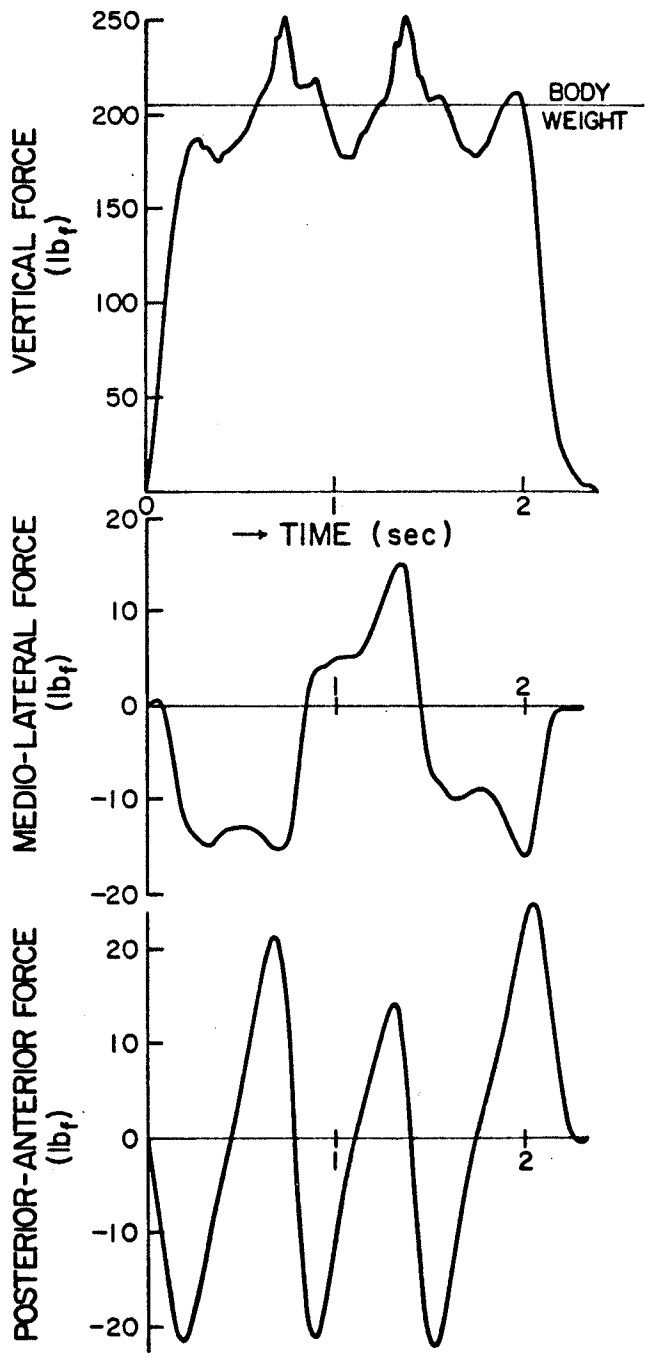

Figure 3 Ground reaction forces for normal locomotion

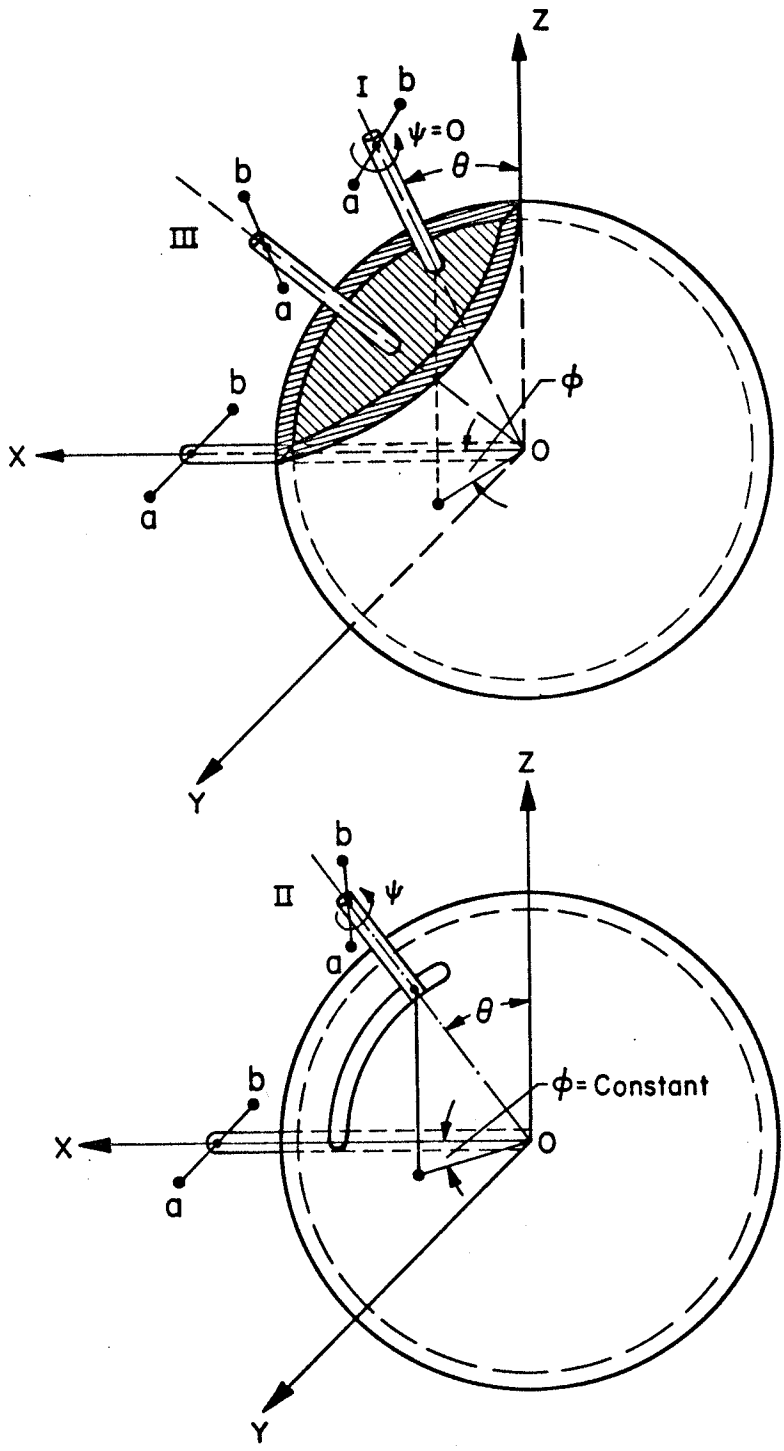

Figure 4 Different types of mechanical joint analogs used by previous investigators

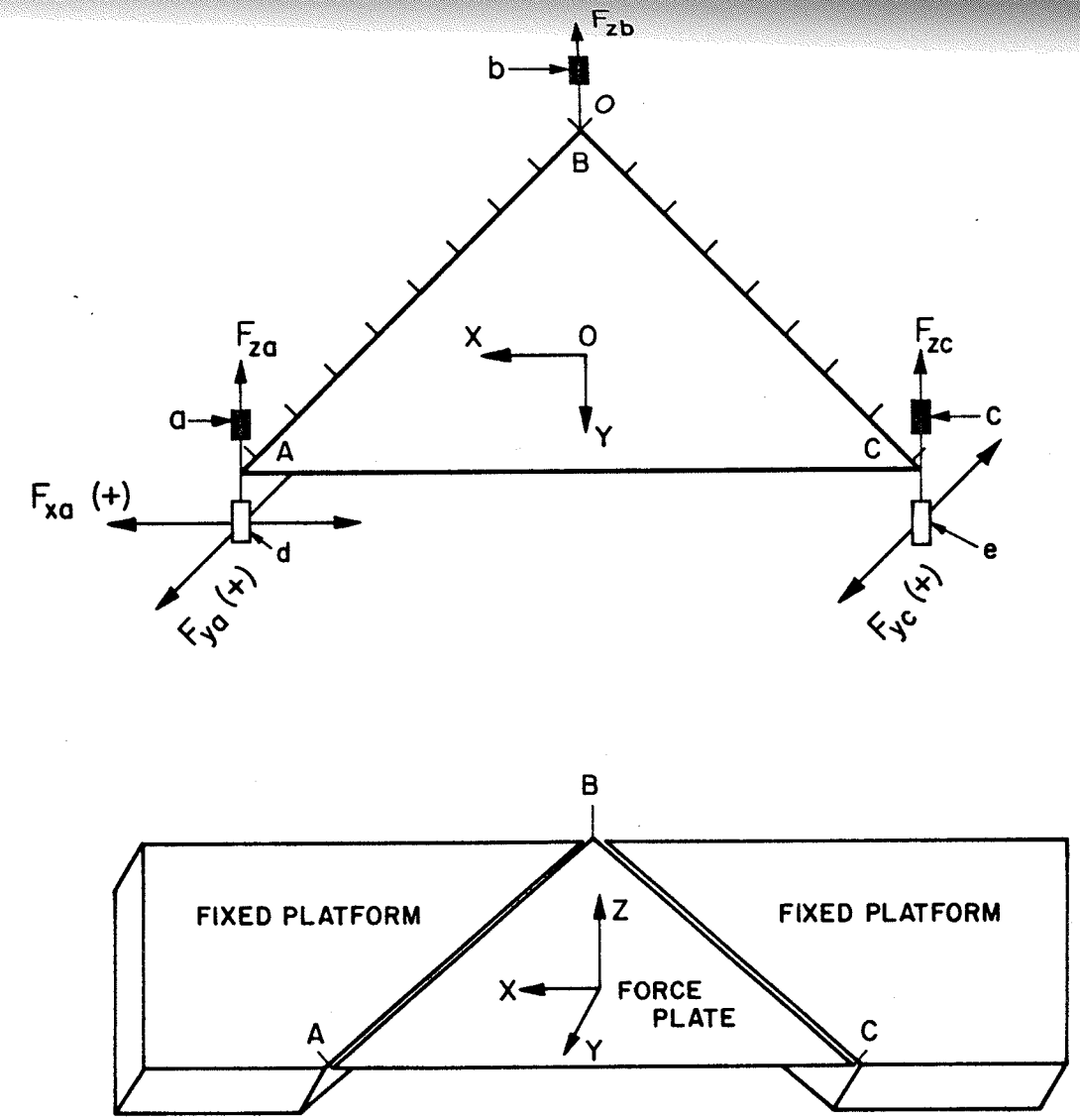

Figure 5 General layout of the force plate and suspension systems

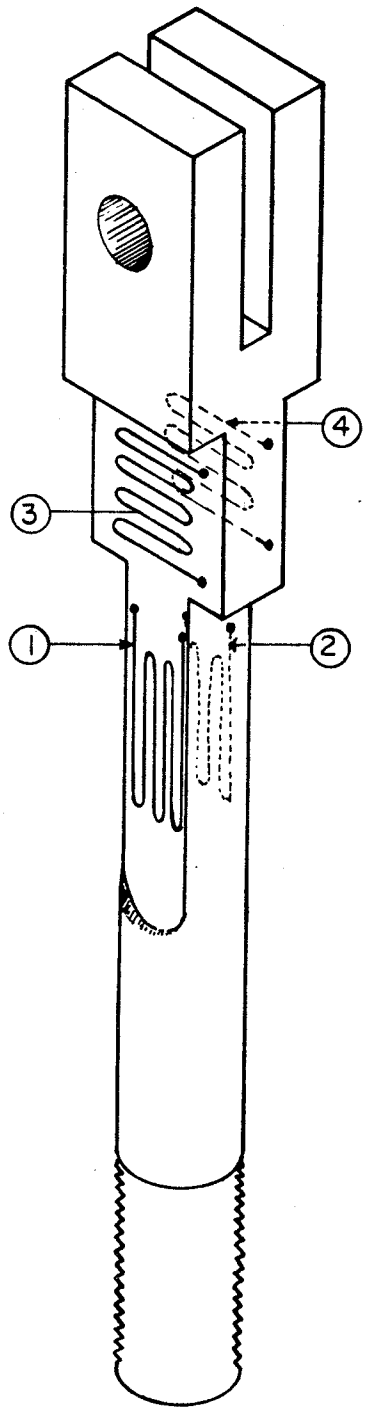

Figure 6 Vertical suspension element showing location of strain gauges

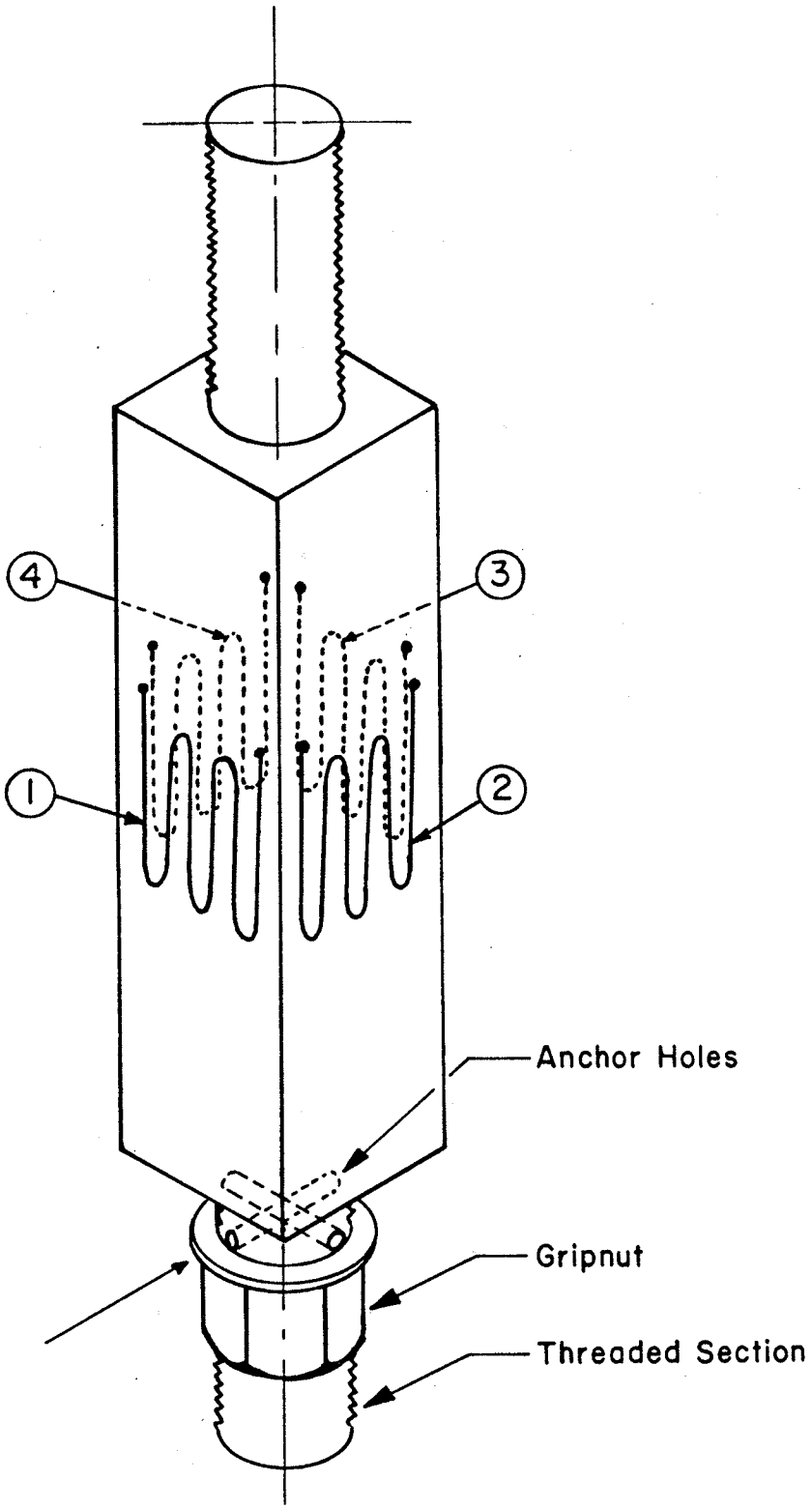

Figure 7 Horizontal suspension element 'd' showing gauge locations

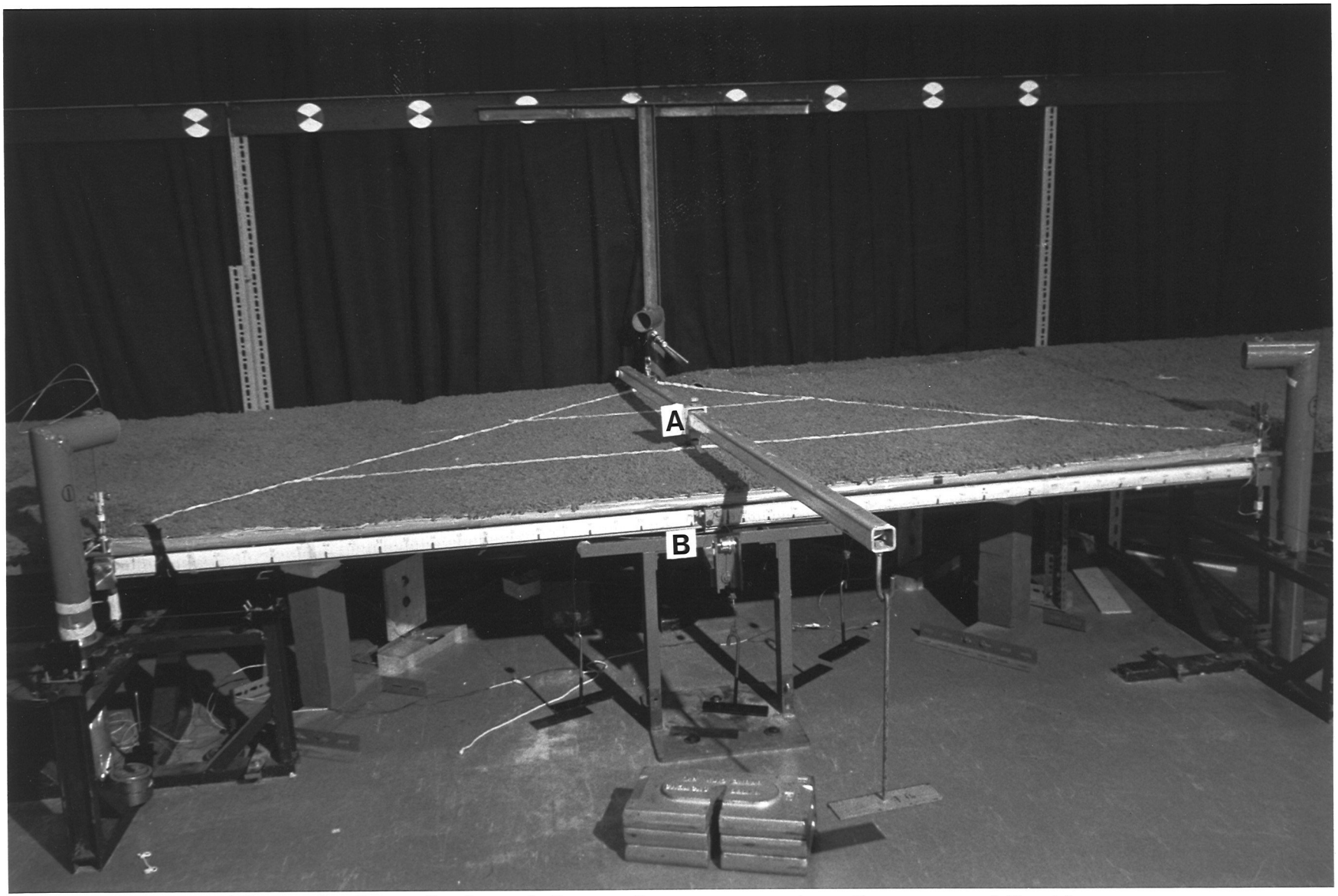

Figure 8 General view of force plate, suspension elements, calibration frame and background markers

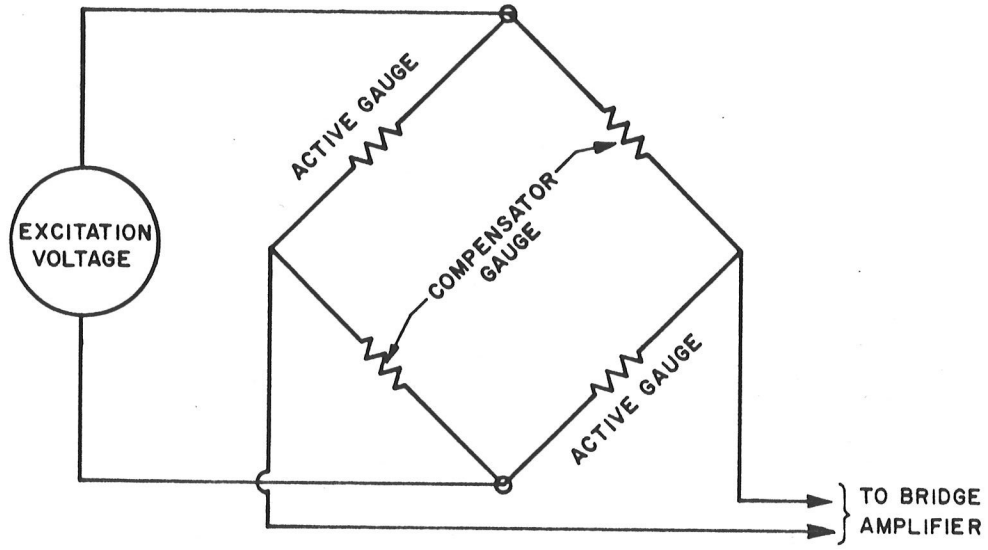

Figure 9 Strain bridge configuration for vertical transducer

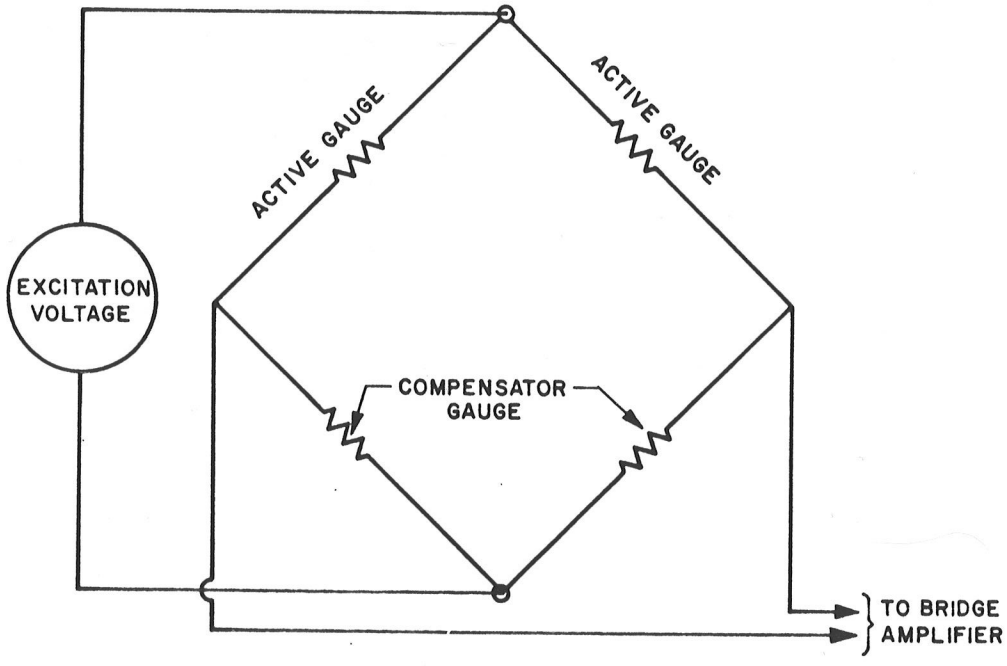

Figure 10 Strain bridge configuration for horizontal transducer

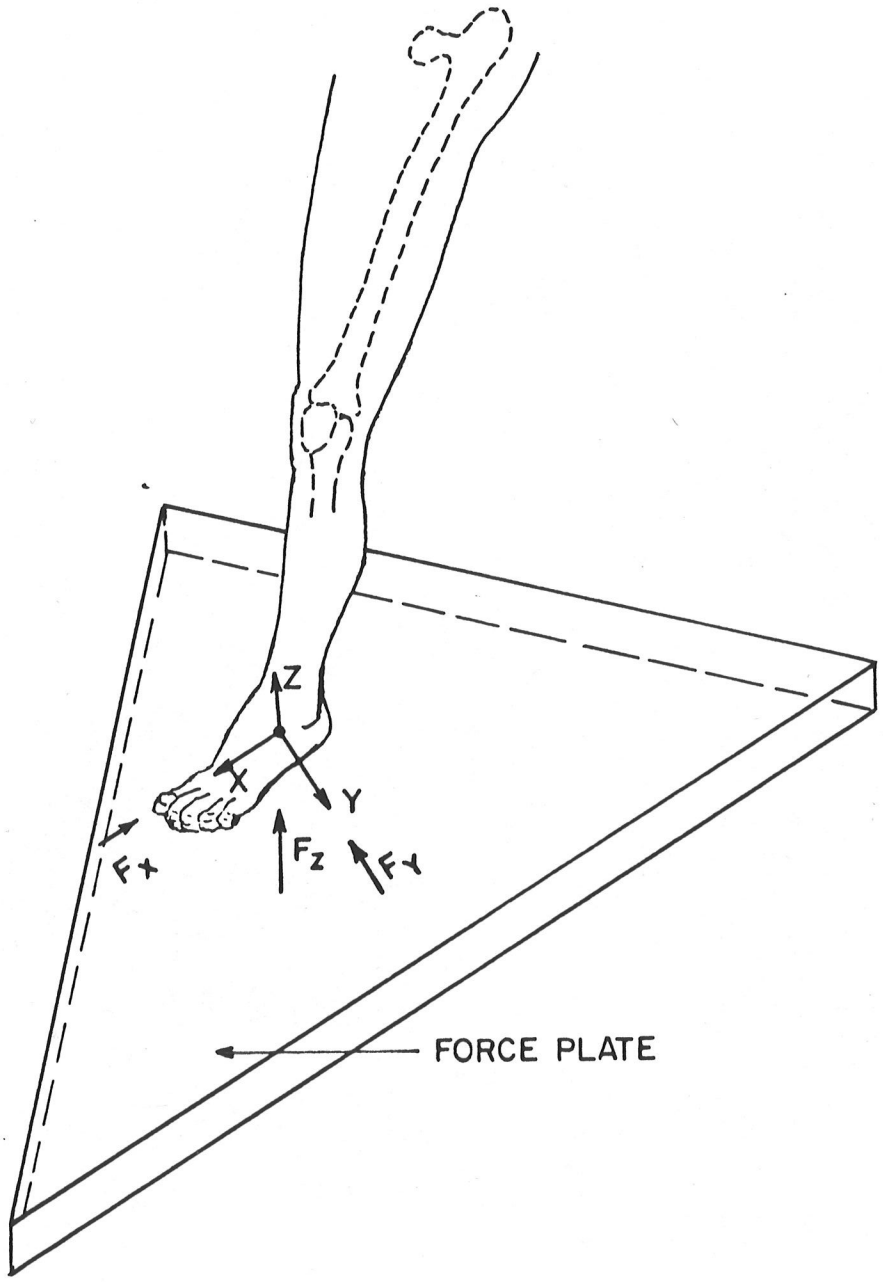

Figure 11 Ground-Reaction force components

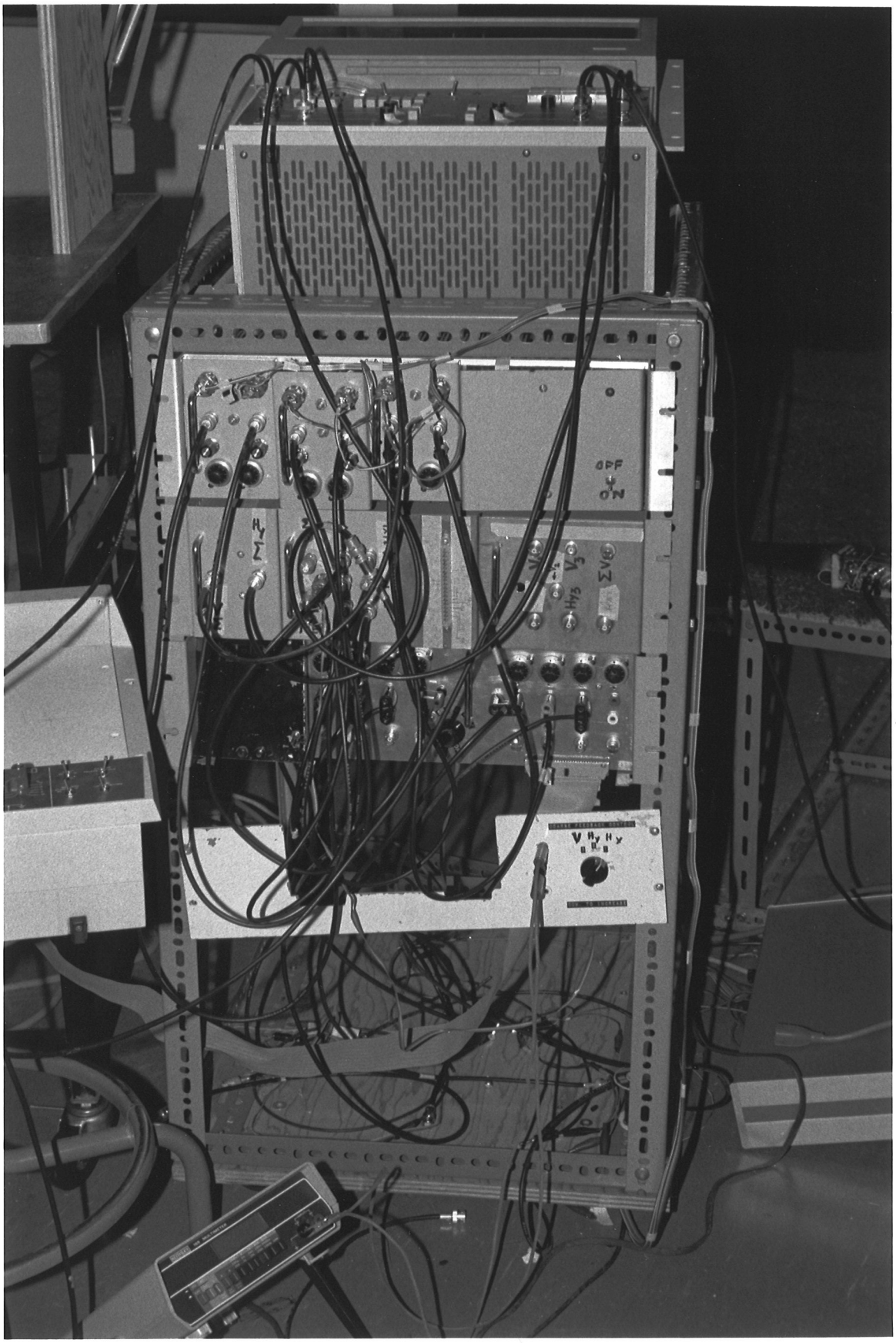

Figure 12 Instrumentation amplifiers for balancing, scaling and signal processing

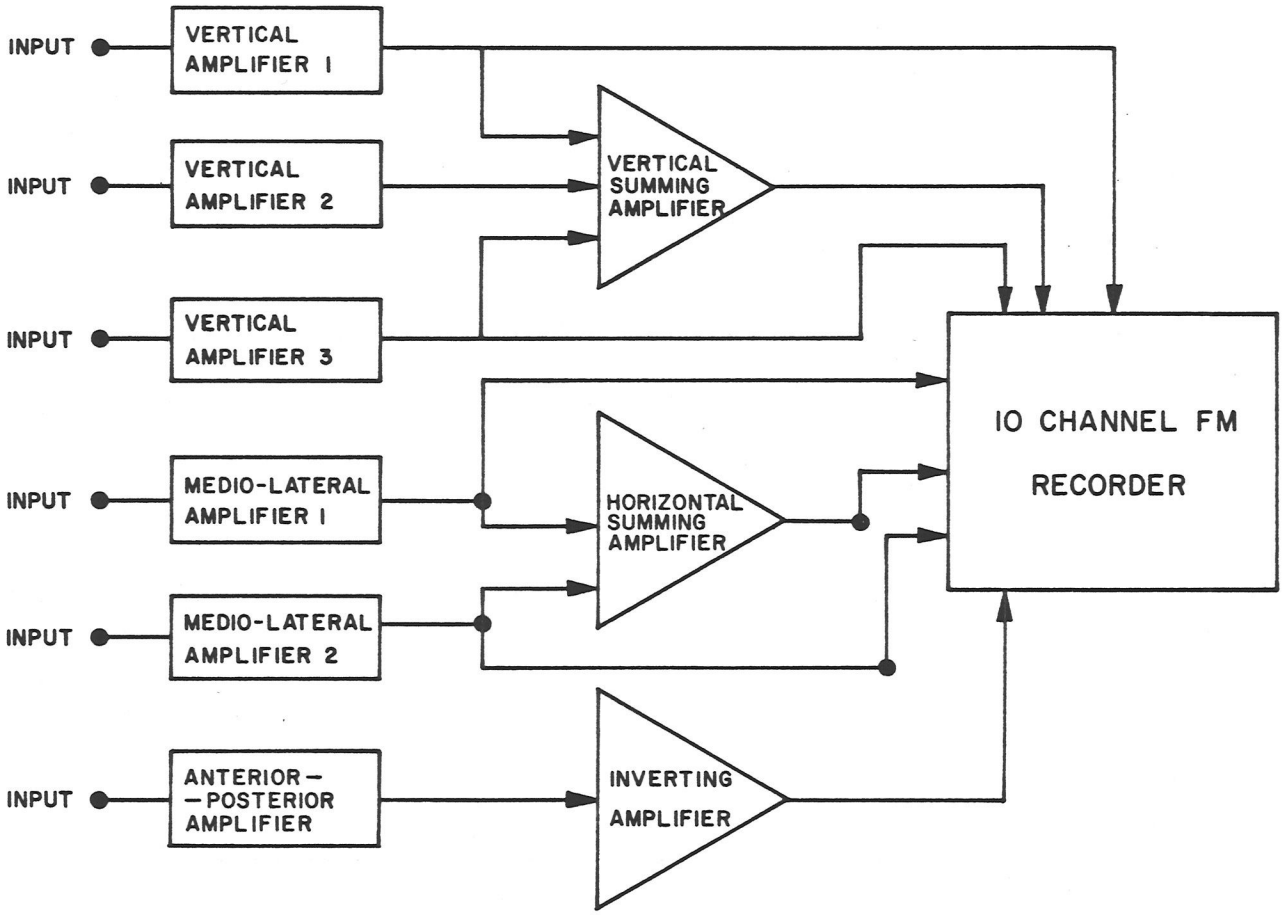

Figure 13 Schematic of the general instrumentation

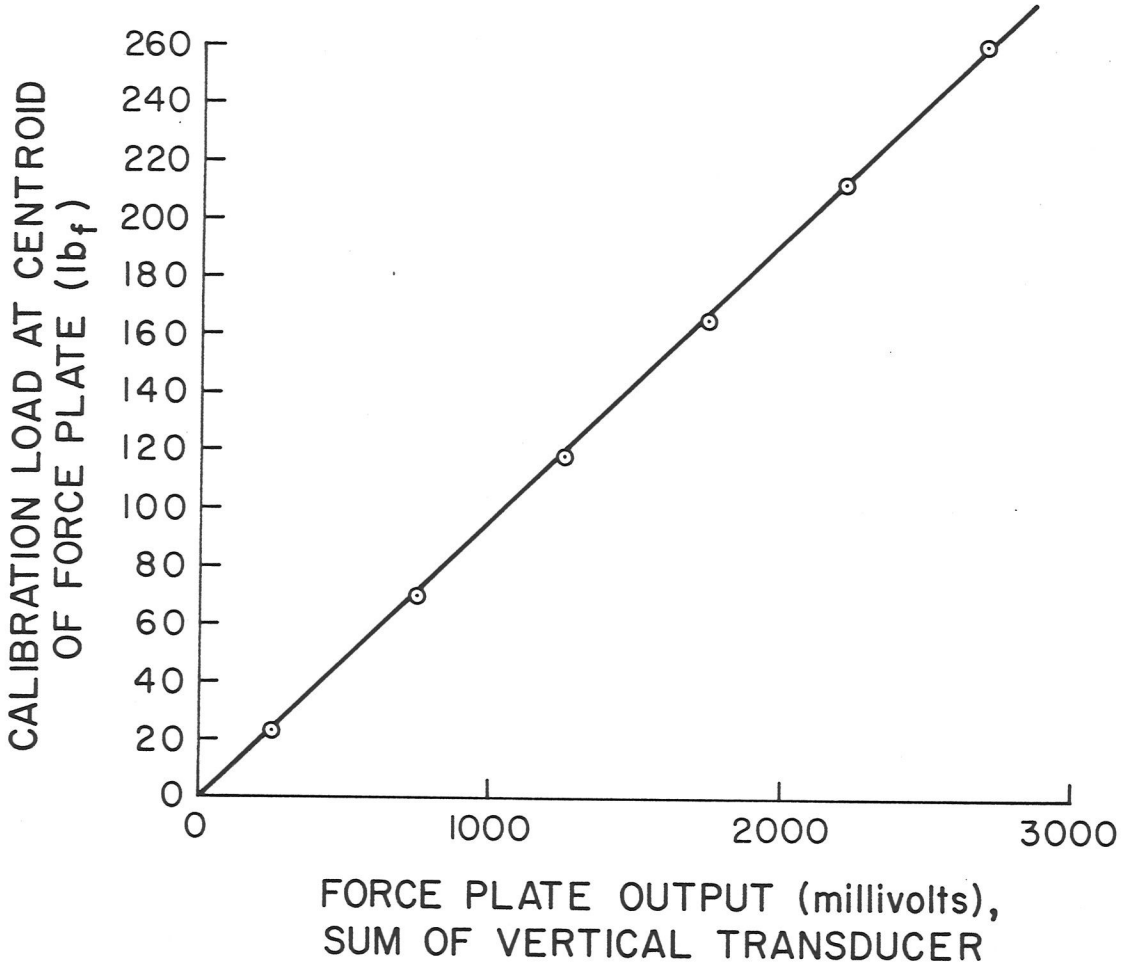

Figure 14 Plot of Load vs Summed output of vertical transducer amplifier signals

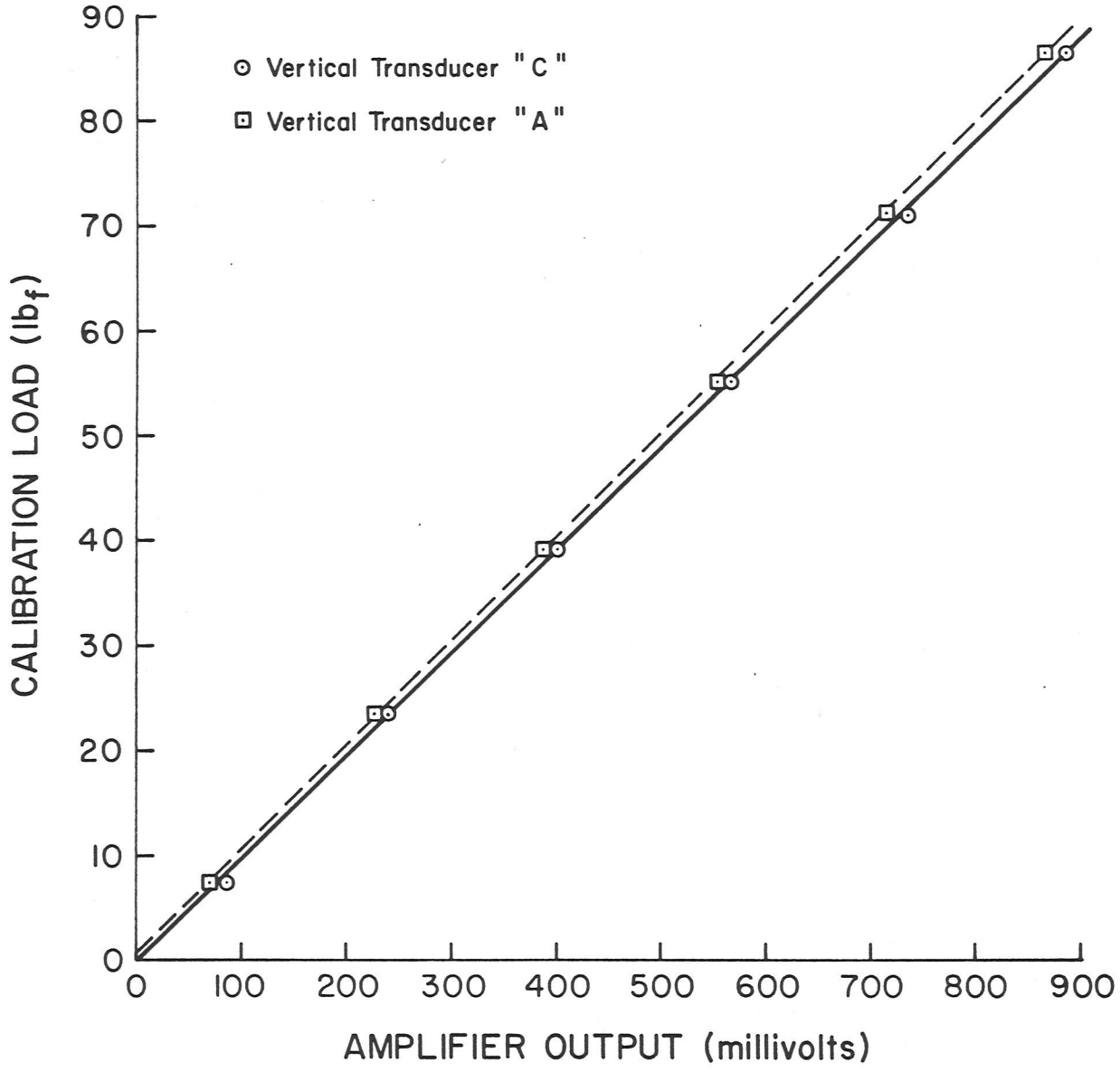

Figure 15 Response of individual transducers for vertical load

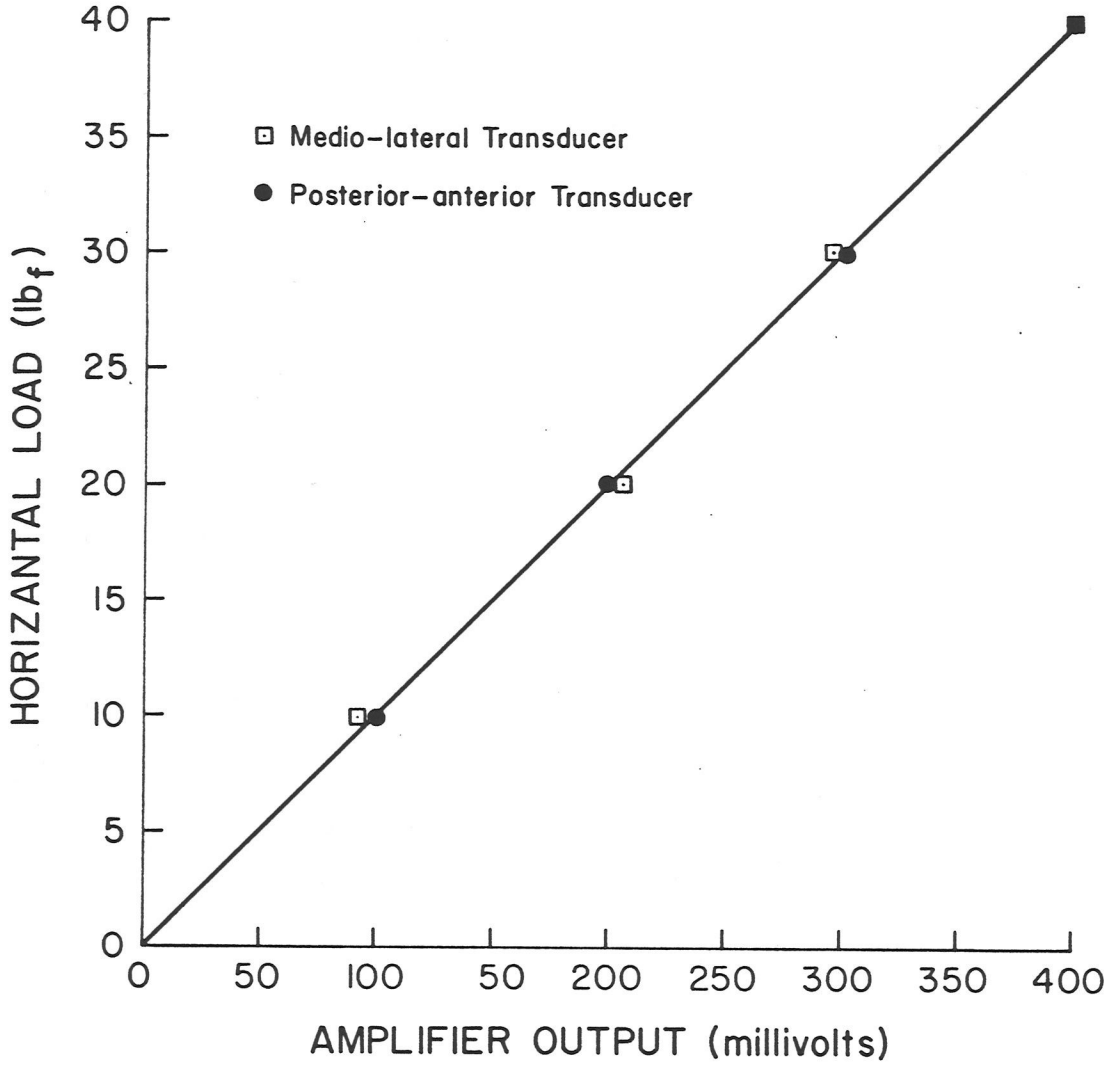

Figure 16 Plot of Load vs Horizontal transducer outputs

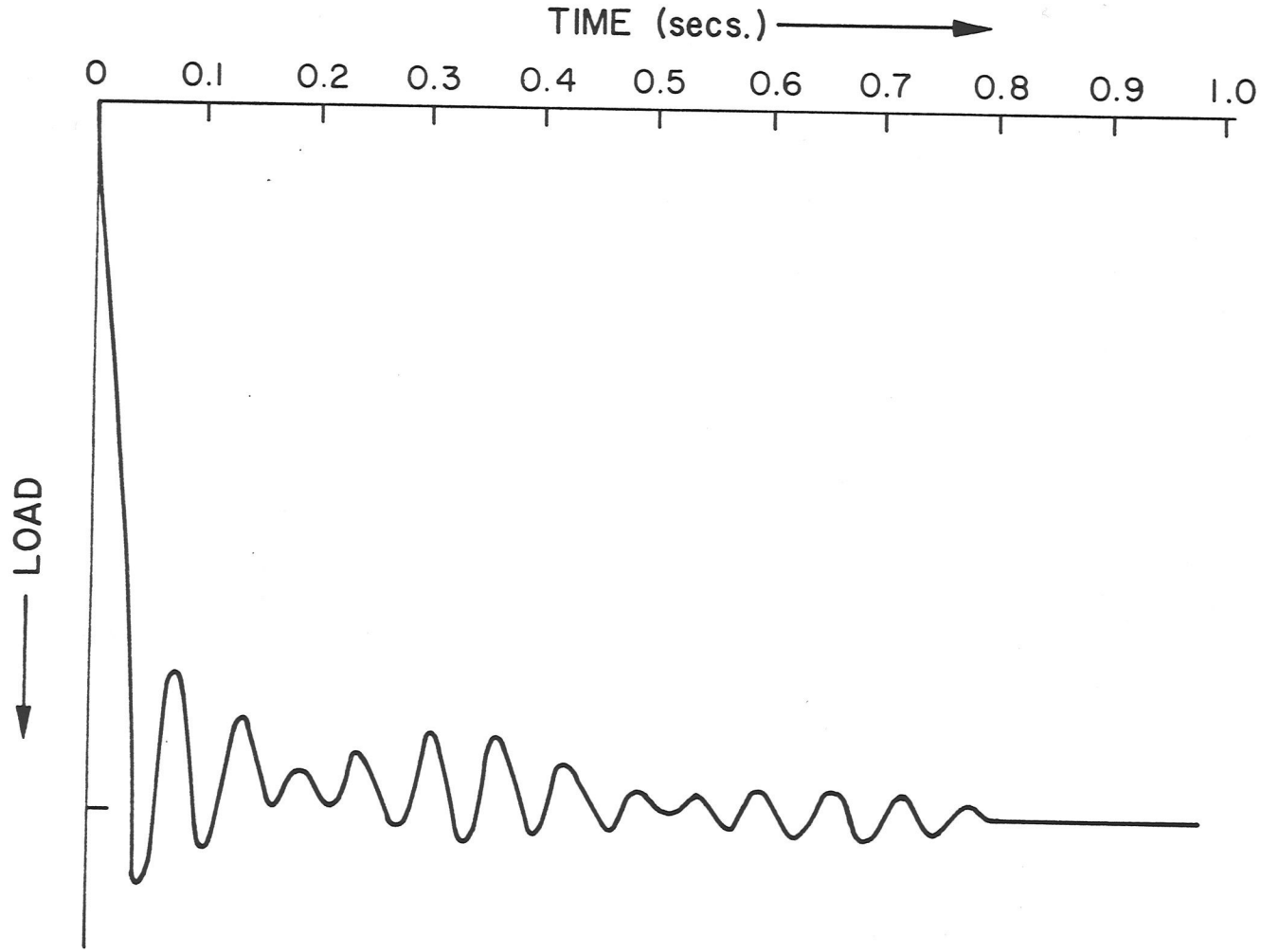

Figure 17 Frequency-time response plot for an impulse load

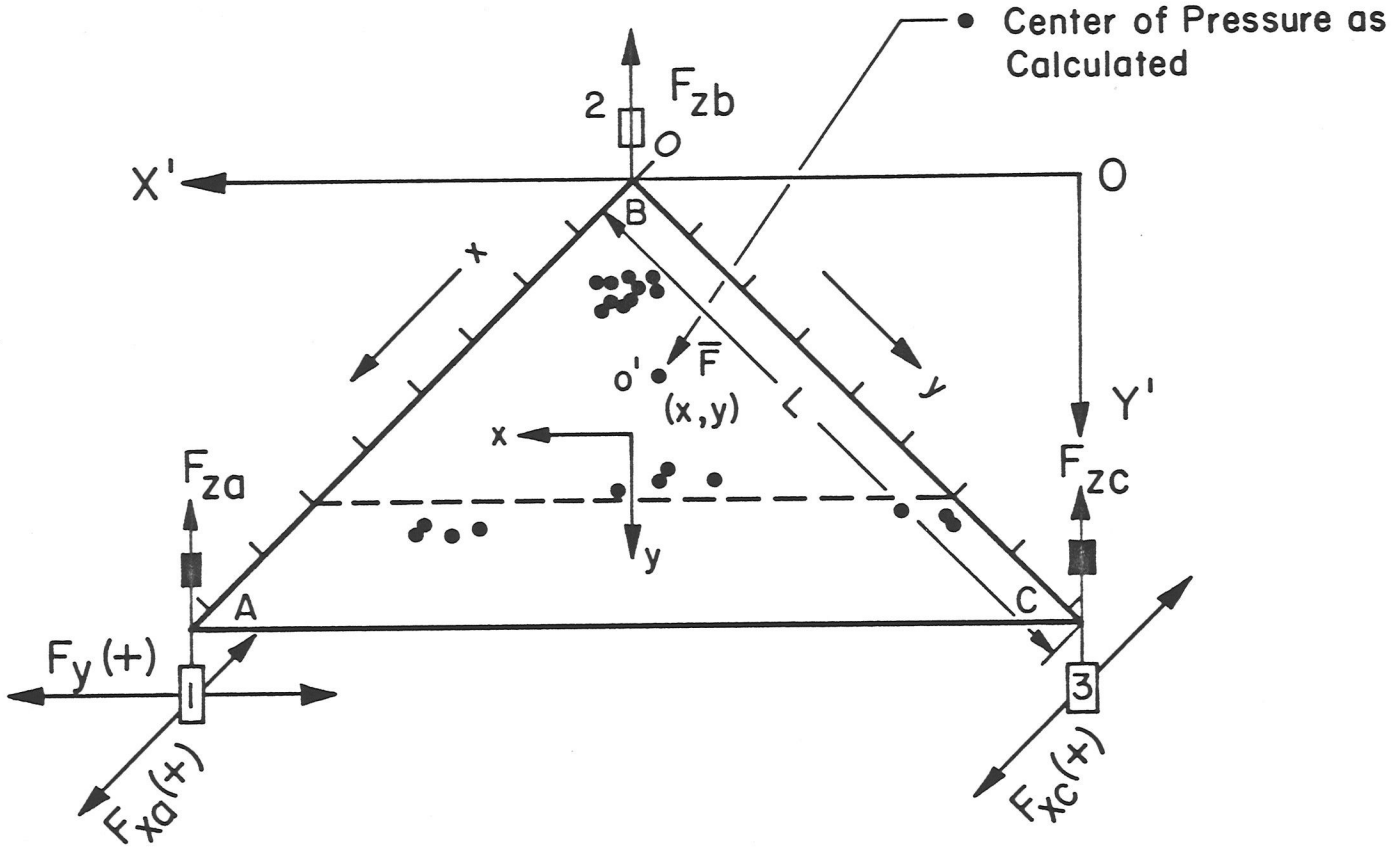

Figure 18 Orientation of plate axes for center of force measurement

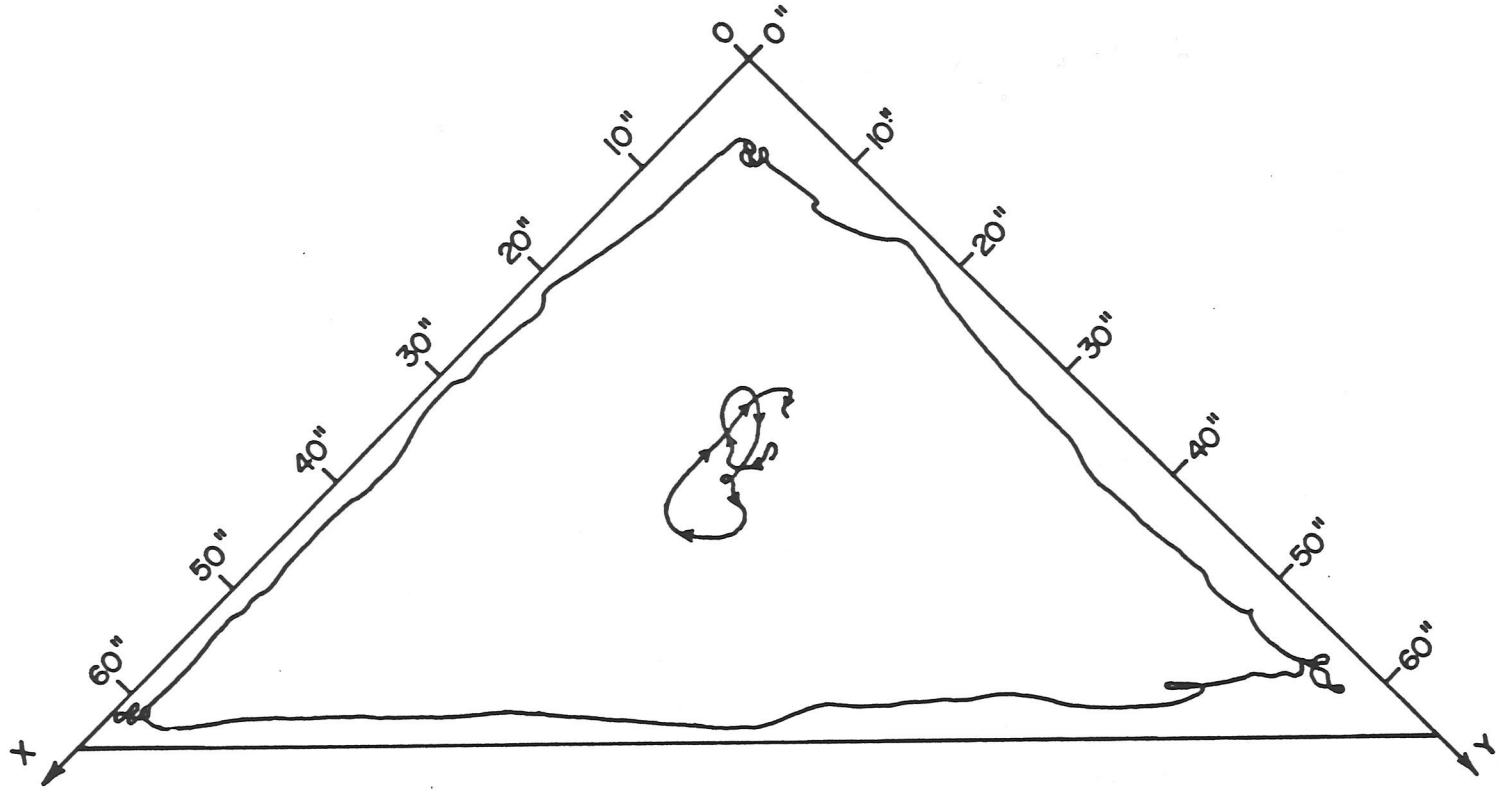

Figure 19 Center of pressure for a specialised maneuver in roller skating (spin)

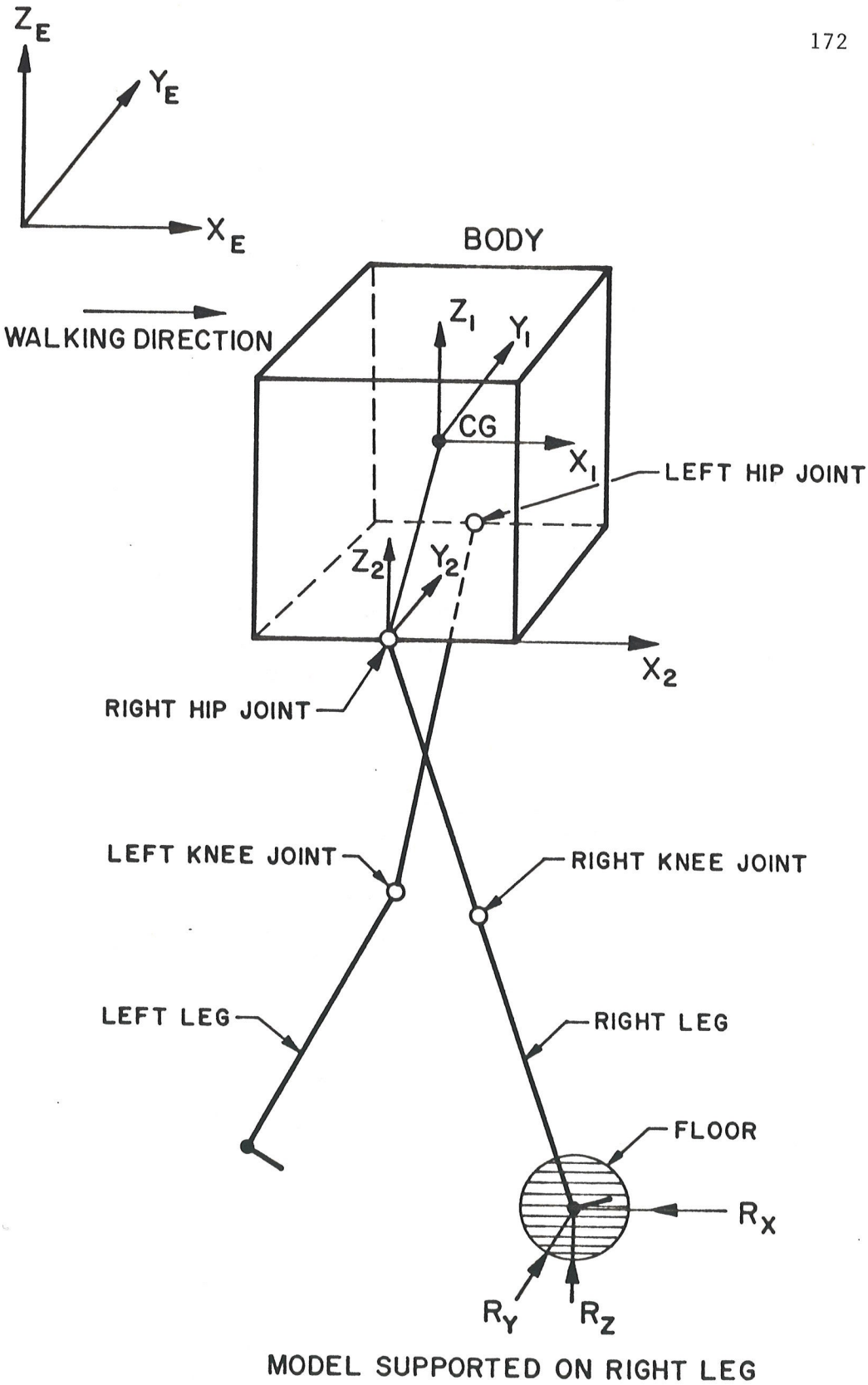

Figure 20 Model on total single support phase

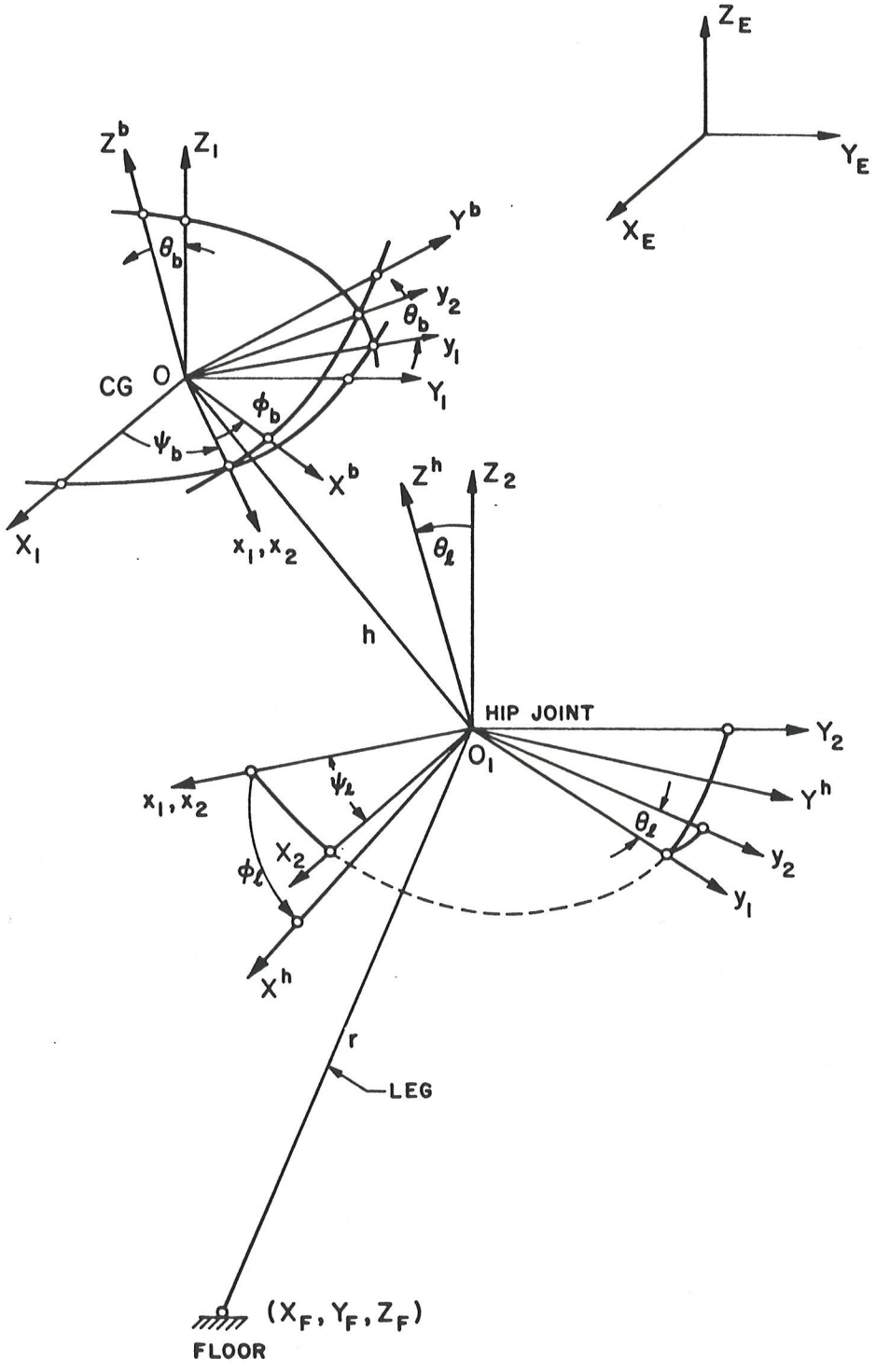

Figure 21 Space and Body coordinate axes at hip and center of gravity

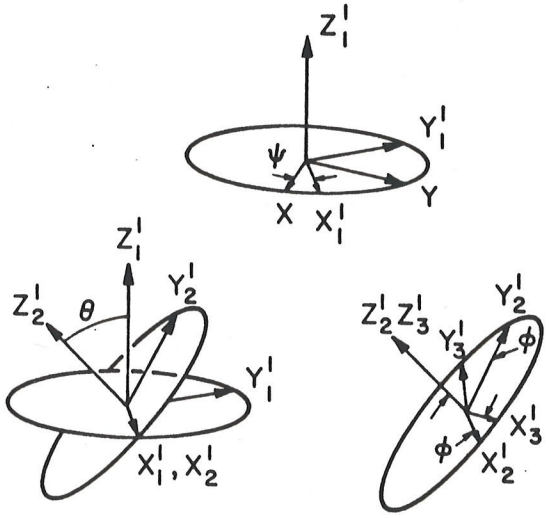

Figure 22 Eulerian angle rotation adopted in this work

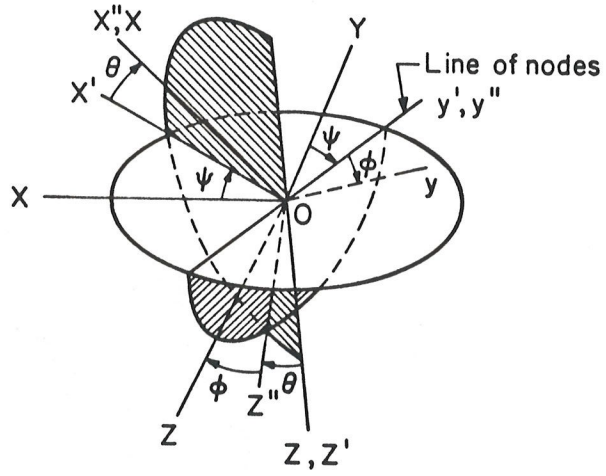

Figure 23 Eulerian angle rotation (Type I in Table 2)

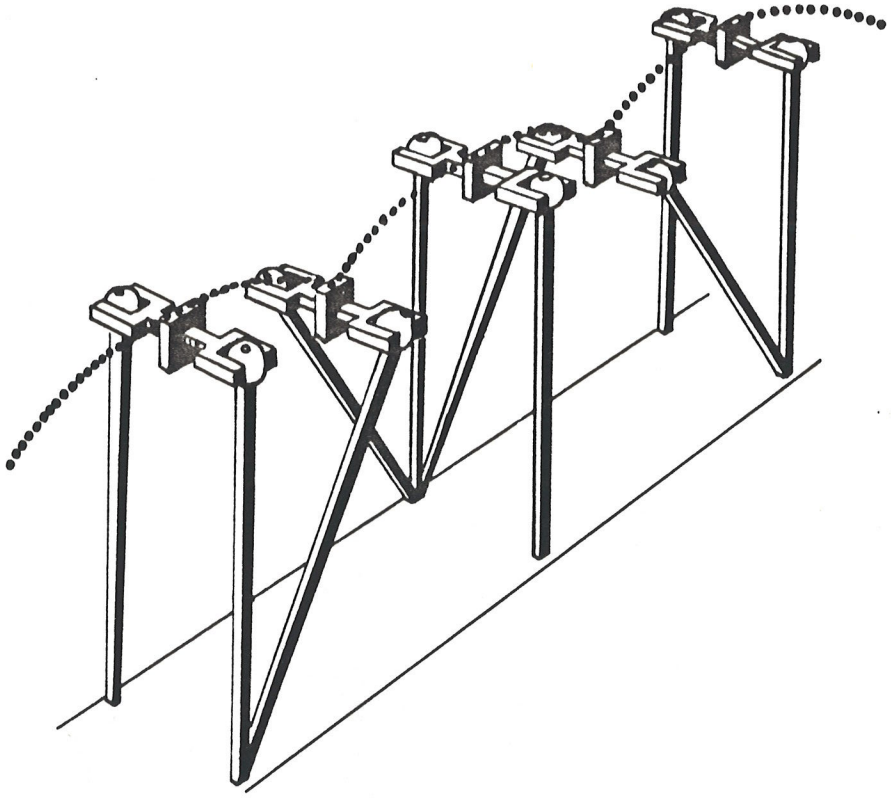

Figure 24 Hypothetical compass gait

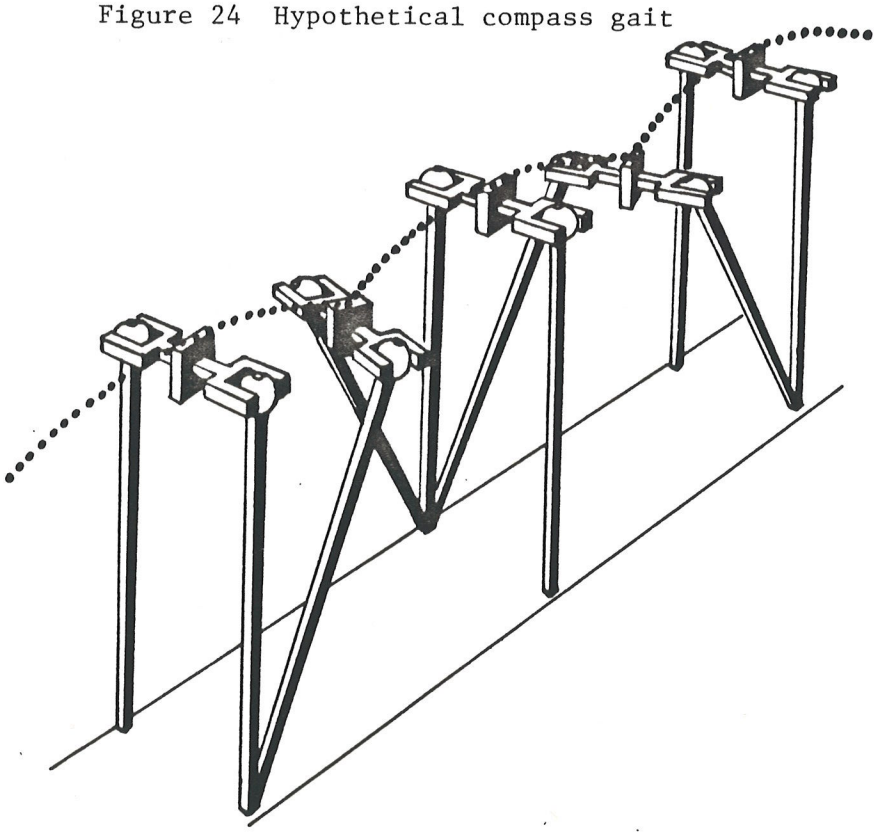

Figure 25 Locomotion with pelvic rotation added to compass gait

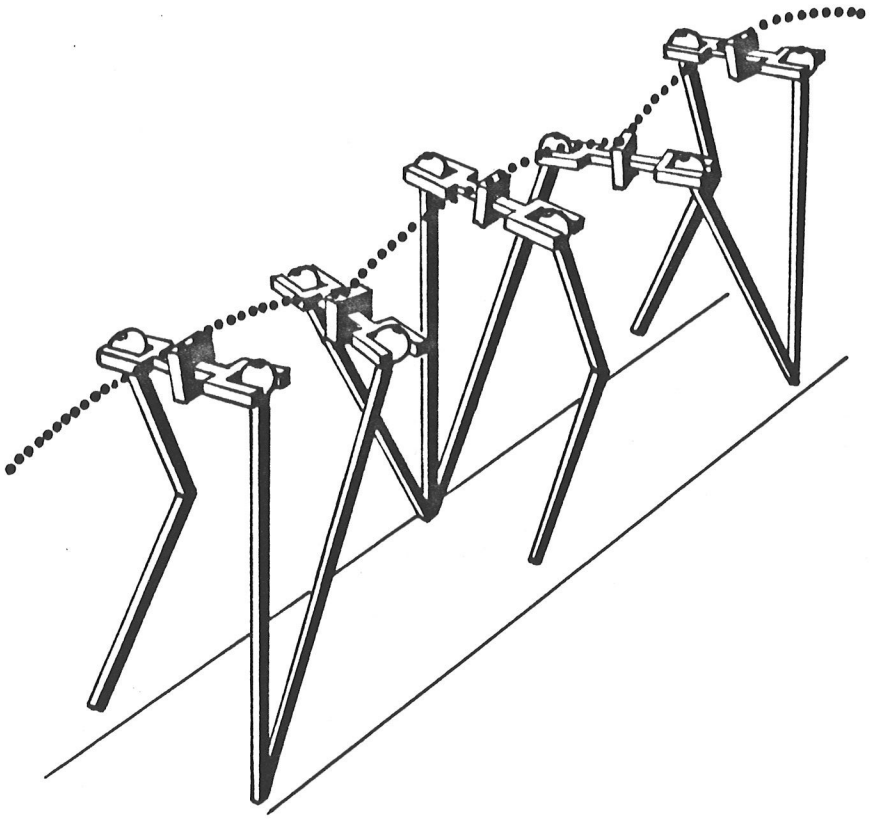

Figure 26 Locomotion with pelvic rotation and pelvic tilt

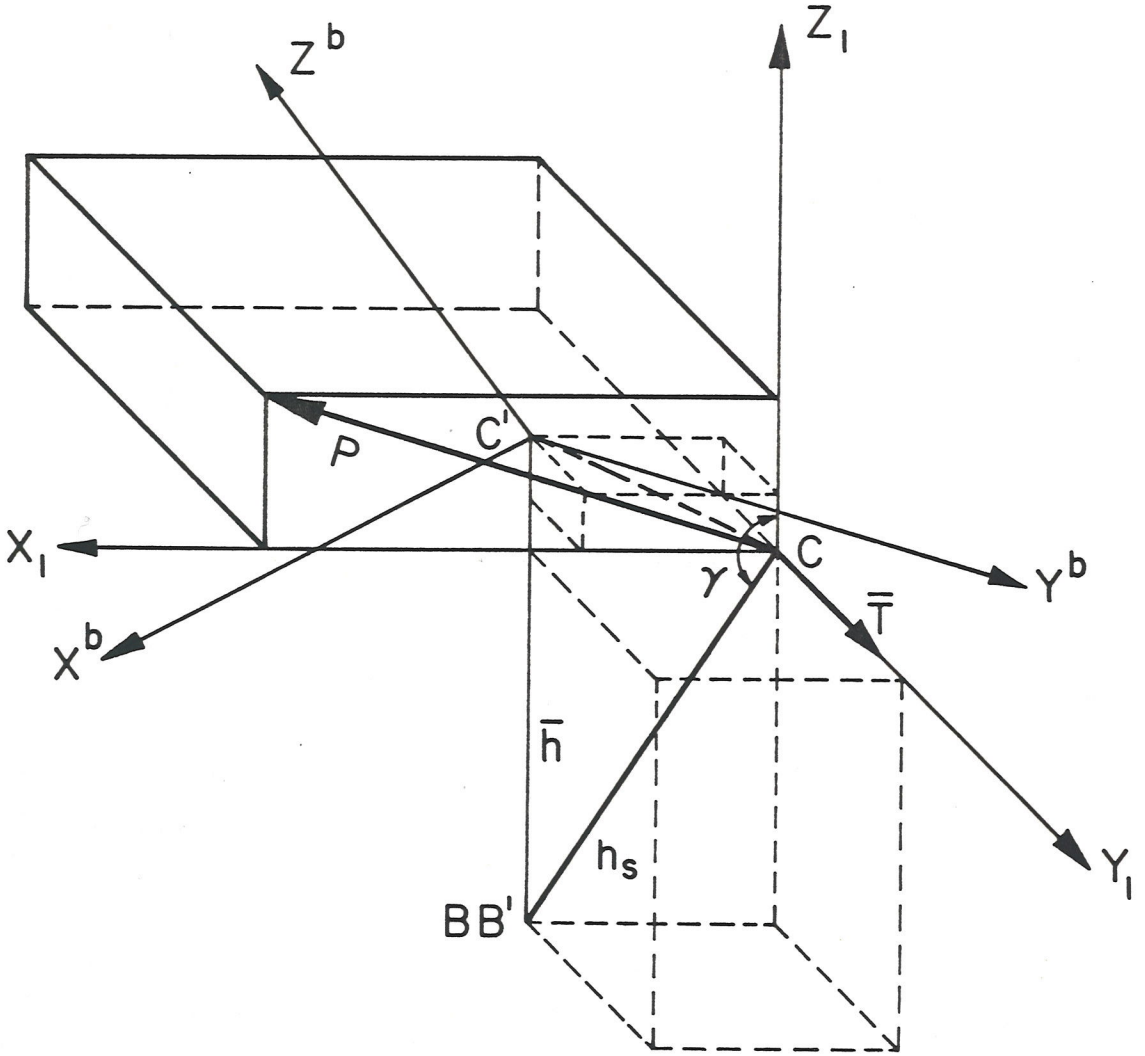

Figure 27 Representation of upper body rotation

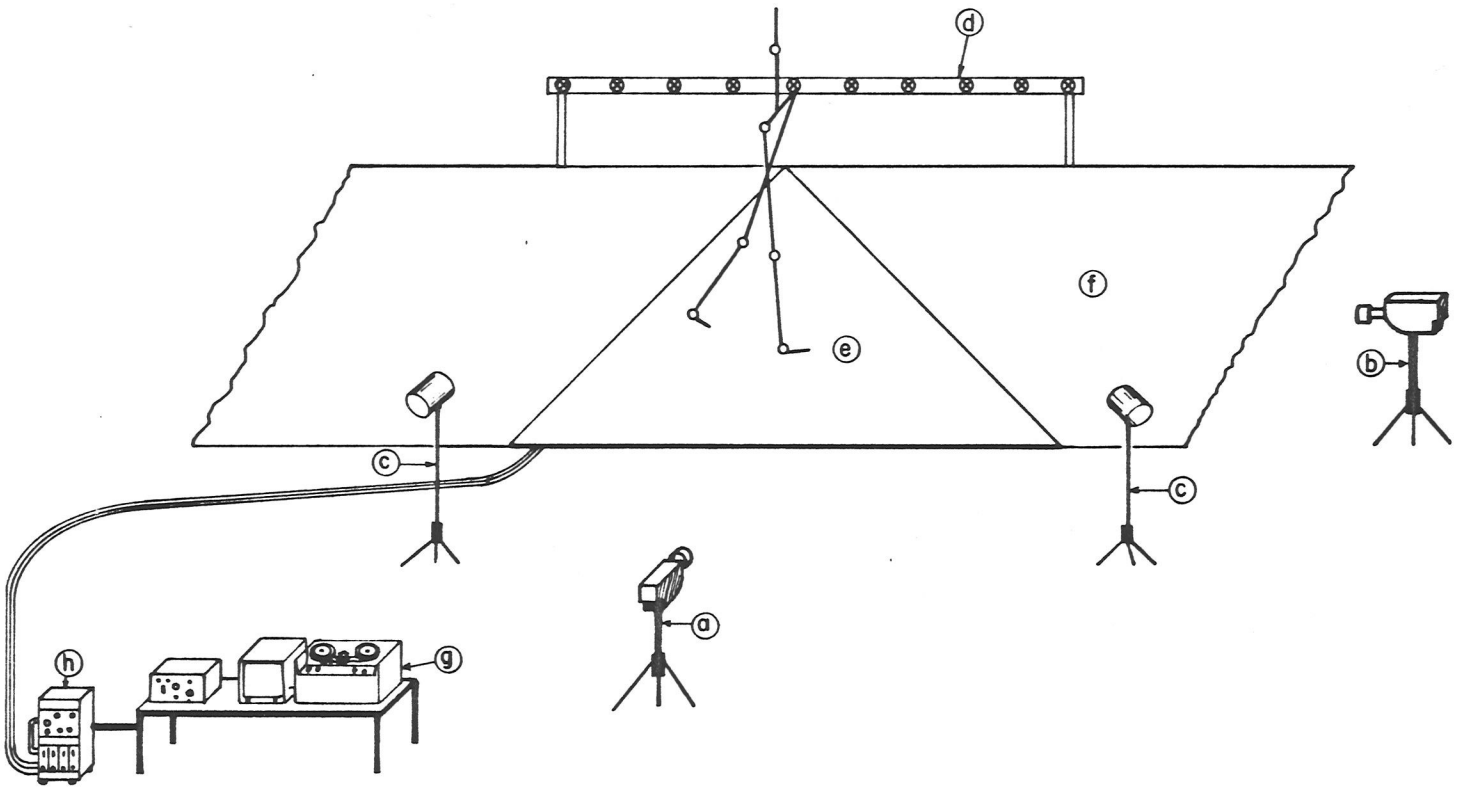

Figure 28 General layout showing position of camera and background markers

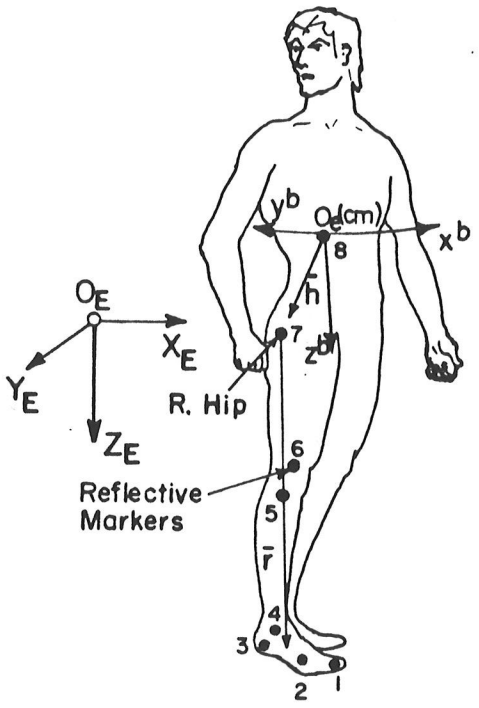

Figure 29 Location of body markers

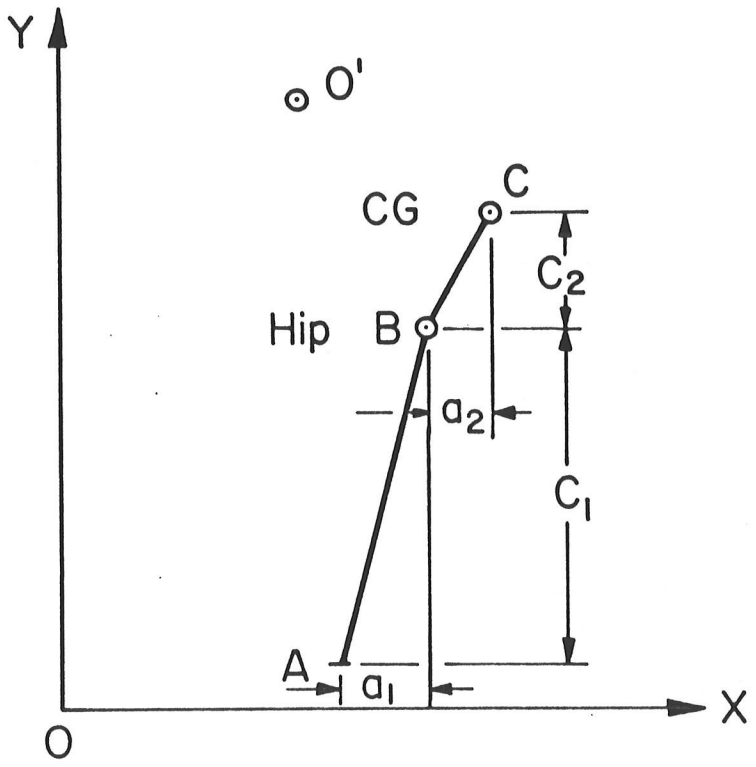

Figure 30 Relative position of markers in the sagittal plane

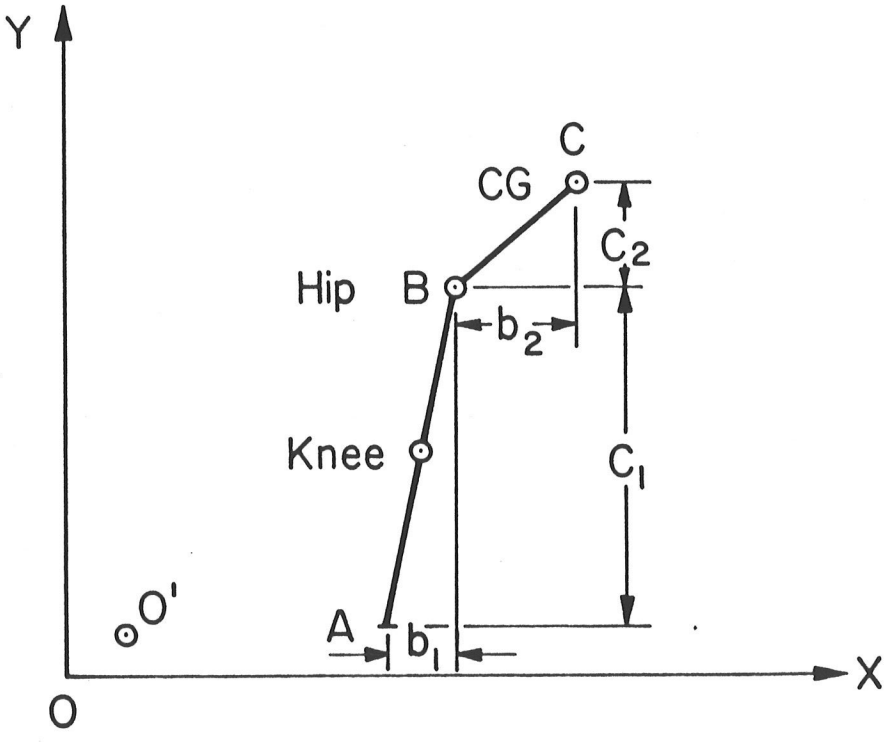

Figure 31 Relative position of markers in the frontal plane

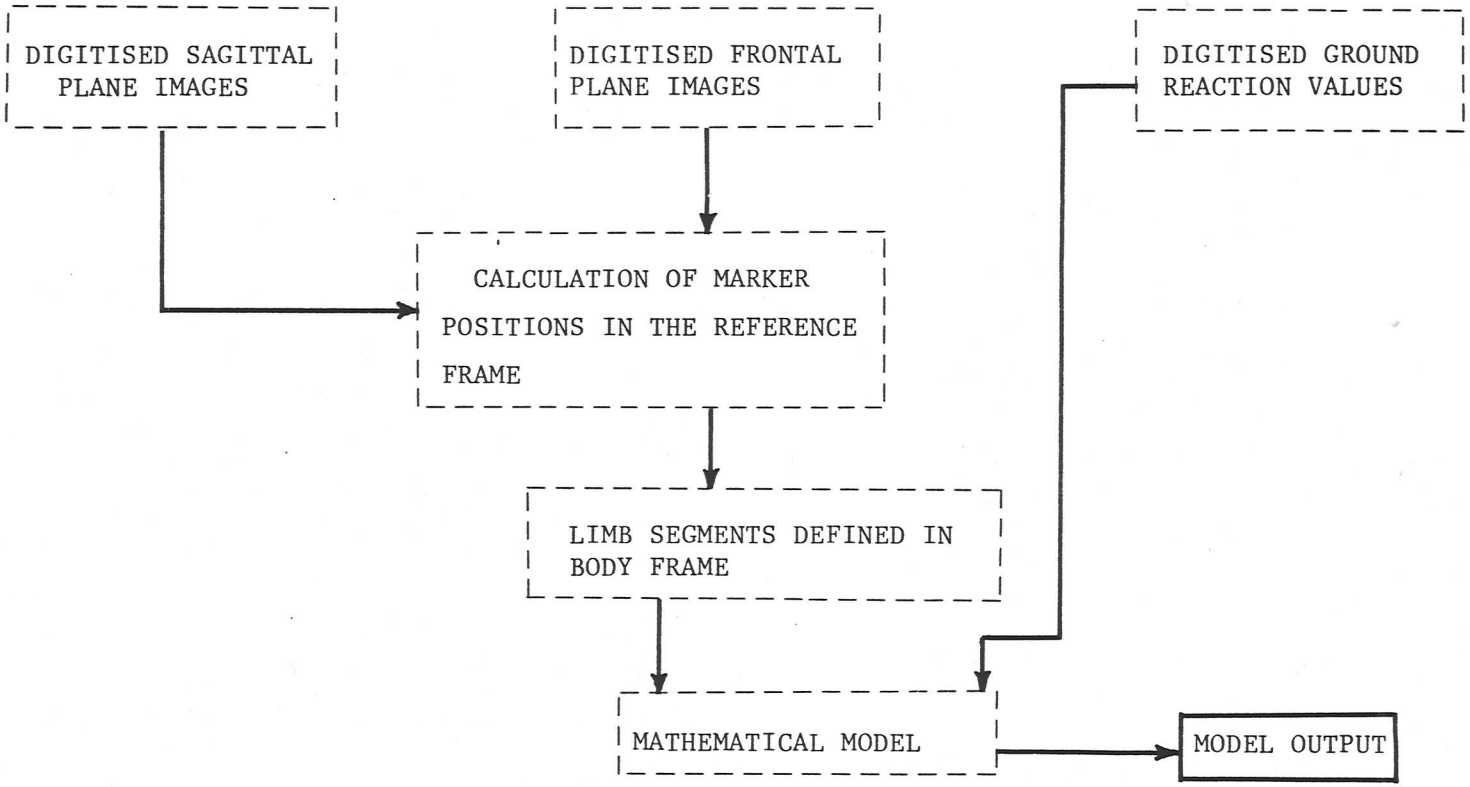

Figure 32 Block diagram of the computer Model

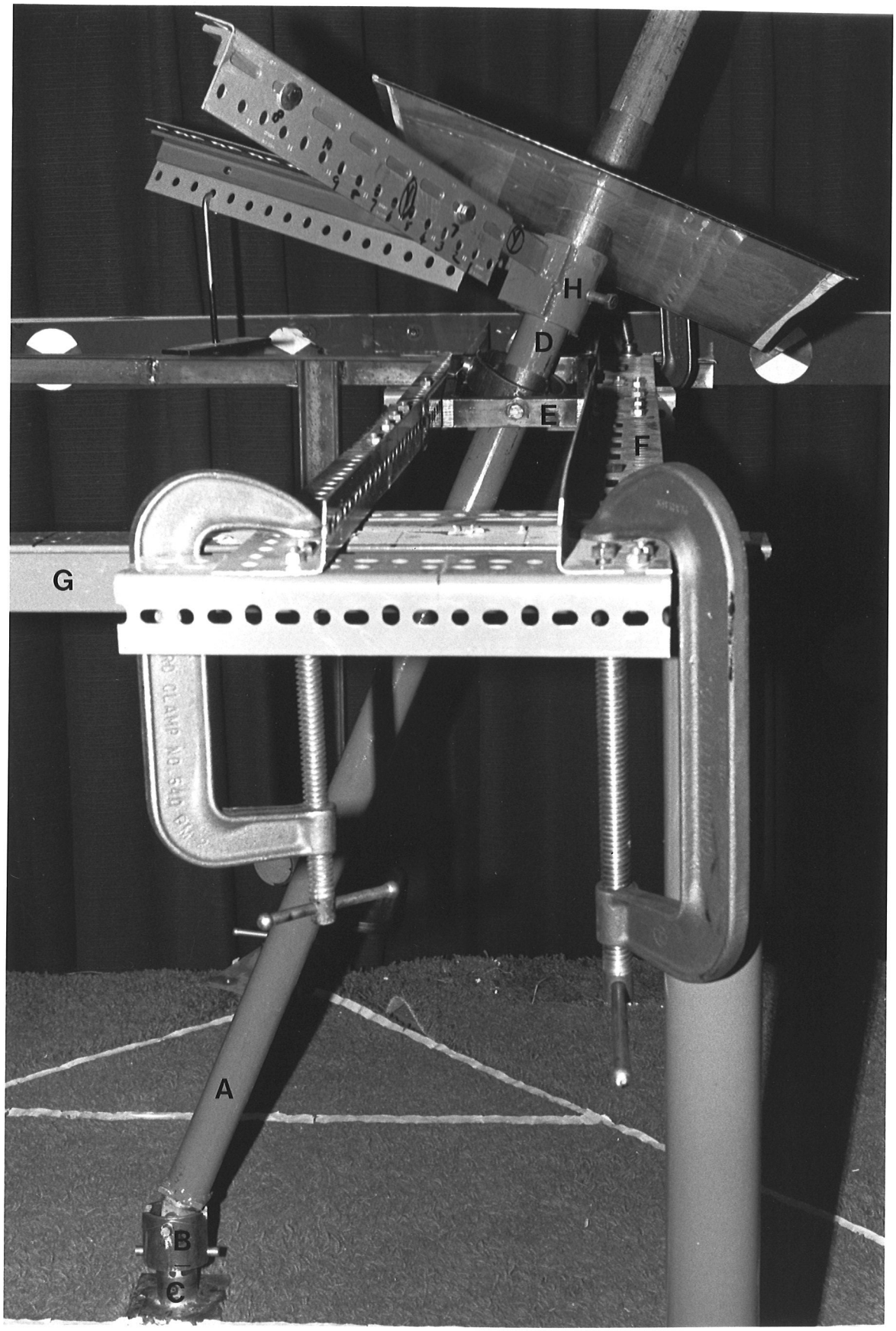

Figure 33 Jig for experimental verification of the model

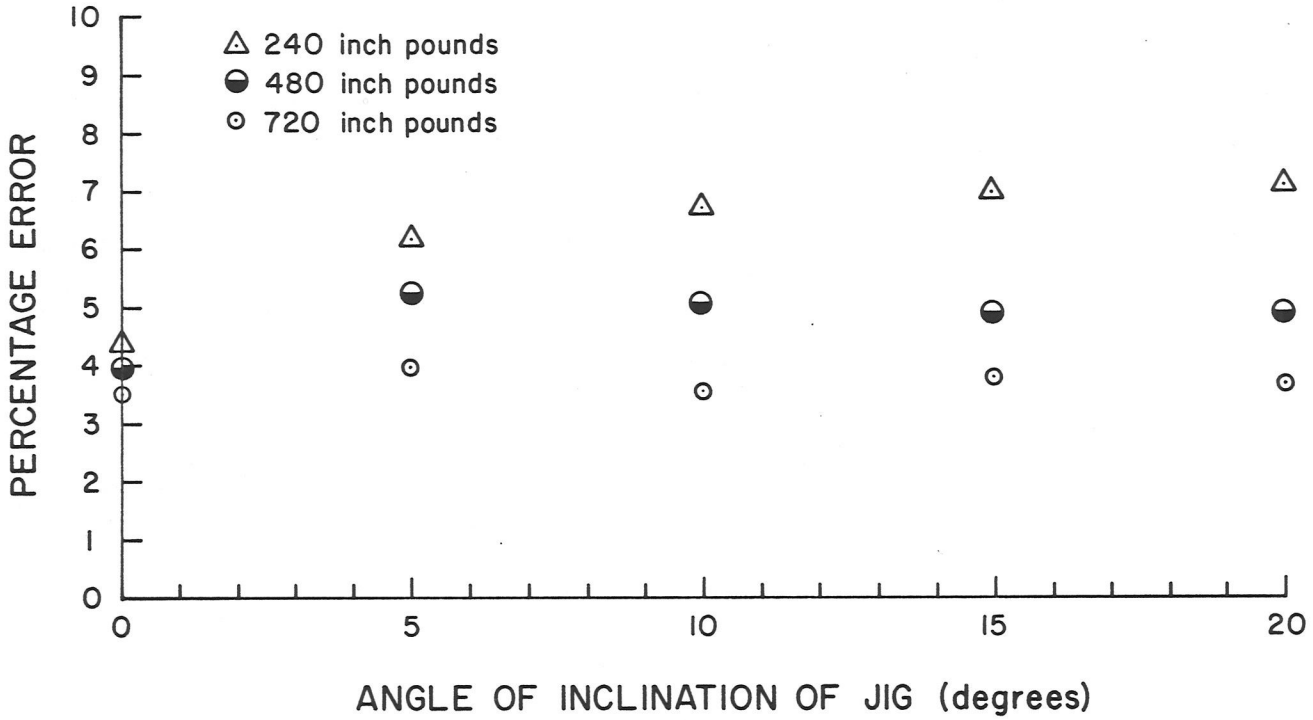

Figure 34 Plot of percentage error in theoretical and experimental moments Vs angle of inclination of jig

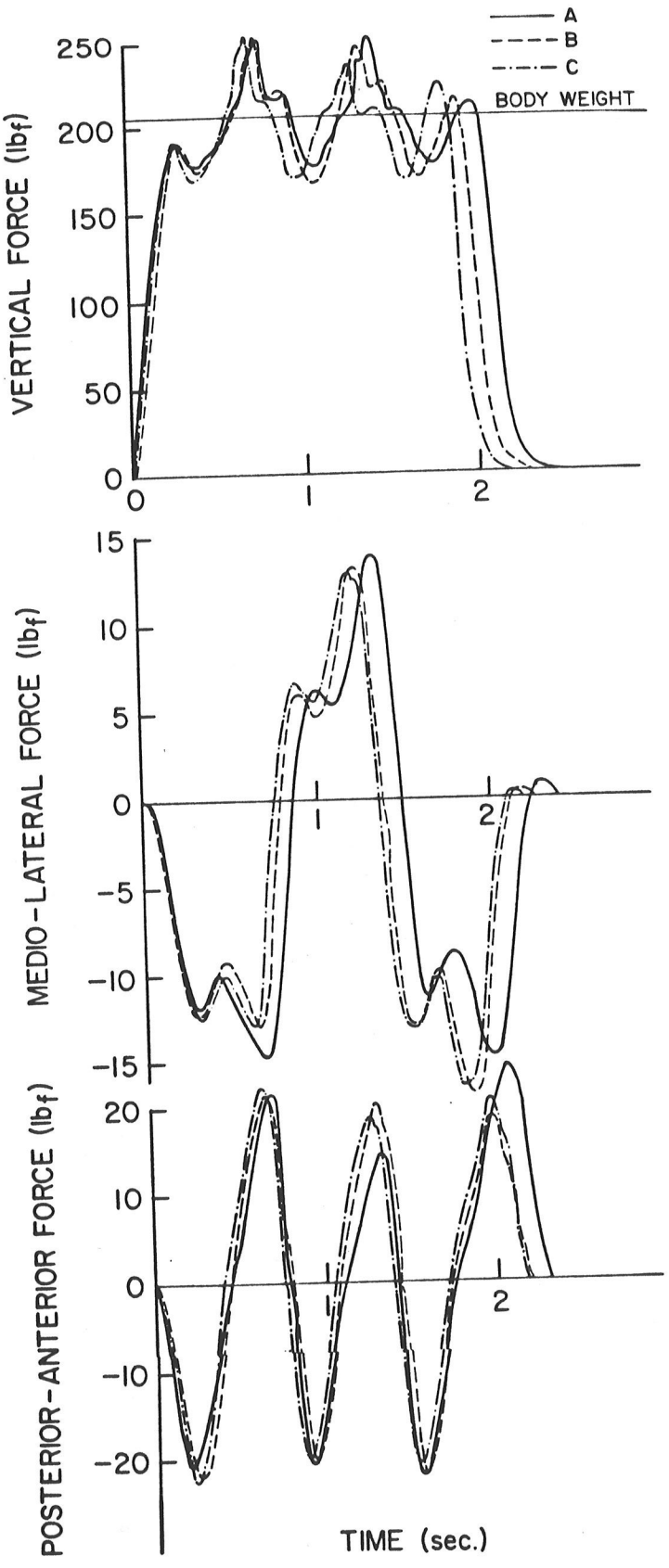

Figure 35 Consistency in ground-reaction forces for a normal locomotion

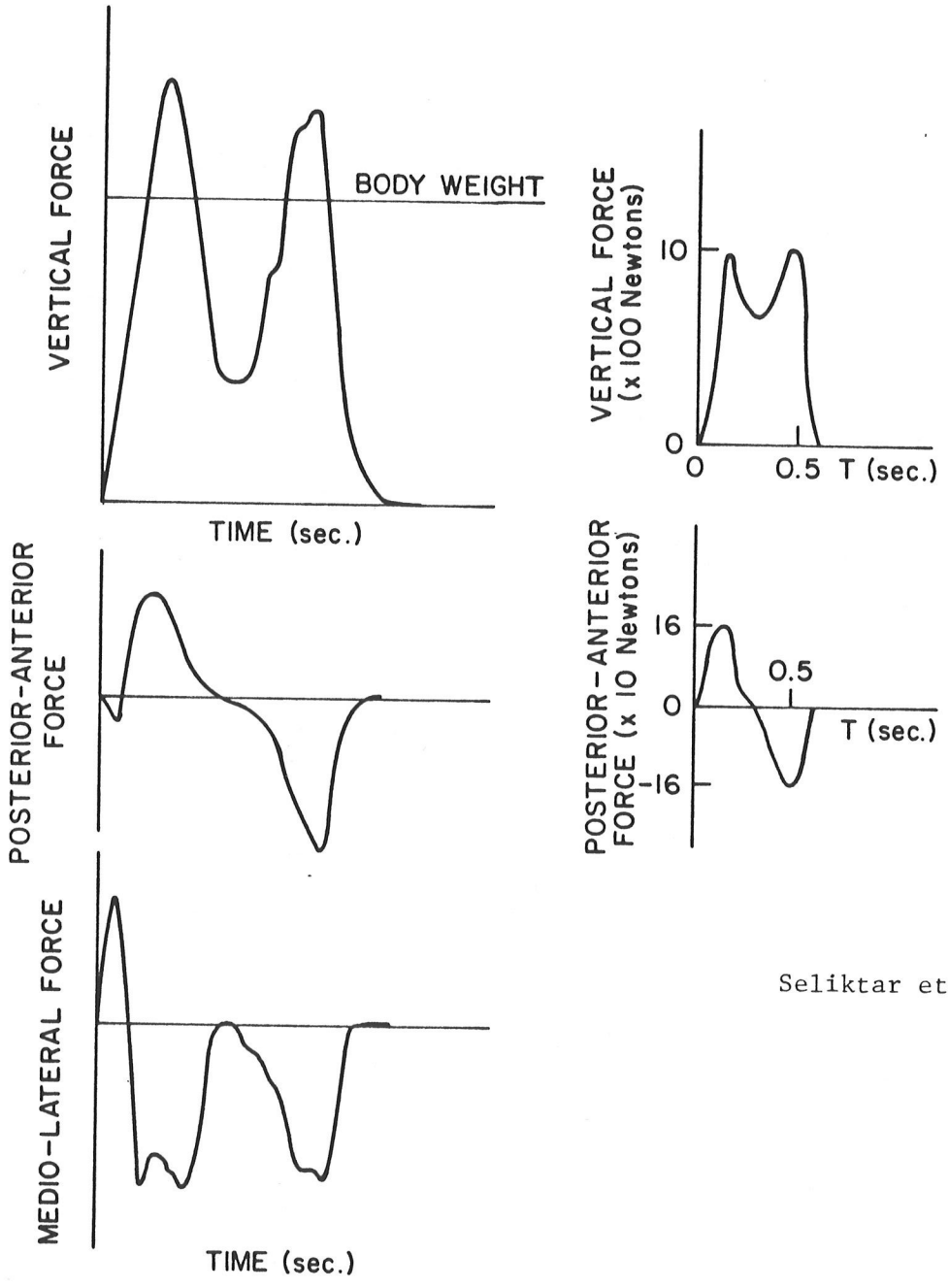

Cunningham et.al (6)

Seliktar et.al(93)

Figure 36 Ground-reaction forces from previous studies

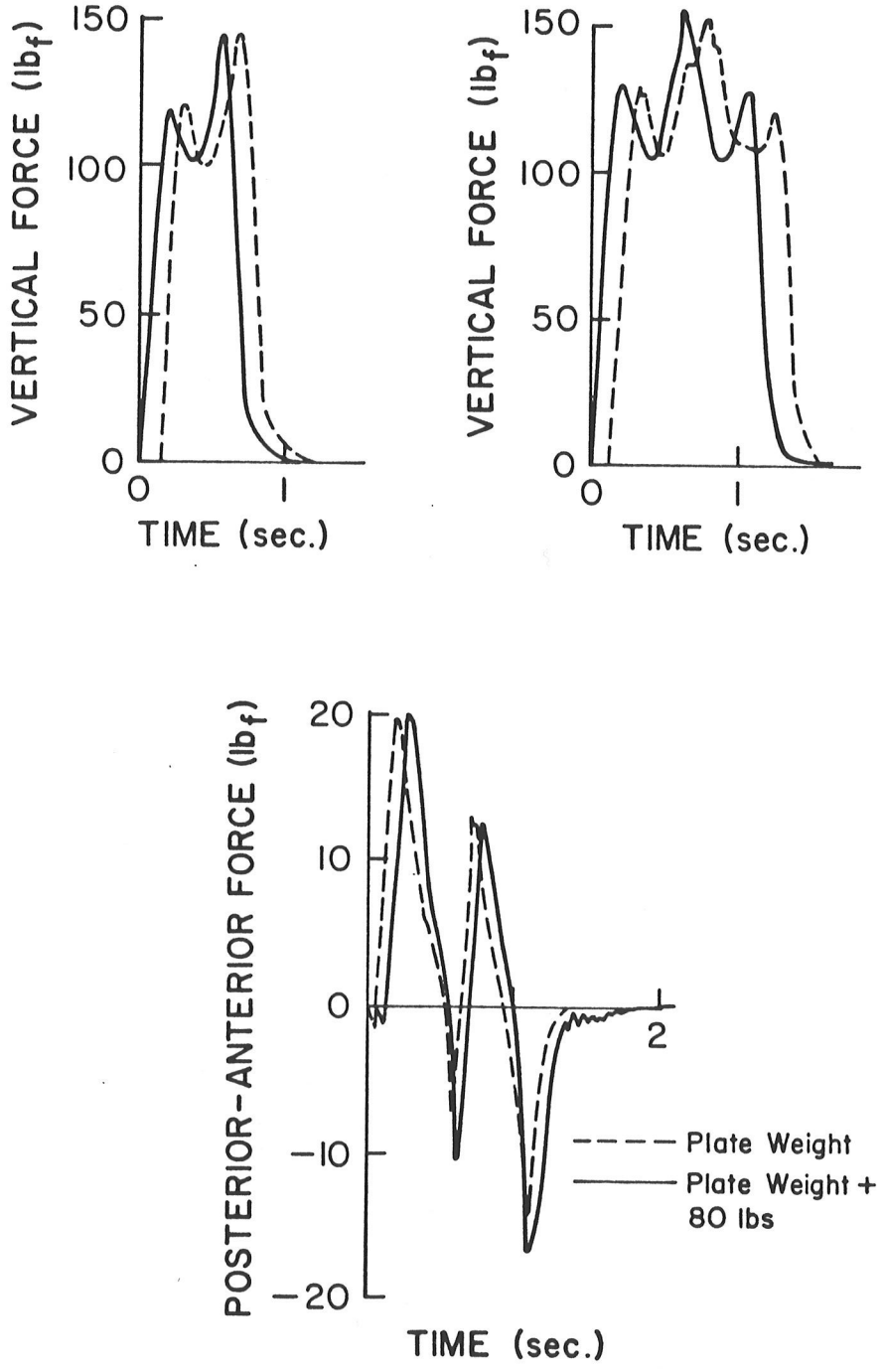

Figure 37 Plots of ground-reaction forces with an increased plate weight

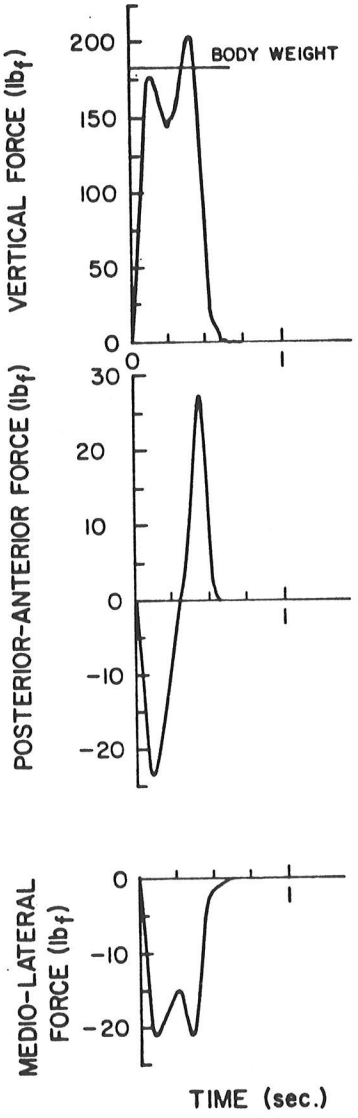

figure 38 Ground-reaction forces for Subject'A'

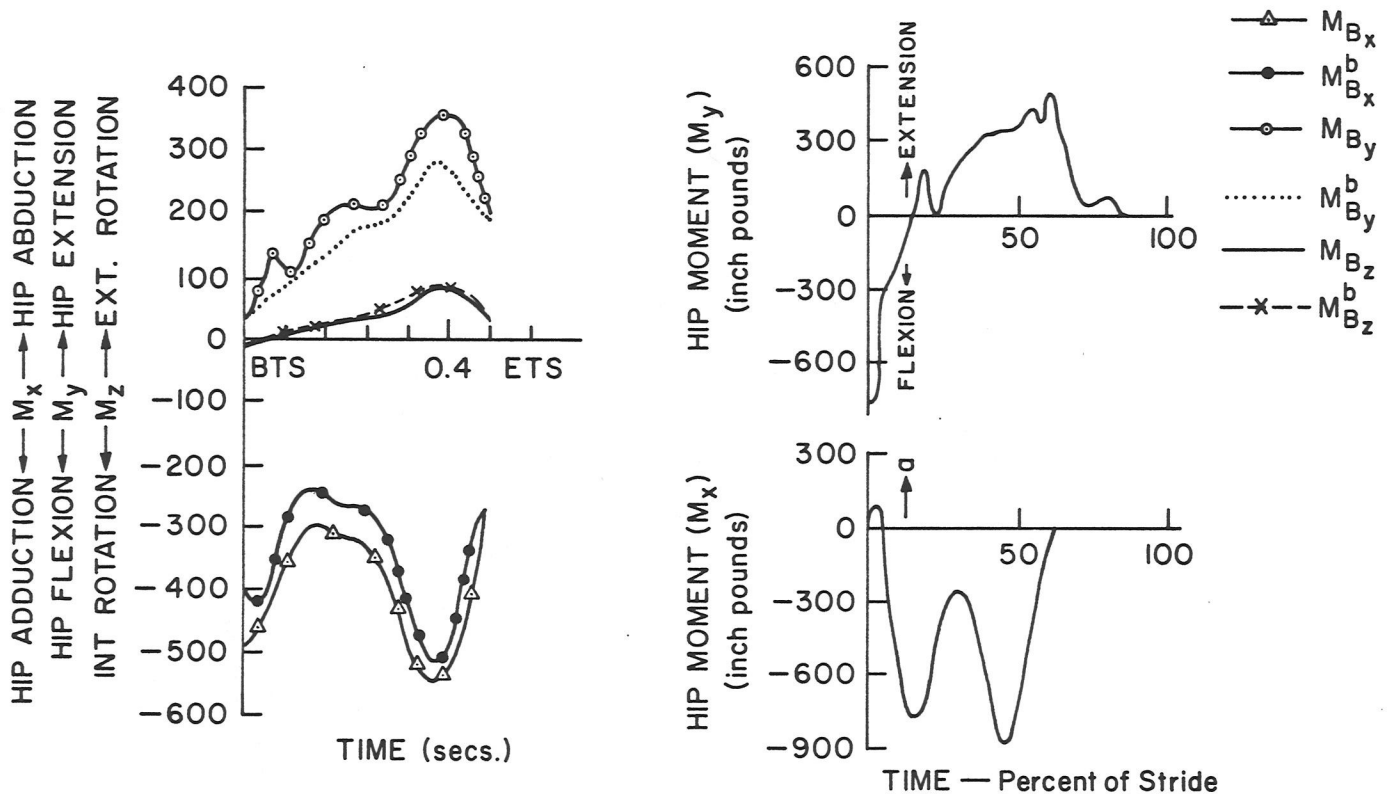

Subject A (this study)

Bresler et.al(22)

Figure 39 Net muscle moment at the hip joint for a normal gait

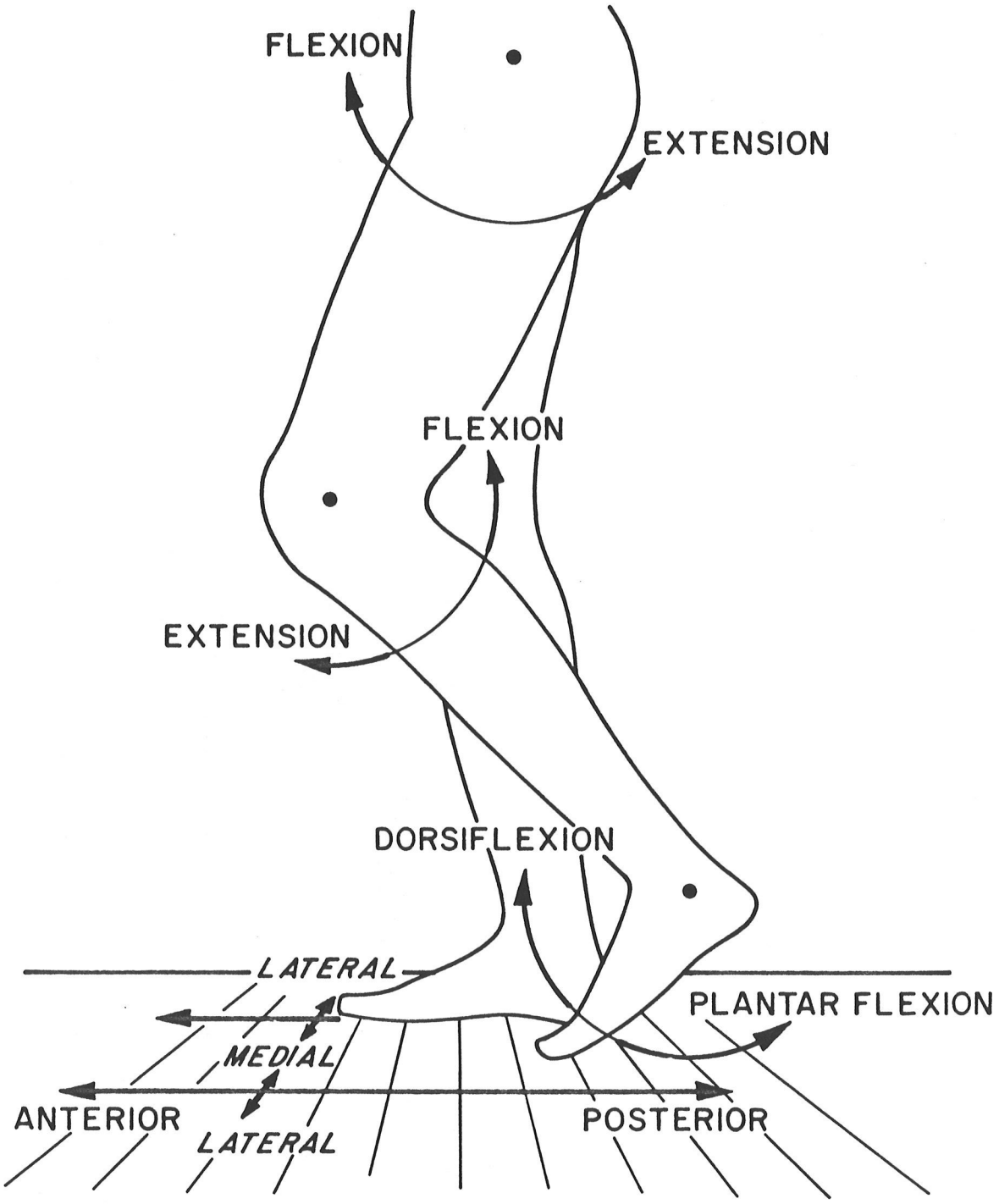

Figure 40 Primary segment movements considered in human locomotion

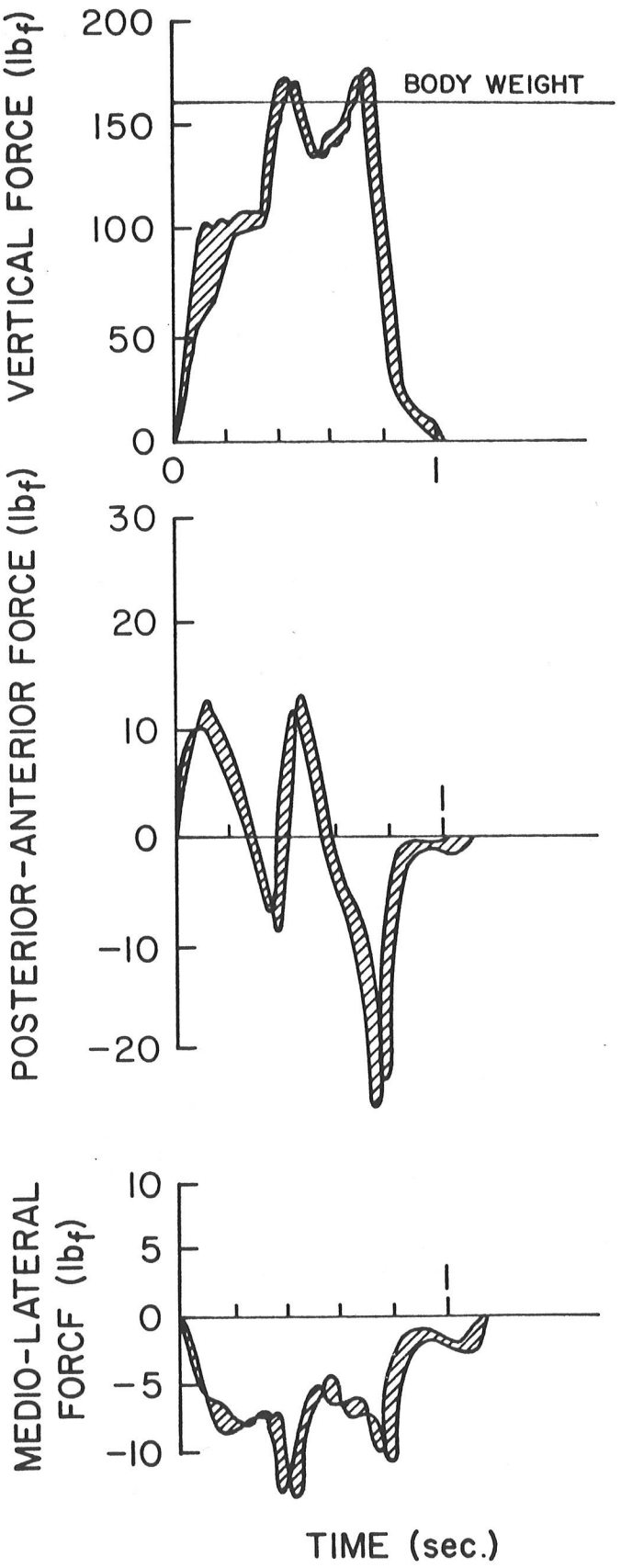

Figure 41 Ground-reaction forces for Subject'B' (first trial)

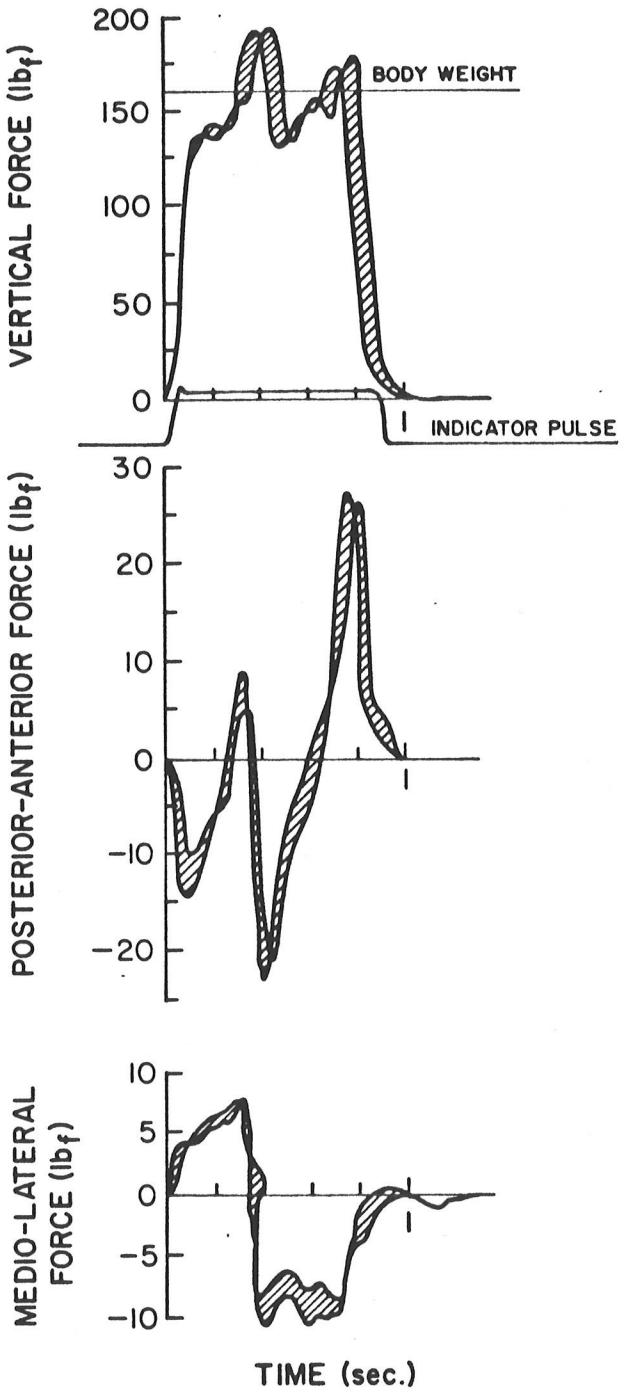

Figure 42 Ground-reaction forces for Subject'B' (subsequent trial)

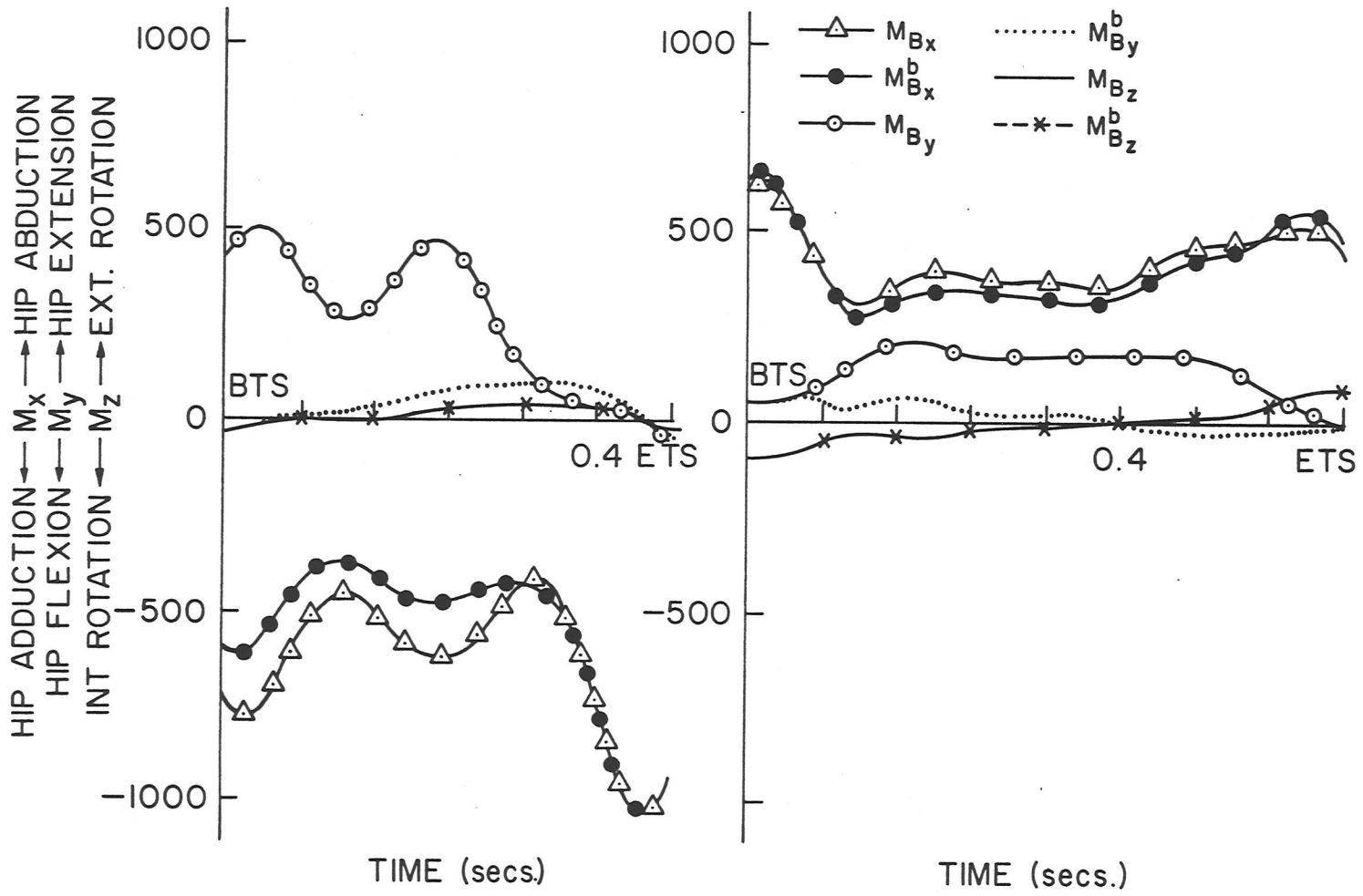

Figure 43 Net muscle moment at the hip joint for subject B (second trial)

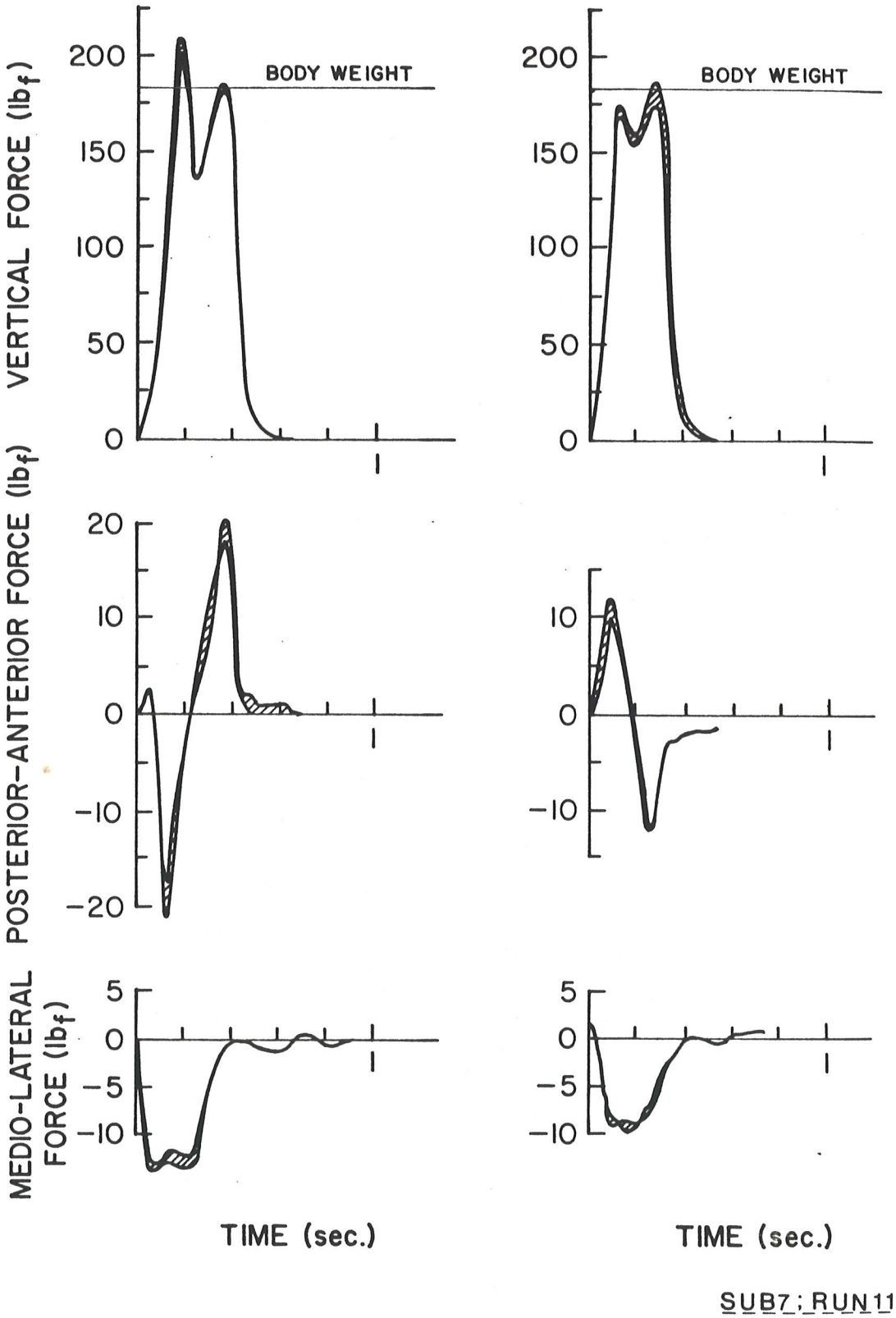

Figure 44 Ground-reaction forces for Subject'C'

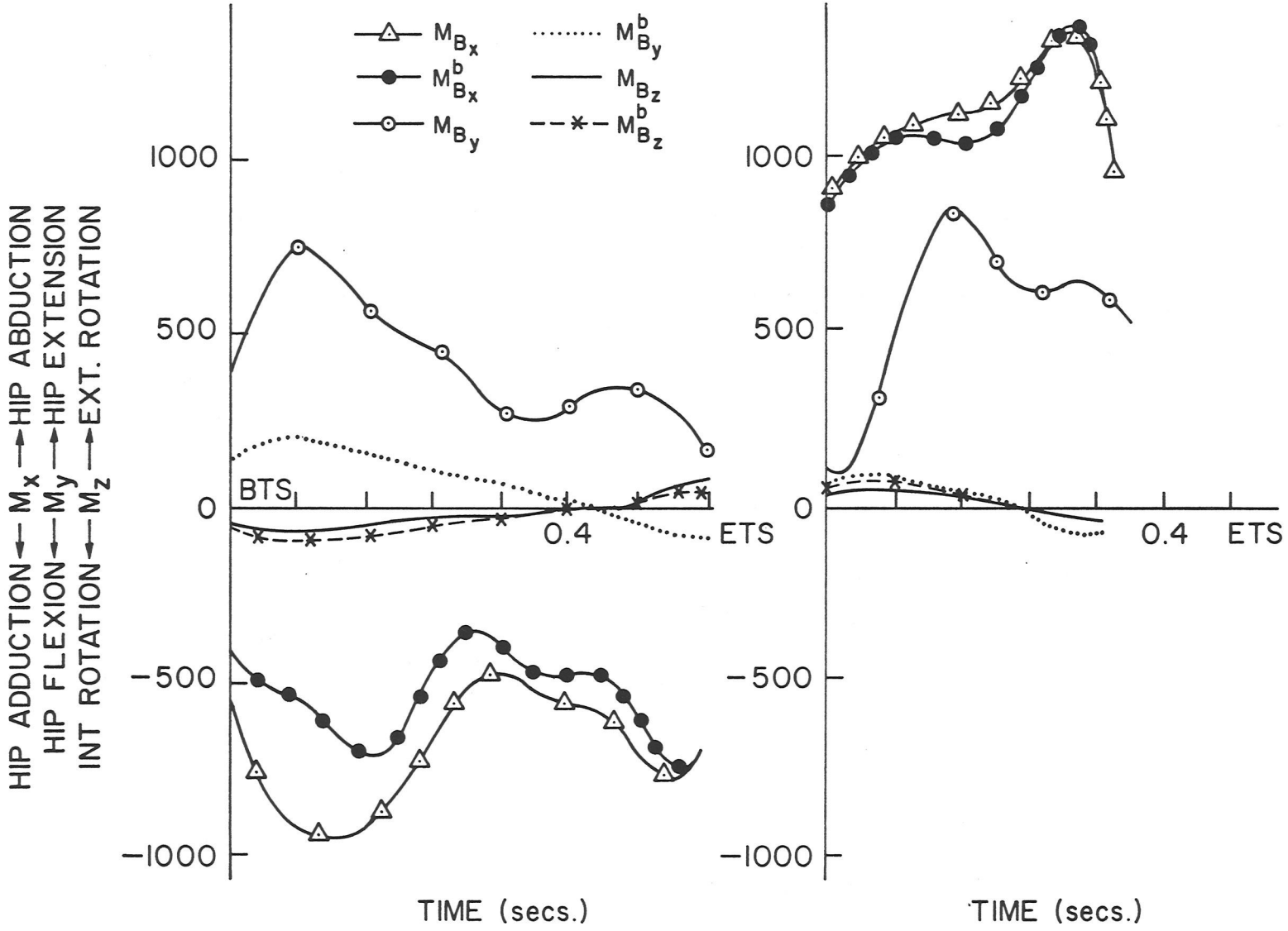

Figure 45 Net muscle moment at the hip joint for subject C

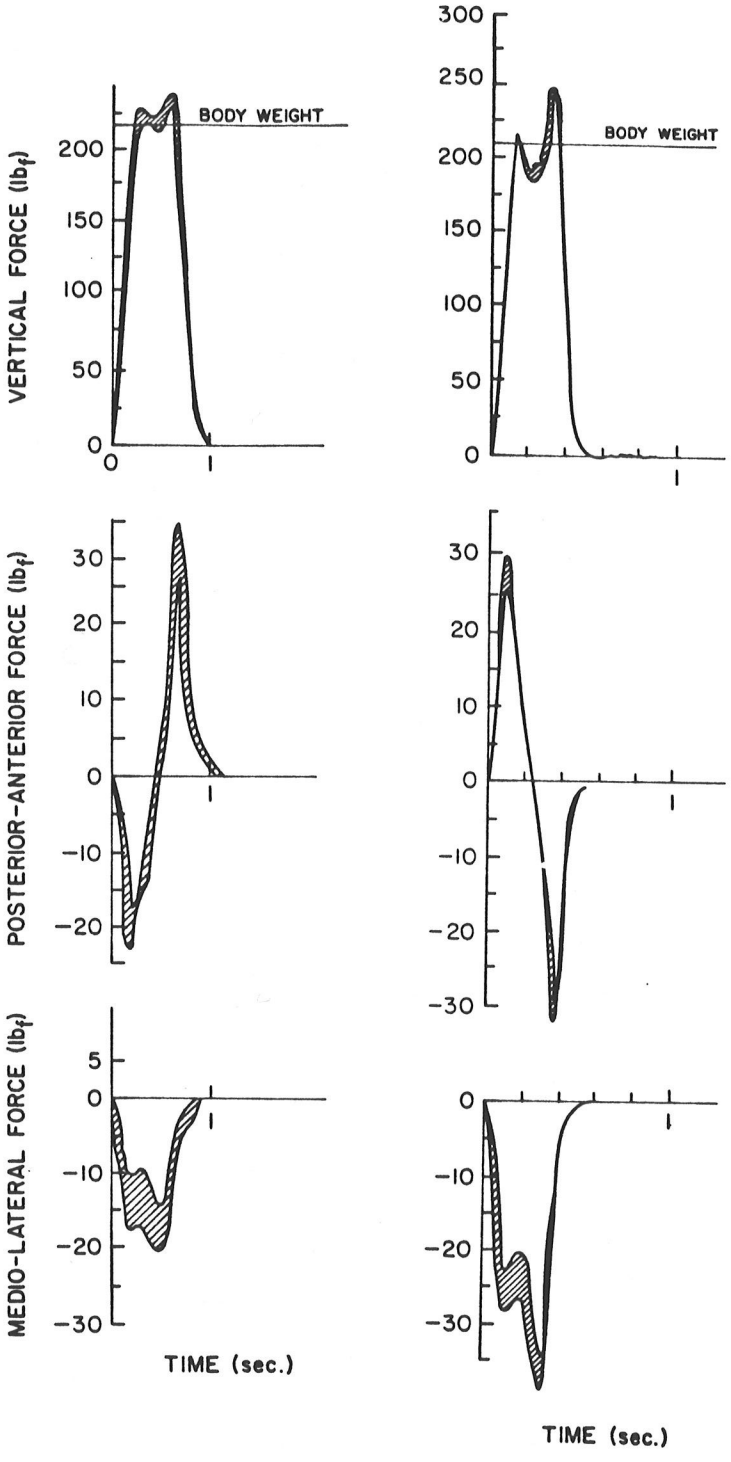

Figure 46 Ground-reaction forces for Subject'D'

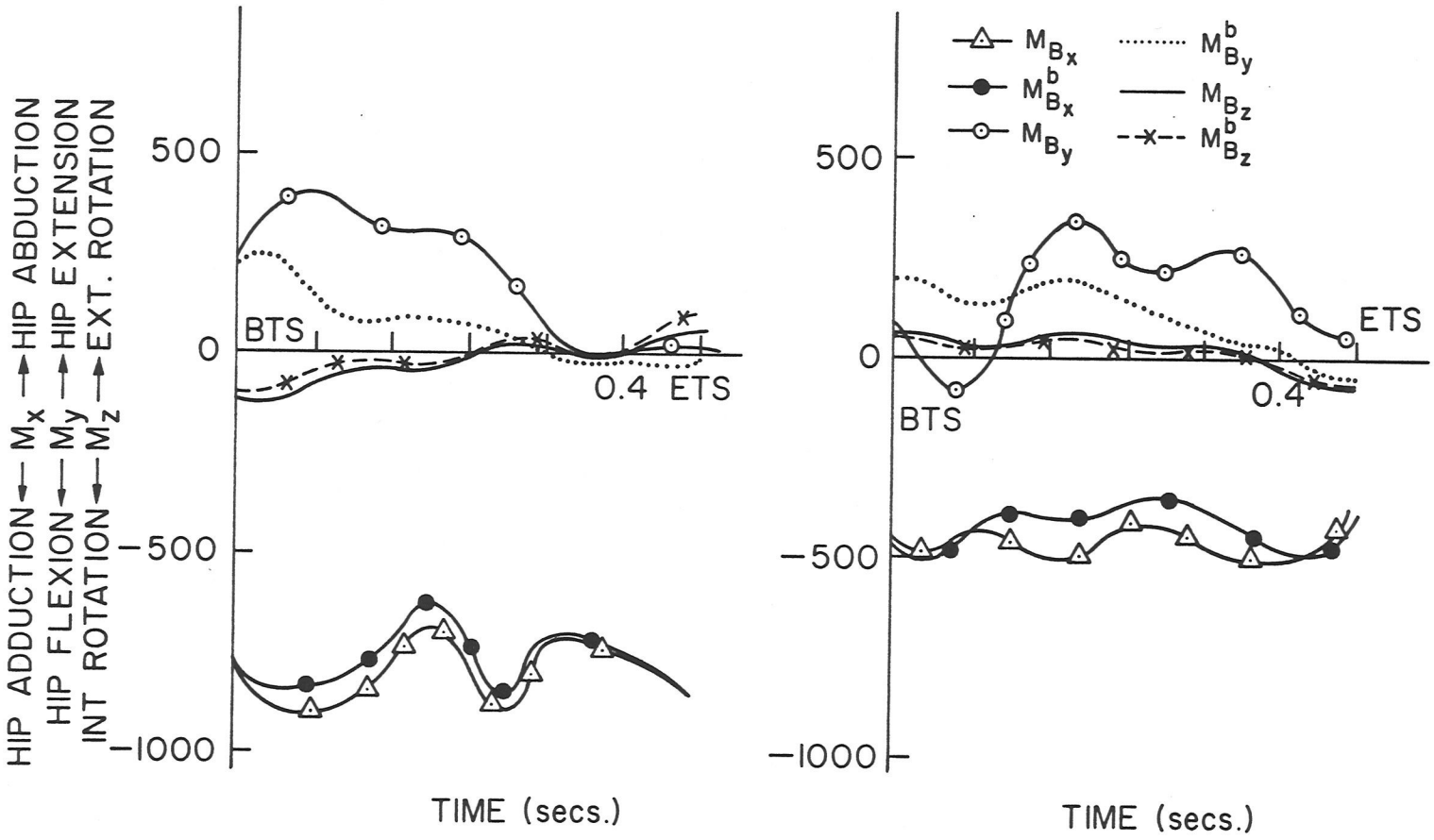

Figure 47 Net muscle moment at the hip joint for subject D (first trial)

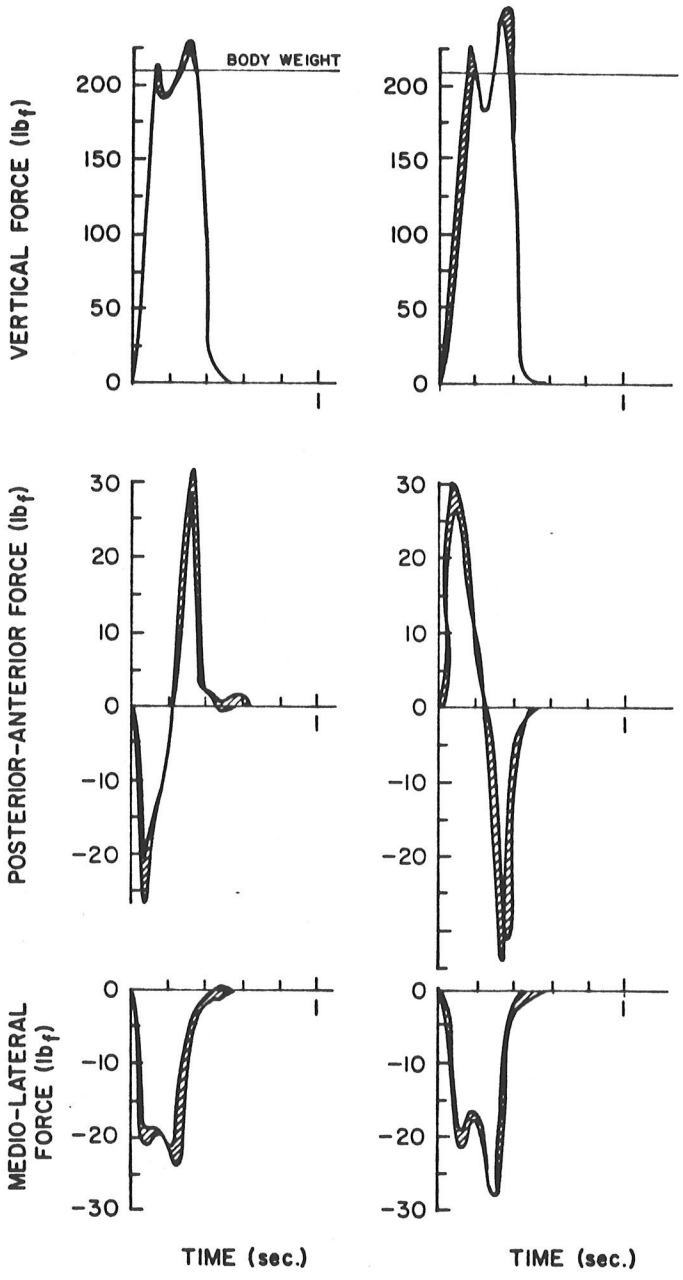

Figure 48 Ground-reaction forces for Subject'D'

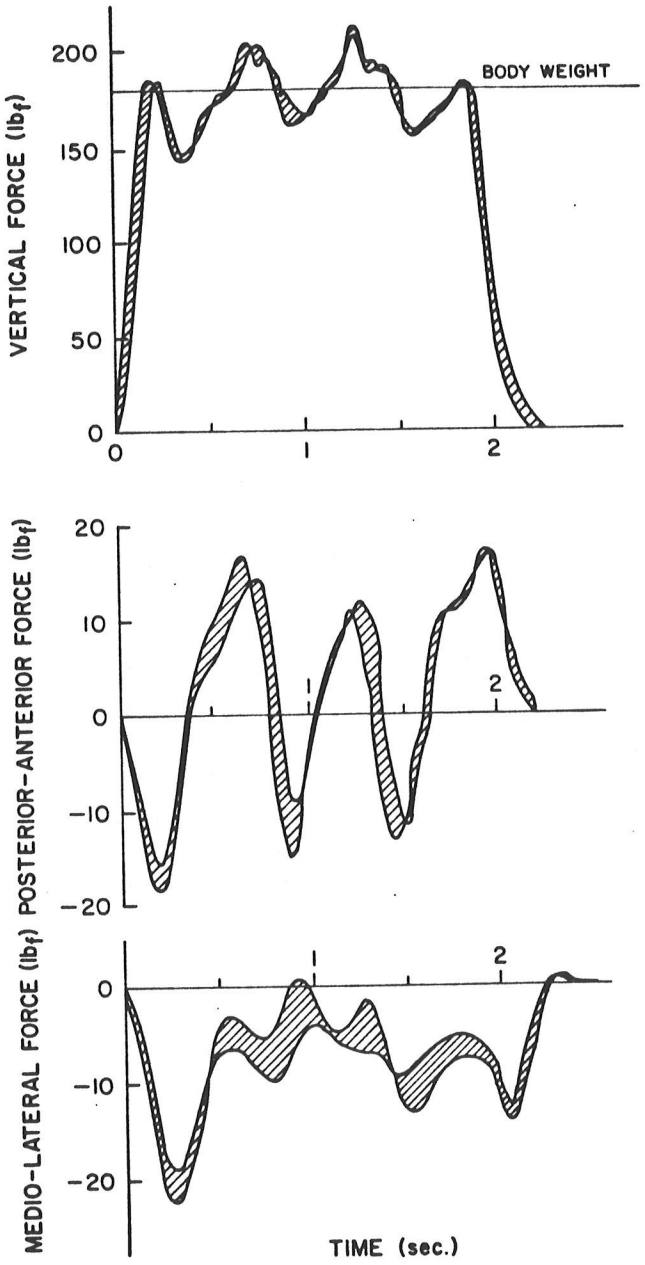

Figure 49 Ground-reaction forces for Subject'E' (with cane)

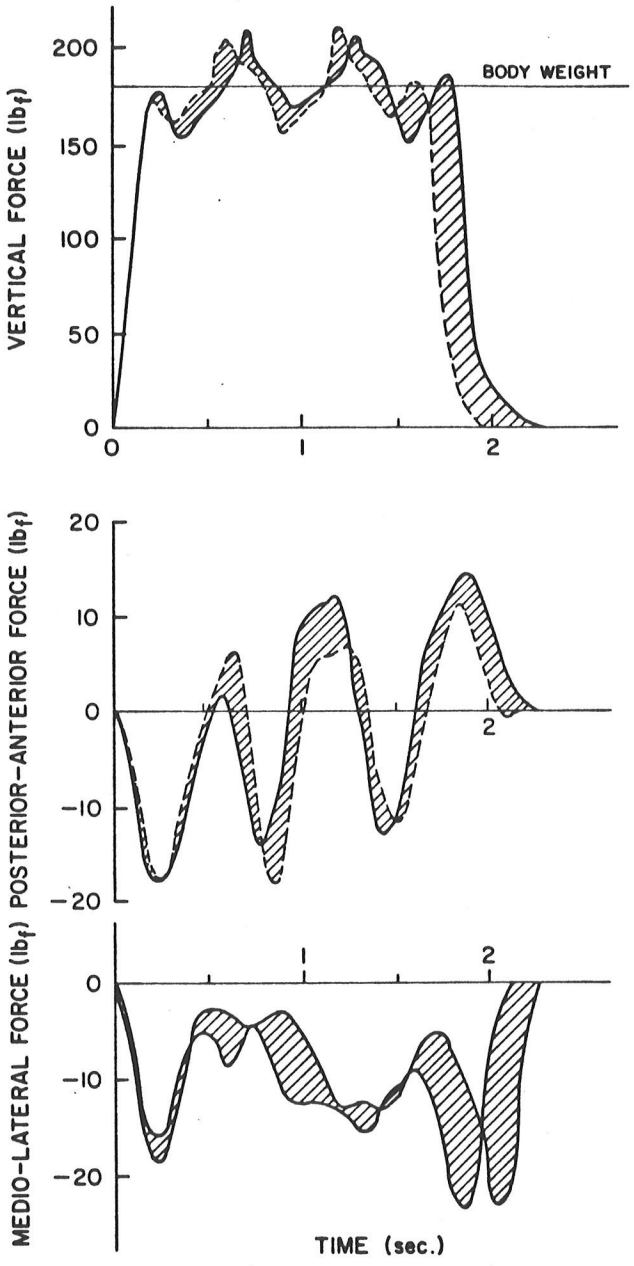

Figure 50 Ground-reaction forces for Subject'E' (without cane)

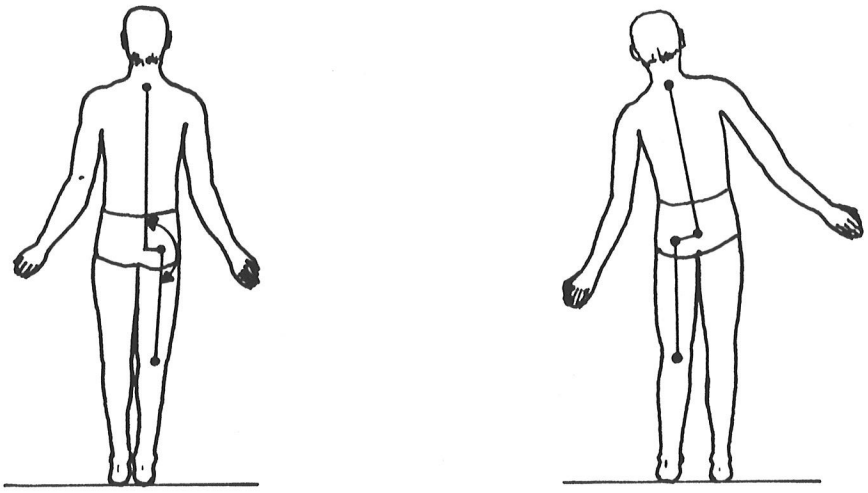

Figure 51 Normal and leaned upper body posture

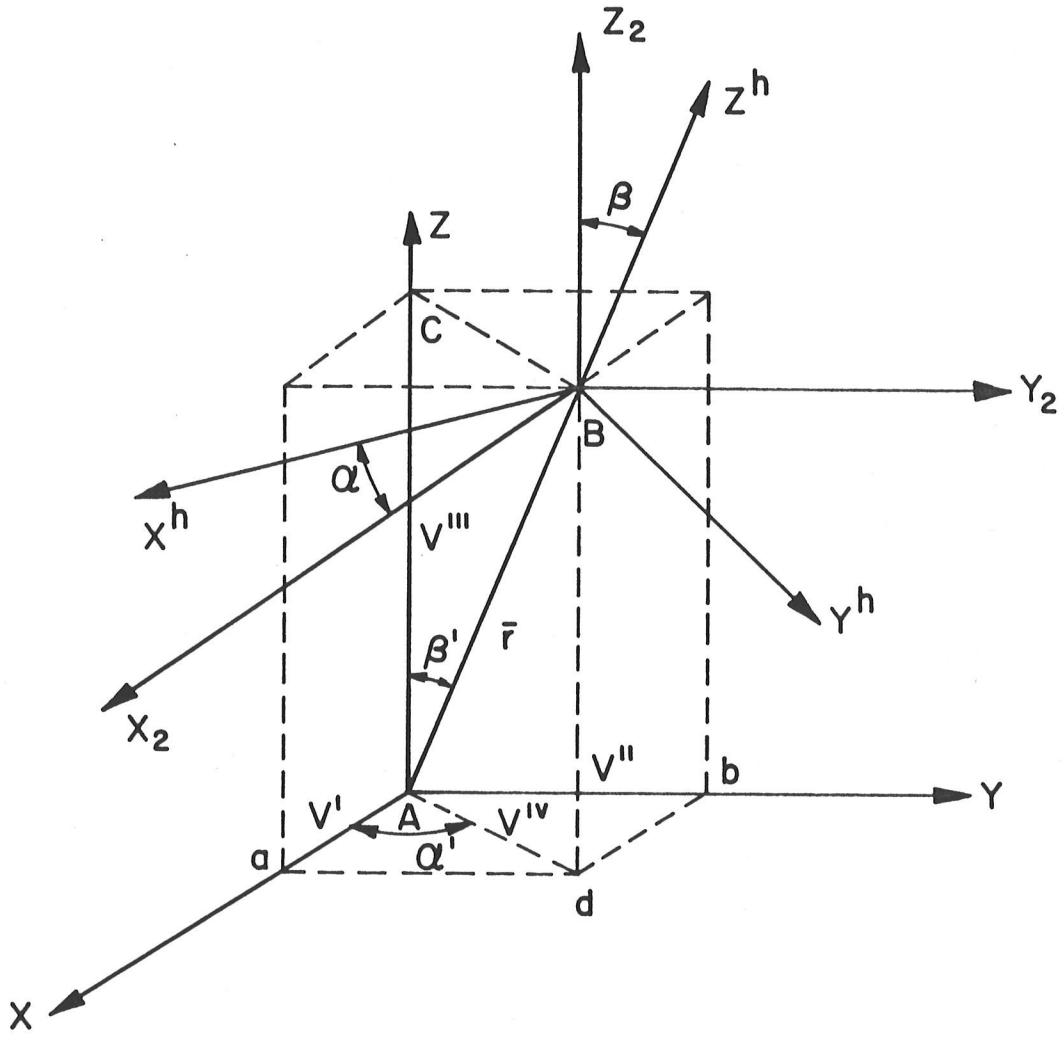

Figure 52 Representation of lower limb rotations